

Investigating Parameters of Lekatech's Electric Hammer

Timo Mayer

Supervisor

Jorma Autio

Advisor

Antti Anttila

Author Timo Mayer

Title Investigating Parameters of Lekatech's Electric Hammer

Degree programme

Major

Code of major MEN.thes

Supervisor Jorma Autio

Advisor Antti Anttila

Date **Number of pages** 166

Language English

Abstract

The parameters of Lekatech's new electric hammer prototype were explored. Initially, 5 different settings on the machine were controlled to explore its whole frequency range. They were tested with 3 different tool types and 2 types of concrete. The vibrations on the machine's tool and housing were measured, as well as the piston's (mover's) position during hammering. The fashion in which the concrete broke was also looked at. The results showed that the blunt tool took the longest to break the rock but also generated the most cracking, and the time taken for the concrete to break increased with frequency. Other conclusions were also drawn from the results.

Keywords Impact Hammering, Electric Hammer, Hydraulic Hammer, Frequency, Vibrations, Fracture, Stress, Kinetic Energy, Energy Efficiency, Lekatech

Contents

Abstract	3
Abstract (in Finnish)	4
Contents	5
Introduction	15
Background/Literature Review	15
Mechanics of Impact Hammering	15
How Hydraulic Hammers Work	26
Impact Hammer Related Products on the Market	28
Customer Needs	28
Types of Rock/Concrete relevant for the study	29
Simulating Rock Breakage	32
Simulating Rock Breakage	34
Parameters influencing rock/concrete breaking	37
Time-dependant Phenomena in Materials	44
Viscoelasticity	45
Types of Fracture	47
Sensors	49
Fatigue Lifetime Prediction	52
Research Problem	52
Hypotheses	52
Aim of the Work	55
Scope	56
Materials and Methods	57
Parameter Combination Codes	57
Example Calculation	59
Energy Efficiency of Machine	60
Colour Penetrant Dye	61
Electric Hammer Prototype	62
Measuring Setup	62
Error Calculations	62
Material Properties	63
Coordinate System	64
Granite Used	64
Normal Concrete Used	64
Results	64
First Iteration Results	64
Energy Efficiency Results	66
Hammering Frequency: 0.9 Hz	66
Hammering Frequency: 5 Hz	67

Hammering Frequency: 8 Hz	68
Hammering Frequency: 14 Hz	68
Hammering Frequency: 18 Hz	69
Energy Efficiency Variation with Frequency	74
Rock Mechanics Testing Results	74
Broken Sample Results	74
Time Taken to Break	75
Material Stress	76
Vibration Results	76
Kinetic Energy	77
Fatigue Analysis	78
Tool	78
Housing	79
Discussion	79
First Testing Iteration	80
Hypotheses	80
Suspected Reasons for Results	83
Possible Improvements to Experiment	85
Relevance of Results for Lekatech	86
Conclusion	89
First Testing Iteration	89
Appendix	96
Rock Mechanics Testing Results	96
CN0.9	96
CN5	98
CN8	100
CN14	102
CN18	104
BN0.9	106
BN5	109
BN8	111
BN14	114
BN18	116
WN0.9	119
WN5	120
WN8	122
WN14	125
WN18	126
WH0.9	129
WH5	131
WH8	133
WH14	136

WH18	138
BH0.9	141
BH5	144
BH8	146
BH14	149
BH18	151
CH0.9	154
CH5	157
CH8	159
CH14	162
CH18	164

List of Figures

1	An illustration of the bit hammering against the rock, creating stress waves which lead to cracking.	16
2	The steps and respective energy split of each stage of one hit of the hammer.	21
3	The amplitude of the vibration increases dramatically the closer the ratio of the two frequencies is to 1 [12].	22
4	Natural (resonance) frequencies of granite and sandstone at 10 and 20 kN input (excitation) frequency [13].	23
5	The mapping of the vibrations measured by the vibrometer [15].	24
6	The different parts of the hydraulic hammer (left) and a hydraulic hammer in action (right) [20].	26
7	The different parts of the hydraulic hammer in more detail [20].	27
8	The Hydraulic Rotary Percussive Hammer Drill invented by Montabert ETS [26].	29
9	A typical piece of red granite [28].	30
10	The stress values from the FEM analysis on the blade [37].	33
11	One corner crack with a circular profile (a) and one side flaw with an elliptical profile (b) were simulated [37].	33
12	The initial flaw, wing cracks and secondary cracks can be seen in the image taken by the camera, giving a good indication of how the rock will fail [39].	34
13	The wing cracks' curved and linear sections can be seen here. [39].	35
14	The grid allows the cracks from different tests to be mapped out and presented conveniently next to each other [39].	35
15	The application of the colour penetrant dye makes the shape and width of the crack clearly visible [40].	36
16	A sawed off section of tunnel flooring. Natural fractures are marked in green and excavation fractures in yellow [41].	36
17	The figure shows the increased tensile strength of the concrete at higher impact loads [44].	37
18	The figure shows the Hopkinson Split Bar setup used to break rock samples [10].	38
19	The figure shows the crack propagation through the sample [10].	38
20	Impact Energy required to fracture each rock type [47].	39
21	The solid lines show the relationship between the frequency of the impact hammer and its maximum load [48].	40
22	Fibres used to reinforce the concrete, from left to right: Polypropylene, Polyvinyl alcohol and Steel Fibre [50].	40
23	The projectile used in the study [51].	41
24	The impactors dropped onto granite in the study [52].	42
25	Vibrations measured in the housing of the hydraulic hammer [59].	43
26	Positions of the different hydraulic hammer reference points. The acceleration sensor was at Point 14 [59].	44

27	Graph showing how an elastic, viscous and viscoelastic material behaves when stress is applied [64].	46
28	The different fracture types when subjected to different types of stresses and material properties [65].	48
29	Different types of fractures appearing geologically in nature [65].	48
30	Mirror Zone, Wallner Lines, Mist Zone and Hackle Zone, as shown in the diagram (a) and the photo of a glass fracture (b) [67] [68].	50
31	The basic strain gauge with its components [69].	50
32	The Wheatstone Bridge described above [69].	51
33	The S-N Curve for 42CrMo4 Steel [71].	52
34	The S-N Curve for En-GJS-700 grade cast iron [72].	53
35	The rock prior to the application of the penetrant dye (a), after its application (b), cleaning the excess dye off (c), and the final result after drying revealing the cracks (d).	62
36	The granite surface after the application of the colour penetrant dye magnified 10 times.	63
37	Cracking in the concrete through and around the aggregate granular shown by the colour penetrant dye.	67
38	Pictures showing: (a) the wedge and cone tool used, (b) the length of the cone part of the tool, and (c) the diameter of the tools and the width of the wedge on the wedge tool.	67
39	The position of the two lasers and two acceleration sensors relative to the excavator and coordinate system.	68
40	The coordinate reference system used for the experiment relative to the excavator and hammer.	68
41	The granite used for the experiment; shown are a sawed and a broken section, although this piece is just a demonstration to show the grain size better, and the actual test blocks had no smooth sawed of section prior to testing.	69
42	The normal concrete used for the experiment; shown are the sawed and broken sections of each block, as well as the concrete's aggregate granular and steel fibre reinforcement.	69
43	Pictures showing (a) the diamond saw used and (b) a close-up of its diamond-tipped blade.	70
44	Kinetic energy calculated from the displacement graph of the laser on top of the mover.	70
45	Power Consumption and displacement graph for 0.9 Hz.	70
46	Kinetic energy calculated from the displacement graph of the laser on top of the mover.	71
47	Power Consumption and displacement graph for 5 Hz.	71
48	Kinetic energy calculated from the displacement graph of the laser on top of the mover.	71
49	Power Consumption and displacement graph for 8 Hz.	72
50	Kinetic energy calculated from the displacement graph of the laser on top of the mover.	72

51	Power Consumption and displacement graph for 8 Hz.	72
52	Kinetic energy calculated from the displacement graph of the laser on top of the mover.	73
53	Power Consumption and displacement graph for 18 Hz.	73
54	The efficiency with each of the 5 different frequency settings tested. . .	74
55	Time taken from the start of hammering until fracturing occurred. . .	75
56	Stress calculated using the same force for each frequency with varying cross sectional areas.	76
57	Vibration data recorded for all 30 tests.	77
58	Average Kinetic Energy of the mover recorded at each frequency. . . .	77
59	Results from the Laser Measurements on the Tool.	96
60	Results of acceleration sensor on material.	97
61	Results of acceleration sensor on material.	97
62	The area around the impact zone.	98
63	Results from the Laser Measurements on the Tool.	98
64	Results of acceleration sensor on material.	99
65	Results of acceleration sensor on material.	99
66	The area around the impact zone.	100
67	Results from the Laser Measurements on the Tool.	100
68	Results of acceleration sensor on material.	101
69	Results of acceleration sensor on material.	101
70	The area around the impact zone.	102
71	Results from the Laser Measurements on the Tool.	102
72	Results of acceleration sensor on material.	103
73	Results of acceleration sensor on material.	103
74	The area around the impact zone.	104
75	Results from the Laser Measurements on the Tool.	104
76	Results of acceleration sensor on material.	105
77	Results of acceleration sensor on material.	105
78	The area around the impact zone.	106
79	Results from the Laser Measurements on the Tool.	107
80	Results of acceleration sensor on material.	107
81	Results of acceleration sensor on material.	108
82	Results of acceleration sensor on material.	108
83	The area around the impact zone.	109
84	Results from the Laser Measurements on the Tool.	109
85	Results of acceleration sensor on material.	110
86	Results of acceleration sensor on material.	110
87	Results of acceleration sensor on material.	111
88	The area around the impact zone.	111
89	Results from the Laser Measurements on the Tool.	112
90	Results of acceleration sensor on material.	112
91	Results of acceleration sensor on material.	113
92	Results of acceleration sensor on material.	113
93	The area around the impact zone.	114

94	Results from the Laser Measurements on the Tool.	114
95	Results of acceleration sensor on material.	115
96	Results of acceleration sensor on material.	115
97	Results of acceleration sensor on material.	116
98	The area around the impact zone.	116
99	Results from the Laser Measurements on the Tool.	117
100	Results of acceleration sensor on material.	117
101	Results of acceleration sensor on material.	118
102	Results of acceleration sensor on material.	118
103	The area around the impact zone.	119
104	The area around the impact zone.	120
105	Results from the Laser Measurements on the Tool.	120
106	Results of acceleration sensor on material.	121
107	Results of acceleration sensor on material.	121
108	Results of acceleration sensor on material.	122
109	The area around the impact zone.	122
110	Results from the Laser Measurements on the Tool.	123
111	Results of acceleration sensor on material.	123
112	Results of acceleration sensor on material.	124
113	Results of acceleration sensor on material.	124
114	The area around the impact zone.	125
115	The area around the impact zone.	125
116	Results from the Laser Measurements on the Tool.	126
117	Results of acceleration sensor on material.	127
118	Results of acceleration sensor on material.	127
119	Results of acceleration sensor on material.	128
120	The area around the impact zone.	128
121	Results from the Laser Measurements on the Tool.	129
122	Results of acceleration sensor on material.	129
123	Results of acceleration sensor on material.	130
124	Results of acceleration sensor on material.	130
125	The area around the impact zone.	131
126	Results from the Laser Measurements on the Tool.	131
127	Results of acceleration sensor on material.	132
128	Results of acceleration sensor on material.	132
129	Results of acceleration sensor on material.	133
130	The area around the impact zone.	133
131	Results from the Laser Measurements on the Tool.	134
132	Results of acceleration sensor on material.	134
133	Results of acceleration sensor on material.	135
134	Results of acceleration sensor on material.	135
135	The area around the impact zone.	136
136	Results from the Laser Measurements on the Tool.	136
137	Results of acceleration sensor on material.	137
138	Results of acceleration sensor on material.	137

139	Results of acceleration sensor on material.	138
140	The area around the impact zone.	138
141	Results from the Laser Measurements on the Tool.	139
142	Results of acceleration sensor on material.	139
143	Results of acceleration sensor on material.	140
144	Results of acceleration sensor on material.	140
145	The area around the impact zone.	141
146	Results from the Laser Measurements on the Tool.	142
147	Results of acceleration sensor on material.	142
148	Results of acceleration sensor on material.	143
149	Results of acceleration sensor on material.	143
150	The area around the impact zone.	144
151	Results from the Laser Measurements on the Tool.	144
152	Results of acceleration sensor on material.	145
153	Results of acceleration sensor on material.	145
154	Results of acceleration sensor on material.	146
155	The area around the impact zone.	146
156	Results from the Laser Measurements on the Tool.	147
157	Results of acceleration sensor on material.	147
158	Results of acceleration sensor on material.	148
159	Results of acceleration sensor on material.	148
160	The area around the impact zone.	149
161	Results from the Laser Measurements on the Tool.	149
162	Results of acceleration sensor on material.	150
163	Results of acceleration sensor on material.	150
164	Results of acceleration sensor on material.	151
165	The area around the impact zone.	151
166	Results from the Laser Measurements on the Tool.	152
167	Results of acceleration sensor on material.	152
168	Results of acceleration sensor on material.	153
169	Results of acceleration sensor on material.	153
170	The area around the impact zone.	154
171	Results from the Laser Measurements on the Tool.	155
172	Results of acceleration sensor on material.	155
173	Results of acceleration sensor on material.	156
174	Results of acceleration sensor on material.	156
175	The area around the impact zone.	157
176	Results from the Laser Measurements on the Tool.	157
177	Results of acceleration sensor on material.	158
178	Results of acceleration sensor on material.	158
179	Results of acceleration sensor on material.	159
180	The area around the impact zone.	159
181	Results from the Laser Measurements on the Tool.	160
182	Results of acceleration sensor on material.	160
183	Results of acceleration sensor on material.	161

184	Results of acceleration sensor on material.	161
185	The area around the impact zone.	162
186	Results from the Laser Measurements on the Tool.	162
187	Results of acceleration sensor on material.	163
188	Results of acceleration sensor on material.	163
189	Results of acceleration sensor on material.	164
190	The area around the impact zone.	164
191	Results from the Laser Measurements on the Tool.	165
192	Results of acceleration sensor on material.	165
193	Results of acceleration sensor on material.	166
194	Results of acceleration sensor on material.	166

List of Tables

1	Material Properties of Granite [31].	31
2	Material Properties of Standard Concrete [34].	31
3	Material Properties of High Strength Concrete [36].	32
4	The 5 different settings used for testing.	57
5	Parameter Combinations for the first testing iteration	58
6	Relevant material properties of materials tested	63
7	Results of the first testing iteration	64
8	More results of the first testing iteration	65
9	Rock mechanics results from the first testing iteration	74
10	Tool stresses and lifetime cycles of each frequency	78
11	Tool stresses and lifetime cycles of each frequency	78
12	Tool stresses and lifetime cycles of each frequency.	79

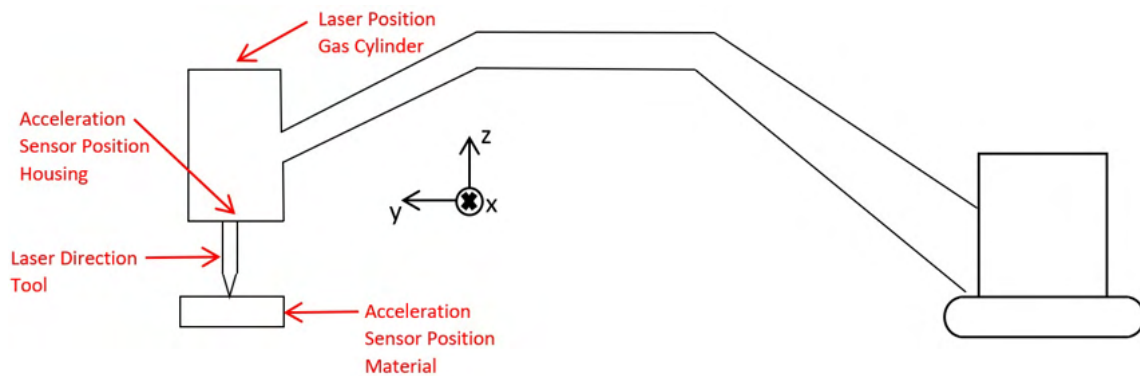


Figure 39: The position of the two lasers and two acceleration sensors relative to the excavator and coordinate system.

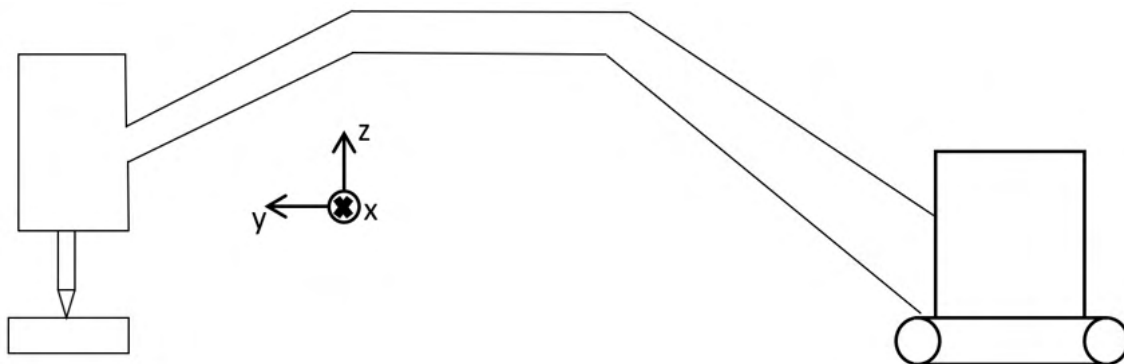


Figure 40: The coordinate reference system used for the experiment relative to the excavator and hammer.

Figure 47 below shows the power consumption of the inverter in the same graph as the position of the mover for 5 Hz.

Hammering Frequency: 8 Hz

The following graph in Figure 48 below shows the kinetic energy of the mover at a frequency of 8 Hz.

Figure 49 below shows the power consumption of the inverter in the same graph as the position of the mover for 8 Hz.

Hammering Frequency: 14 Hz

The following graph in Figure 50 below shows the kinetic energy of the mover at a frequency of 14 Hz.

Figure 51 below shows the power consumption of the inverter in the same graph as the position of the mover for 14 Hz.



Figure 41: The granite used for the experiment; shown are a sawed and a broken section, although this piece is just a demonstration to show the grain size better, and the actual test blocks had no smooth sawed of section prior to testing.

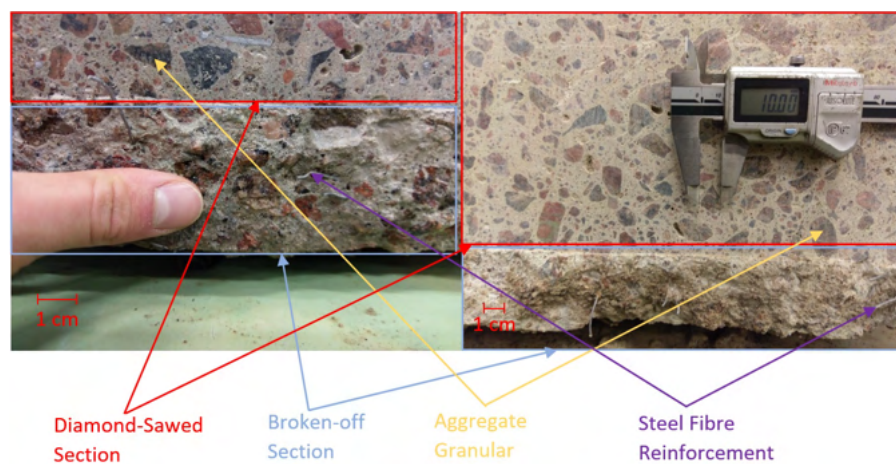


Figure 42: The normal concrete used for the experiment; shown are the sawed and broken sections of each block, as well as the concrete's aggregate granular and steel fibre reinforcement.

Hammering Frequency: 18 Hz

The following graph in Figure 52 below shows the kinetic energy of the mover at a frequency of 18 Hz.

Figure 53 below shows the power consumption of the inverter in the same graph as the position of the mover for 18 Hz.

The power consumption graphs shown above clearly show that the power consumption of the inverter is constant when the mover's position goes up, and decreases quickly to zero as the mover is accelerated rapidly downwards onto the tool.



Figure 43: Pictures showing (a) the diamond saw used and (b) a close-up of its diamond-tipped blade.

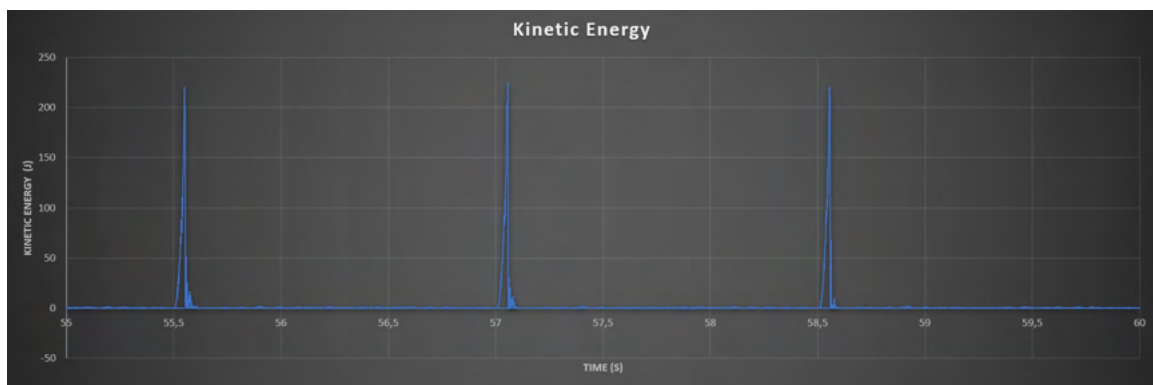


Figure 44: Kinetic energy calculated from the displacement graph of the laser on top of the mover.

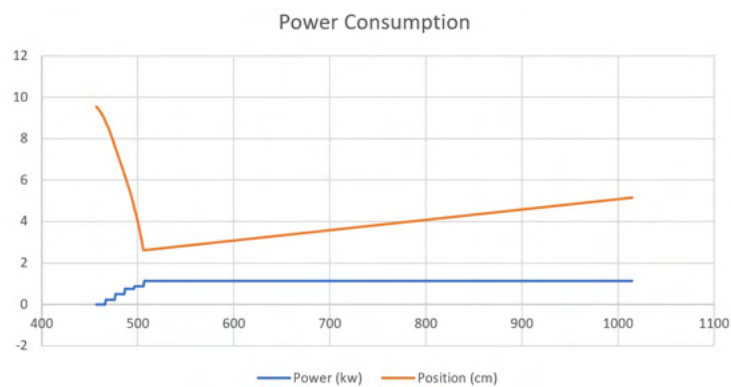


Figure 45: Power Consumption and displacement graph for 0.9 Hz.

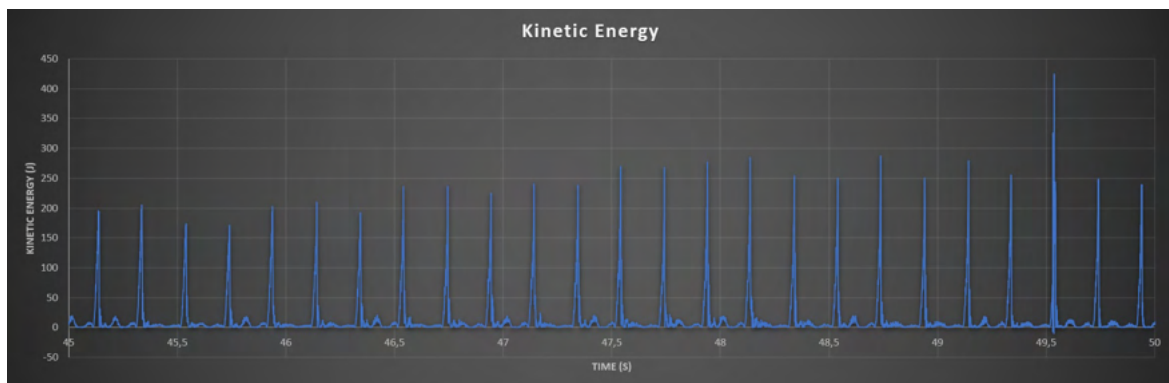


Figure 46: Kinetic energy calculated from the displacement graph of the laser on top of the mover.

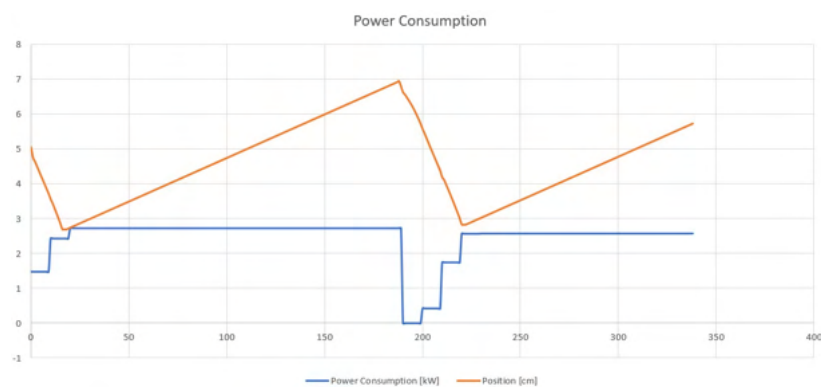


Figure 47: Power Consumption and displacement graph for 5 Hz.

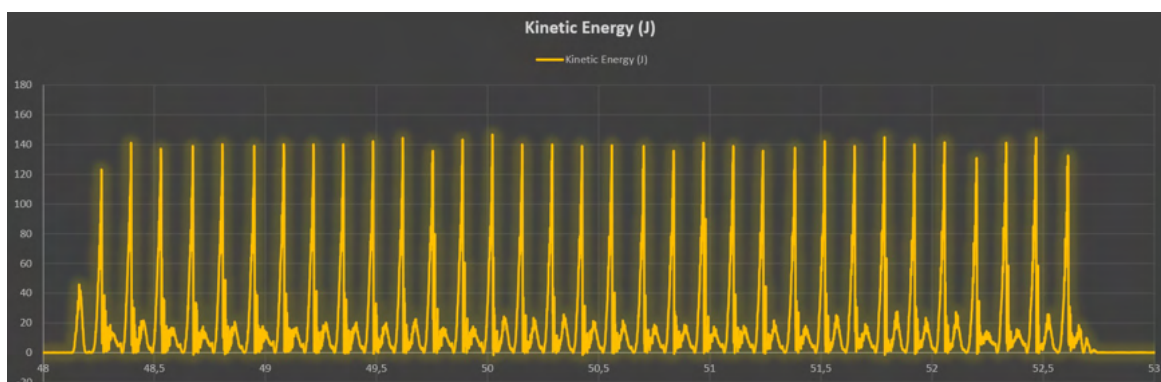


Figure 48: Kinetic energy calculated from the displacement graph of the laser on top of the mover.

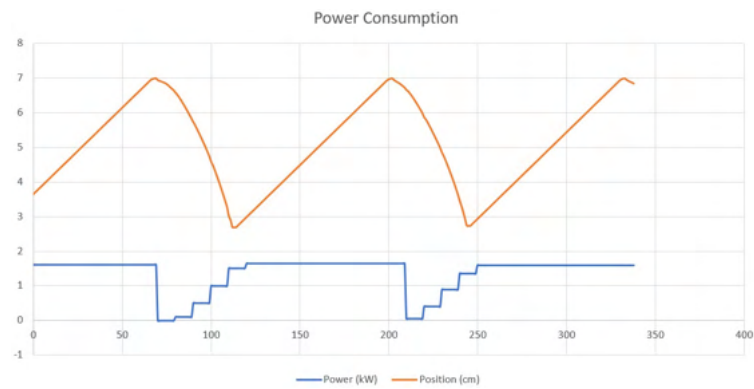


Figure 49: Power Consumption and displacement graph for 8 Hz.

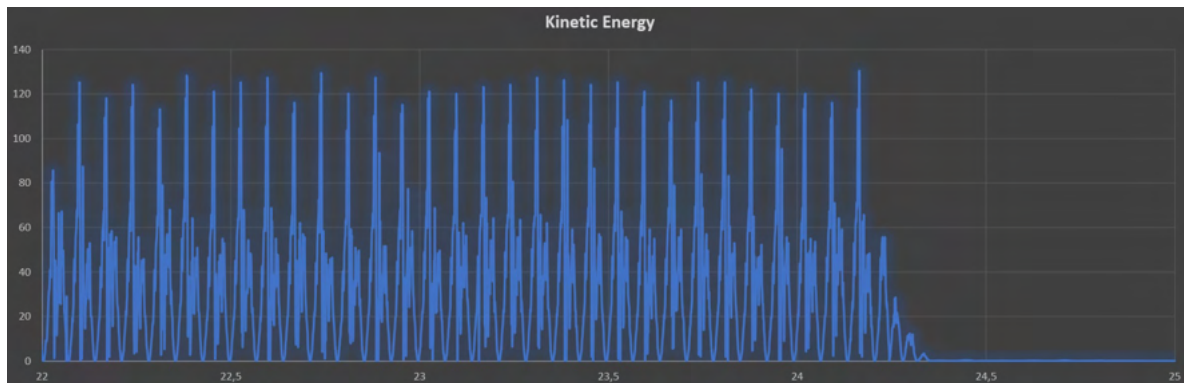


Figure 50: Kinetic energy calculated from the displacement graph of the laser on top of the mover.

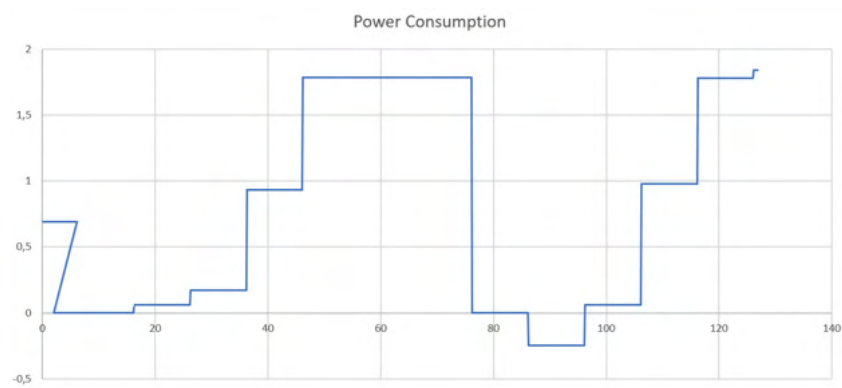


Figure 51: Power Consumption and displacement graph for 8 Hz.

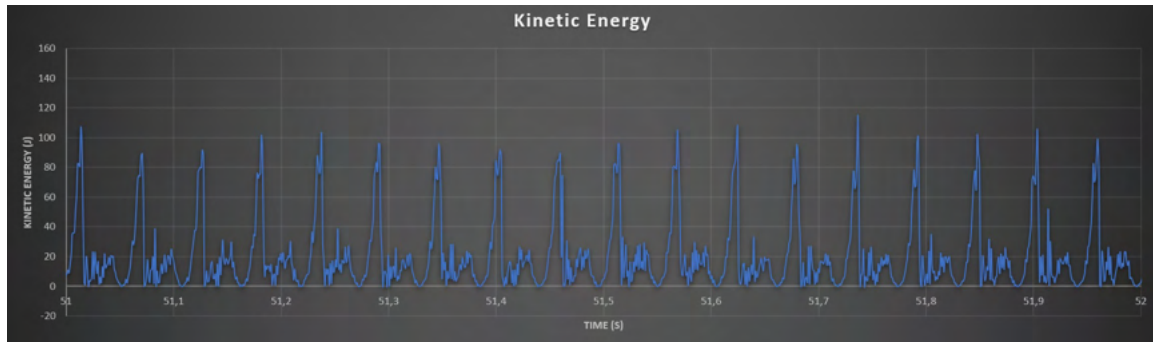


Figure 52: Kinetic energy calculated from the displacement graph of the laser on top of the mover.

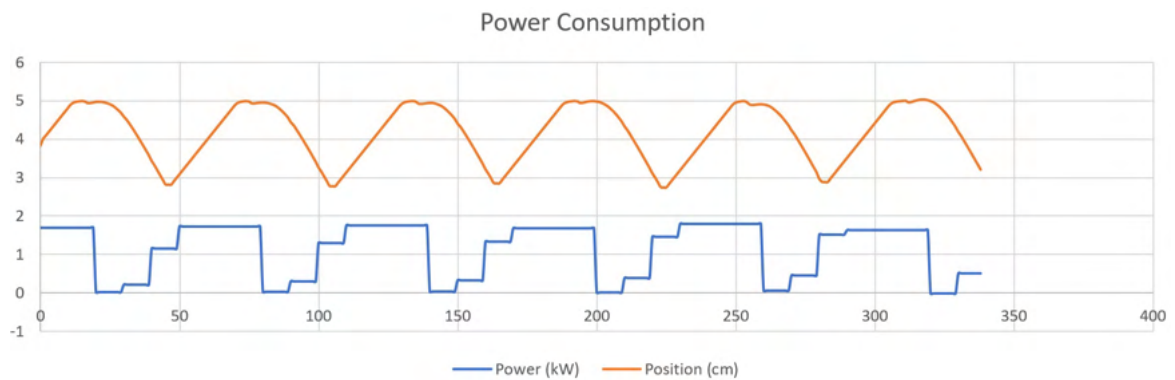


Figure 53: Power Consumption and displacement graph for 18 Hz.

Energy Efficiency Variation with Frequency

As can be seen in Figure 54 below, the energy efficiency varied significantly with frequency at the relatively low energy levels tested. The clearly recognisable trend is that the efficiency is lower for the low frequencies and higher for the high frequencies. It will be interesting in the second testing iteration to see the behaviour of the machine's energy efficiency with higher impact energies.

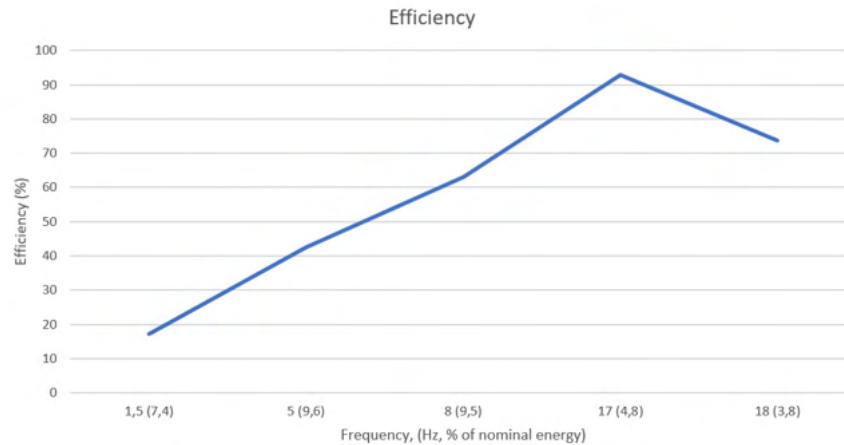


Figure 54: The efficiency with each of the 5 different frequency settings tested.

Rock Mechanics Testing Results

The results of the vibration measurements as well as the state of the tested samples after the test can be seen for each of the 30 tests in the Appendix. In this section, a summary of the results will be shown.

Broken Sample Results

Table 9 below shows the variations between the results of the different material-tool combinations. It should be noted that the last column shows the 5 tests for each tool-material combination in order of lowest to highest frequency (0.9 Hz, 5 Hz, 8 Hz, 14 Hz, 18 Hz).

Table 9: Rock mechanics results from the first testing iteration

<u>Tool & Material Code</u>	<u>Amount of Cracks Ranking</u>	<u>Amount of Fragmentation Ranking</u>	<u>Cracking more around/ more through Agg. Granular</u>	<u>Cracking near Impact Zone (Yes/No)</u>
Cone - N	2	2	even	N, N, Y, N, N

Blunt - N	1	1	more around	N, Y, Y, Y, Y
Wedge - N	T3	3	more through	Y, N, N, N, N
Wedge - HS	T3	T5	more through	N, Y, Y, Y, N
Blunt - HS	T5	T5	even	Y, Y, Y, Y, Y
Cone - HS	T5	4	even	N, Y, N, Y, Y

Table 9 shows that the blunt tool consistently causes more cracking (both around and away from the impact zone) and fragmentation, especially in the normal concrete. It is also the only tool with which the cracking goes around, rather than through, the impact zone.

Time Taken to Break

Figure 55 below shows the difference between the different samples and the time it took for them to break.

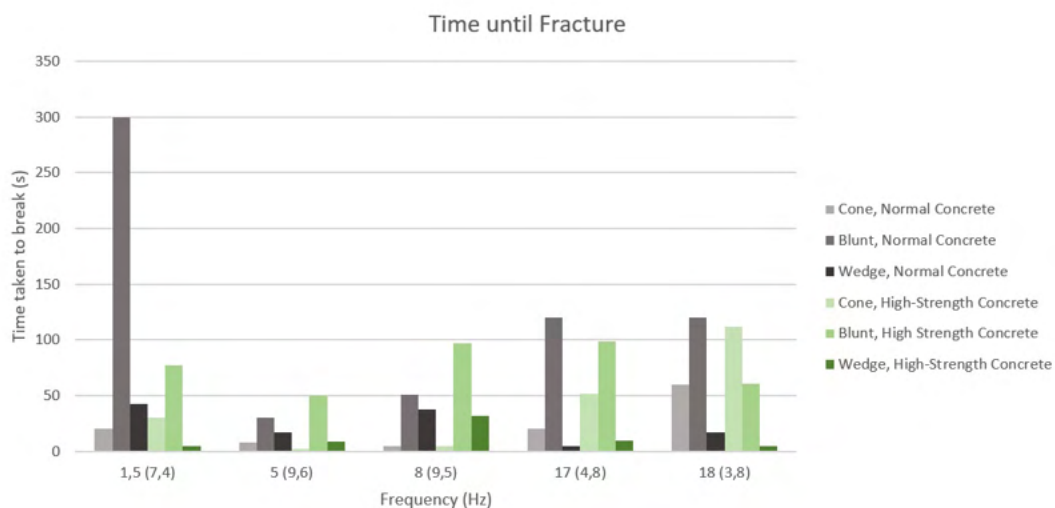


Figure 55: Time taken from the start of hammering until fracturing occurred.

Figure 55 above shows that the blunt tool consistently takes the longest time to break the sample. There is no significant difference between the wedge and cone tool types.

The time required to break increases with frequency, with the exception of the lowest frequency.

There is no significant difference between the time taken until fracture between the two types of concrete.

Material Stress

Figure 56 below shows how the stress varies with stress and tool type. The value was the average of all the peaks in the acceleration graphs for each frequency, which were obtained by differentiating the laser displacement graph twice. The error bars were a half population standard deviation above and below the mean, after any outliers had been removed.

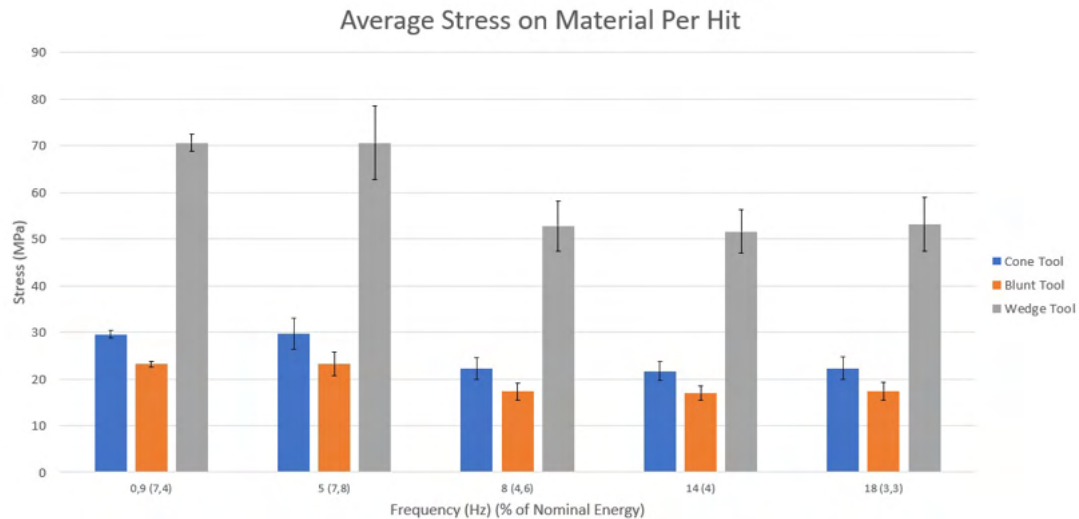


Figure 56: Stress calculated using the same force for each frequency with varying cross sectional areas.

Figure 56 above shows that the wedge tool clearly exerts more stress on the material than the other two tools. There is no significant difference between the other two tool types in terms of stress.

Vibration Results

Figure 57 below compares all recorded tool vibrations for all 30 tests. Unfortunately, some data was unavailable or unusable, leading to some gaps in the graphs but the majority of it is usable.

Figure 57 shows that using the blunt tool on the normal concrete consistently causes more vibrations than the other tools in the material, housing, and tool itself. The other tool-material combinations do not have significant discernible differences each other in terms of the vibrations they cause.

The vibrations in the material are significantly higher than the housing and tool vibrations. The housing vibrations are significantly larger than the vibrations in the tool.

There is no significant, clear trend regarding changes of vibration magnitudes with changes in frequency.

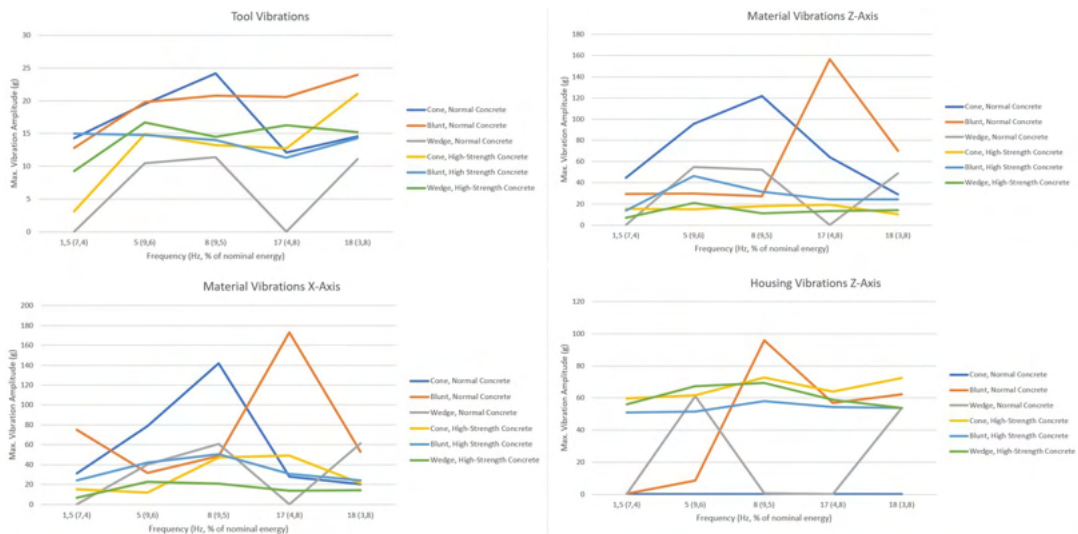


Figure 57: Vibration data recorded for all 30 tests.

Kinetic Energy

Figure 58 below shows the variations in the maximum Kinetic Energy of the mover with varying frequencies. Only the variations in the graph will be discussed here, the energy efficiency is discussed in the ‘‘Energy Efficiency’’ section.

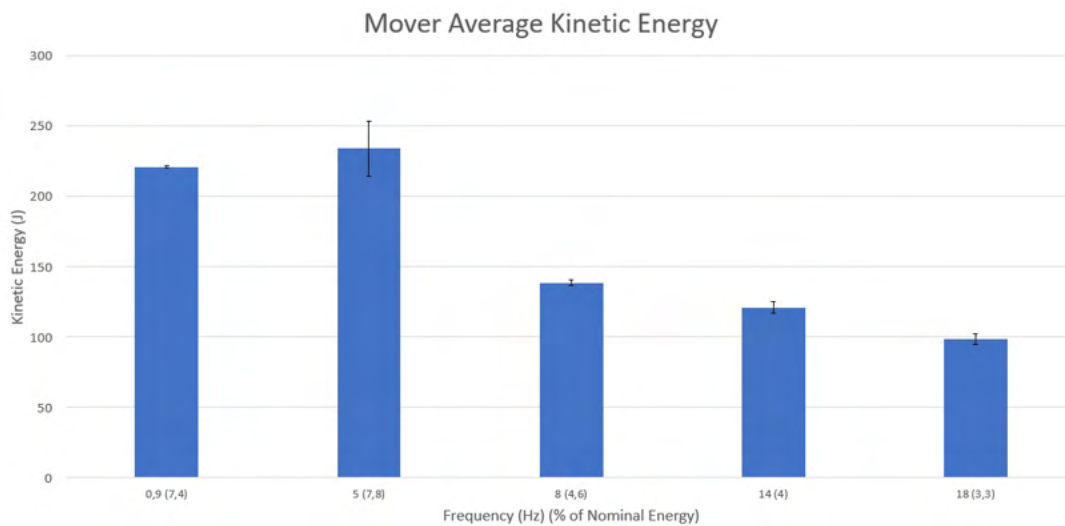


Figure 58: Average Kinetic Energy of the mover recorded at each frequency.

Figure 58 above shows that the kinetic energy of the mover is highest at the settings for the 0.9 and 5 Hz frequencies. For the 8, 14, and 18 Hz frequencies it is significantly lower than for 0.9 and 5 Hz frequencies, although variation between the former three is statistically insignificant.

Conclusion

First Testing Iteration

The project, at the beginning, set out to obtain data for Lekatech's electric hammer prototype which could benefit product by identifying how the machine performs under settings and parameters. The intention was to firstly show/assess whether the electric hammer could function in the same manner as the conventional hydraulic hammer, and secondly to explore what additional features and capabilities the electric hammer had compared to the hydraulic hammer.

By the end of the first round of testing (halfway through the project), data had been obtained on material, tool and housing vibrations as well as on how and how quickly *concrete* broke. What had not been done yet was testing with *homogenous rock*. Different tools and machine settings were also tested and their different effects on the concrete assessed. This obtained data is useable for e.g. an instruction manual for the product. It will also be useful for programming a new, more user-friendly PLC (Programmable Logic Controller). While frequency was the main parameter being varied, the second round of testing can focus on varying the impact energy, and hitting with significantly higher energy levels.

In terms of comparing the energy efficiency and vibrations to those of the hydraulic hammer, partial progress has been made. Energy efficiency and vibration data was collected, but it could not yet be compared to the same measured data from a hydraulic hammer because this had not yet been obtained. The energy efficiency results did, however, indicate an efficiency in the same ball park as that theoretically calculated when designing the electric hammer, at least for some of the frequencies, although a couple of frequencies also gave unrealistic efficiencies. In the second testing iteration, this data must be obtained from the hydraulic hammer. A second testing iteration will also allow for measuring of the power consumption more accurately and reliably.

Overall, the first 3 months of this project have gone well and a lot has been achieved, laying the groundwork for the second round of testing. There is, however, a significant amount of work left to do and it will also bring new challenges.

References

- [1] (2020, May) Impact (mechanics). Wikipedia. [Online]. Available: [https://en.wikipedia.org/wiki/Impact_\(mechanics\)](https://en.wikipedia.org/wiki/Impact_(mechanics))
- [2] H. Tunçdemir, “Impact hammer applications in istanbul metro tunnels,” *Tunnelling and Underground Space Technology*, vol. 23, no. 3, pp. 264 – 272, 2008. [Online]. Available: <http://www.sciencedirect.com/science/article/pii/S0886779807000533>
- [3] T. Bell. (2018, Dec.) Ductility Explained: Tensile Stress and Metals. ThoughtCo. [Online]. Available: <https://www.thoughtco.com/ductility-metallurgy-4019295>
- [4] D. Collins. (2019, Nov.) Mechanical properties of materials: stiffness and deflection. Linear Motion Tips. [Online]. Available: <https://www.linearmotiontips.com/mechanical-properties-of-materials-stiffness-and-deflection/#:~:text=Amaterial'sstiffnessindicatesits,itexperiencesstressandstrain.>
- [5] NTD. Fracture Toughness. NTD Resource Center. [Online]. Available: <https://www.nde-ed.org/EducationResources/CommunityCollege/Materials/Mechanical/FractureToughness.htm>
- [6] (2020) Material Hardness Review - Strength Mechanics of Materials. Engineers Edge. [Online]. Available: https://www.engineersedge.com/material_science/hardness.htm#:~:text=Hardnessisthepropertyof,watergenerallyincreaseswithhardness.
- [7] (2016, Apr.) Plasticity. Britannica. [Online]. Available: <https://www.britannica.com/science/plasticity>
- [8] D. Olsen. (2016, Sep.) Material Applications: Wear Resistance. Metal Tek International. [Online]. Available: <https://marketing.metalk.com/smart-blog/material-applications-wear-resistance>
- [9] (2019, Nov.) Split-Hopkinson pressure bar. Wikipedia. [Online]. Available: https://en.wikipedia.org/wiki/Split-Hopkinson_pressure_bar
- [10] B. Bohloli, “Effects of the geological parameters on rock blasting using the hopkinson split bar,” *International Journal of Rock Mechanics and Mining Sciences*, vol. 34, no. 3, pp. 32.e1 – 32.e9, 1997. [Online]. Available: <http://www.sciencedirect.com/science/article/pii/S1365160997002281>
- [11] (2020) Natural Frequency. The Physics Classroom. [Online]. Available: <https://www.physicsclassroom.com/class/sound/Lesson-4/Natural-Frequency>
- [12] MasterHD. (2019, Nov.) Resonance transmissability. Wikipedia. [Online]. Available: https://en.wikipedia.org/wiki/Mechanical_resonance#/media/File:Resonance.PNG

- [13] C. Shi, S. Li, S. Tian, W. Li, T. Yan, and F. Bi, "Research on the resonance characteristics of rock under harmonic excitation," *Shock and Vibration*, vol. 2019, p. 6326510, 2019. [Online]. Available: <https://doi.org/10.1155/2019/6326510>
- [14] M. Cerpinska and M. Irbe, "Specifics of Natural Frequency Measurements for Floor Vibration," *Engineering for Rural Development*, 2017.
- [15] M. Retze, Ulrich; Schüssler, "Dynamic Stress and Strain Measurement," *Polytech Aerospace Technical Papers*, 2010. [Online]. Available: https://www.polytec.com/fileadmin/d/Vibrometrie/OM_TP_InFocus_Strain_2010_02_E.pdf
- [16] (2020, Sep.) Proximity sensor. Wikipedia. [Online]. Available: https://en.wikipedia.org/wiki/Proximity_sensor
- [17] (2020, Jul.) Measuring Vibration with Accelerometers. NI. [Online]. Available: <https://www.ni.com/fi-fi/innovations/white-papers/06/measuring-vibration-with-accelerometers.html#section--692732068>
- [18] A. Eitzenberger, "Wave Propagation in Rock and the Influence of Discontinuities," *Luleå University of Technology*, 2012.
- [19] P Wave. Byju's The Learning App. [Online]. Available: <https://byjus.com/physics/p-wave/>
- [20] Anshita. (2018, Feb.) What is Hydraulic Hammer and how does it work? Engineering Insider. [Online]. Available: <https://engineeringinsider.org/hydraulic-hammer-working/>
- [21] C. Hodanbosi and J. G. Fairman. (1996, Aug.) Pascal's Principle and Hydraulics. National Aeronautics and Space Administration. [Online]. Available: https://www.grc.nasa.gov/www/k-12/WindTunnel/Activities/Pascals_principle.html
- [22] Gorilla. (2020) Practical Tips for Using Heavy Demolition Tools. Gorilla Hammers. [Online]. Available: <https://gorillahammers.com/hydraulic-hammer-breaker-usage/>
- [23] K. Andersson and J. Rodert, "Hammer device," EU patenteu EP1 089 854A1, Apr. 11, 2001.
- [24] M. Pettersson and A. Johansson, "Hydraulic impact mechanism for use in equipment for treating rock and concrete," EU patenteu EP2 611 579A1, Jul. 10, 2013.
- [25] I. Masayoshi, "Electromagnetic type hammering device," Japanese Patent JP6 081 574A, Mar. 22, 1994.
- [26] "Hydraulic rotary percussive hammer drill," Israel patent IL163 897A, Nov. 26, 2008. [Online]. Available: <https://worldwide.espacenet.com/publicationDetails/biblio?DB=worldwide.espacenet.com&II=0&ND=3&adjacent=true&FT=D&date=20081126&CC=IL&NR=163897A&KC=A>

- [27] W.-L. Zhao, “Impact piston and hydraulic breaking hammer with same,” Chinese Patent CN102 818 018A, Dec. 12, 2012.
- [28] I. Friman, “Granite,” *Wikipedia*, 2020. [Online]. Available: <https://en.wikipedia.org/wiki/Granite#/media/File:Fj\T1\aeregranitt3.JPG>
- [29] H. M. King, “Granite,” *Geology.com*, 2020. [Online]. Available: <https://geology.com/rocks/granite.shtml>
- [30] H. Blatt and R. Tracy, *Petrology, Second Edition: Igneous, Sedimentary, and Metamorphic*. W. H. Freeman, 1995. [Online]. Available: <https://books.google.fi/books?id=5aSIQgAACAAJ>
- [31] MatWeb. (2020) Granite. MatWeb: Material Property Data. [Online]. Available: <http://www.matweb.com/search/datasheet.aspx?matguid=3d4056a86e79481cb6a80c89caae1d90&ckck=1>
- [32] P. A. S. Håkan, *Rock Engineering*. ICE Publishing, 2010. [Online]. Available: <https://app.knovel.com/hotlink/toc/id:kpRE00002O/rock-engineering/rock-engineering>
- [33] Concrete Basics: Essential Ingredients For a Concrete Mixture. Concrete Supply Co. [Online]. Available: <https://concretesupplyco.com/concrete-basics/>
- [34] EngineeringToolBox. (2008) Concrete - properties. The Engineering ToolBox. [Online]. Available: https://www.engineeringtoolbox.com/concrete-properties-d_1223.html
- [35] Testing Compressive Strength of Concrete. NRMCA. [Online]. Available: <https://centralconcrete.com/wp-content/themes/centralconcrete/images/cip/35pr.pdf>
- [36] P. Song and S. Hwang, “Mechanical properties of high-strength steel fiber-reinforced concrete,” *Construction and Building Materials*, vol. 18, no. 9, pp. 669 – 673, 2004. [Online]. Available: <http://www.sciencedirect.com/science/article/pii/S095006180400073X>
- [37] K. Barlow and R. Chandra, “Fatigue crack propagation simulation in an aircraft engine fan blade attachment,” *International Journal of Fatigue*, vol. 27, no. 10, pp. 1661 – 1668, 2005, fatigue Damage of Structural Materials V. [Online]. Available: <http://www.sciencedirect.com/science/article/pii/S0142112305001040>
- [38] L. E. Chiang and D. A. Elías, “A 3d fem methodology for simulating the impact in rock-drilling hammers,” *International Journal of Rock Mechanics and Mining Sciences*, vol. 45, no. 5, pp. 701 – 711, 2008. [Online]. Available: <http://www.sciencedirect.com/science/article/pii/S136516090700127X>
- [39] Q. Li, Q. Yang, J.-c. Jia, and L.-h. Liu, “Experimental research on crack propagation and failure in rock-type materials under compression,” *Electronic Journal of Geotechnical Engineering*, vol. 13, 01 2008.

- [40] WEICONinternational. (2017, Sep.) Crack inspection, nondestructive testing, colour penetration test | weicon crack testing agent. WEICON. [Online]. Available: <https://www.youtube.com/watch?v=SVLuKfZwJYo>
- [41] L. O. Ericsson, J. Thörn, R. Christiansson, T. Lehtimäki, H. Ittner, K. Hansson, C. Butron, O. Sigurdsson, and P. Kinnbom, “A demonstration project on controlling and verifying the excavation-damaged zone,” *Svensk Kärnbränslehantering AB*, Jan. 2015.
- [42] L. Wu, S. Liu, Y. Wu, and C. Wang, “Precursors for rock fracturing and failure—part i: Irr image abnormalities,” *International Journal of Rock Mechanics and Mining Sciences*, vol. 43, no. 3, pp. 473 – 482, 2006. [Online]. Available: <http://www.sciencedirect.com/science/article/pii/S136516090500122X>
- [43] L. Wu, C. Cui, N. Geng, and J. Wang, “Remote sensing rock mechanics (rsrm) and associated experimental studies,” *International Journal of Rock Mechanics and Mining Sciences*, vol. 37, no. 6, pp. 879 – 888, 2000. [Online]. Available: <http://www.sciencedirect.com/science/article/pii/S1365160999000660>
- [44] P. Sukontasukkul, P. Nimityongskul, and S. Mindess, “Effect of loading rate on damage of concrete,” *Cement and Concrete Research*, vol. 34, no. 11, pp. 2127 – 2134, 2004. [Online]. Available: <http://www.sciencedirect.com/science/article/pii/S000888460400136X>
- [45] S. Kaewunruen and A. M. Remennikov, “Impact capacity of railway prestressed concrete sleepers,” *Engineering Failure Analysis*, vol. 16, no. 5, pp. 1520 – 1532, 2009. [Online]. Available: <http://www.sciencedirect.com/science/article/pii/S1350630708002215>
- [46] I. Evans, “Energy requirements for impact breakage of rocks,” in *Proceedings of the Fluid Power Equipment in Mining, Quarrying and Tunnelling*, London, 1974, pp. 1 – 8.
- [47] T. Kujundžić, G. Bedeković, D. Kuhinek, and T. Korman, “Impact of rock hardness on fragmentation by hydraulic hammer and crushing in jaw crusher,” *Rudarsko-Geološko-Naftni Zbornik*, vol. 20, 12 2008.
- [48] S. Takagawa, “A study on high frequency hammering system and its impact loads — second report,” in *OCEANS 2011 IEEE - Spain*, 2011, pp. 1–5.
- [49] . Metallurgist, “Rock hammering & rock breaking,” *Rock Hammering & Rock Breaking*, 2017. [Online]. Available: <https://www.911metallurgist.com/rock-hammering-rock-breaking/>
- [50] J. Feng, X. Gao, J. Li, H. Dong, Q. He, J. Liang, and W. Sun, “Penetration resistance of hybrid-fiber-reinforced high-strength concrete under projectile multi-impact,” *Construction and Building Materials*, vol. 202, pp. 341 – 352,

2019. [Online]. Available: <http://www.sciencedirect.com/science/article/pii/S0950061819300388>
- [51] M. Zhang, V. Shim, G. Lu, and C. Chew, “Resistance of high-strength concrete to projectile impact,” *International Journal of Impact Engineering*, vol. 31, no. 7, pp. 825 – 841, 2005. [Online]. Available: <http://www.sciencedirect.com/science/article/pii/S0734743X04000740>
- [52] J. D. Hogan, R. J. Rogers, J. G. Spray, and S. Boonsue, “Dynamic fragmentation of granite for impact energies of 6–28j,” *Engineering Fracture Mechanics*, vol. 79, pp. 103 – 125, 2012. [Online]. Available: <http://www.sciencedirect.com/science/article/pii/S0013794411003857>
- [53] P. B. Sob, A. A. Alugongo, and T. B. Tengen, “Cracks Propagation as a Function of Grain Size Variants on Nanocrystalline Materials’ Yield Stress Produced by Accumulative Roll-Bonding,” *Advances in Materials Physics and Chemistry*, 2017.
- [54] A. Kumano and W. Goldsmith, “Projectile impact on soft, porous rock,” *Rock mechanics*, vol. 15, no. 3, pp. 113–132, 1982. [Online]. Available: <https://doi.org/10.1007/BF01238259>
- [55] L. T. Bbosa, M. Powell, and Cloete, “An investigation of impact breakage of rocks using the split hopkinson pressure bar,” *Journal of the South African Institute of Mining and Metallurgy*, pp. 291 – 296, Apr. 2006. [Online]. Available: https://journals.co.za/content/saimm/106/4/AJA0038223X_3114
- [56] S. Kahraman, N. Bilgin, and C. Feridunoglu, “Dominant rock properties affecting the penetration rate of percussive drills,” *International Journal of Rock Mechanics and Mining Sciences*, vol. 40, no. 5, pp. 711 – 723, 2003. [Online]. Available: <http://www.sciencedirect.com/science/article/pii/S1365160903000637>
- [57] K. Tsusaka and T. Tokiwa, “Influence of fracture orientation on excavatability of soft sedimentary rock using a hydraulic impact hammer: A case study in the horonobe underground research laboratory,” *Tunnelling and Underground Space Technology*, vol. 38, pp. 542 – 549, 2013. [Online]. Available: <http://www.sciencedirect.com/science/article/pii/S0886779813001272>
- [58] A. Afrouz and F. Hassani, “An investigation into rock breaking by direct impact,” *Mining Science and Technology*, vol. 4, no. 2, pp. 167 – 176, 1987. [Online]. Available: <http://www.sciencedirect.com/science/article/pii/S0167903187902799>
- [59] F. Ubertini, C. Song, D. J. Kim, J. Chung, K. W. Lee, S. S. Kweon, and Y. K. Kang, “Estimation of impact loads in a hydraulic breaker by transfer path analysis,” *Shock and Vibration*, vol. 2017, p. 8564381, 2017. [Online]. Available: <https://doi.org/10.1155/2017/8564381>

- [60] C. Paraskevopoulou, M. Perras, M. Diederichs, F. Amann, S. Löw, T. Lam, and M. Jensen, “The three stages of stress relaxation - observations for the time-dependent behaviour of brittle rocks based on laboratory testing,” *Engineering Geology*, vol. 216, pp. 56 – 75, Jan. 2017. [Online]. Available: <https://www.sciencedirect.com/science/article/abs/pii/S0013795216306573?via=ihub>
- [61] J. M. Atienza and M. Elices, “Role of Residual Stresses in Stress Relaxation of Prestressed Concrete Wires,” *Journal of Materials in Civil Engineering*, vol. 19, Aug. 2007. [Online]. Available: [https://ascelibrary-org.libproxy.aalto.fi/doi/abs/10.1061/\(ASCE\)0899-1561\(2007\)19:8\(703\)](https://ascelibrary-org.libproxy.aalto.fi/doi/abs/10.1061/(ASCE)0899-1561(2007)19:8(703))
- [62] L. Hacini, N. Van Lê, and P. Bocher, “Effect of impact energy on residual stresses induced by hammer peening of 304l plates,” *Journal of Materials Processing Technology*, vol. 208, no. 1, pp. 542 – 548, 2008. [Online]. Available: <http://www.sciencedirect.com/science/article/pii/S0924013608000770>
- [63] M. Williams. (2015, Feb.) What is Hooke’s Law? PhysOrg. [Online]. Available: <https://phys.org/news/2015-02-law.html>
- [64] R. Lakes, *Viscoelastic Materials*. Cambridge University Press, 2009. [Online]. Available: https://books.google.fi/books?hl=en&lr=&id=BH6f2hWWBkAC&oi=fnd&pg=PR1&dq=viscoelasticmaterials&ots=ELL11CTeNt&sig=-Kpv3VmtfYCZUY5AEKixDrgzXc&redir_esc=y#v=onepage&q=viscoelasticmaterials&f=false
- [65] Types of fracture. blogspot. Learning Geology. [Online]. Available: <http://geologylearn.blogspot.com/2015/08/types-of-fractures.html>
- [66] B. K. Atkinson. Elsevier, 1987. [Online]. Available: <https://app.knovel.com/hotlink/toc/id:kpFMR00001/fracture-mechanics-rock/fracture-mechanics-rock>
- [67] J. Byous, “Hertzian Fractures and Related Terms - A Glossary,” *A.T. Dows Research*, 2013. [Online]. Available: http://www.dowresearch.org/Hertzian_Cone_Glossary.pdf
- [68] R. A. Schultz, “Cracks and anticracks,” *Geologic Fracture Mechanics*, pp. 143 – 169, Aug. 2019. [Online]. Available: <https://www.cambridge.org/core/books/geologic-fracture-mechanics/cracks-and-anticracks/5F29B9D2961D880EB2B80AAD7E6701CE>
- [69] NI. (2020, Jul.) Measuring Strain with Strain Gages. National Instruments. [Online]. Available: <https://www.ni.com/fi-fi/innovations/white-papers/07/measuring-strain-with-strain-gages.html>
- [70] AManWithNoPlan. (2020, Nov.) Fatigue (material). Wikiwand. [Online]. Available: [https://www.wikiwand.com/en/Fatigue_\(material\)](https://www.wikiwand.com/en/Fatigue_(material))

- [71] P. Strzelecki, J. Sempruch, and T. Tomaszewski, “Analysis of selected mathematical models of high-cycle s-n characteristics,” *Technical Sciences*, vol. 20, 04 2017.
- [72] T. Rausch, P. Beiss, C. Broeckmann, S. Lindlohr, and R. Weber, “Application of quantitative image analysis of graphite structures for the fatigue strength estimation of cast iron materials,” *Procedia Engineering*, vol. 2, pp. 1283–1290, 04 2010.
- [73] (2020, Oct.) Steel Grade - 42CrMo4. Ovako. [Online]. Available: <https://steelnavigator.ovako.com/steel-grades/42crmo4/>

Appendix

Rock Mechanics Testing Results

The results of the vibration measurements as well as the state of the tested samples after the test can be seen for each of the 30 tests in the Appendix. In this section, a summary of the results will be shown.

CN0.9

Laser in y-direction: Figure 59 below shows tool vibrations in the y-direction.

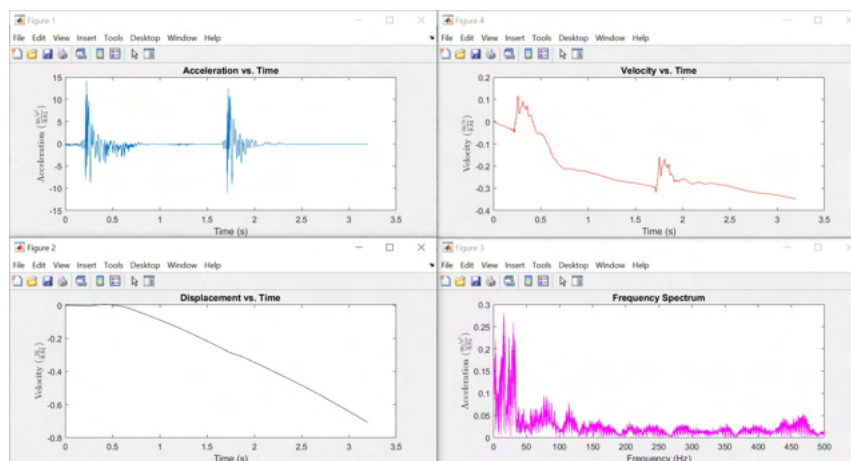


Figure 59: Results from the Laser Measurements on the Tool.

Acceleration Sensor Material in z-direction: Figure 60 below shows material vibrations in the z-direction.

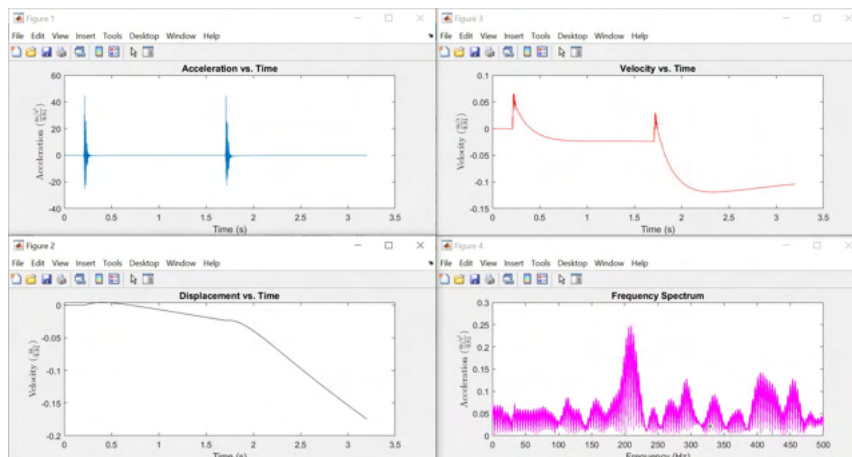


Figure 60: Results of acceleration sensor on material.

Acceleration Sensor Material in x-direction: Figure 61 below shows material vibrations in the x-direction.

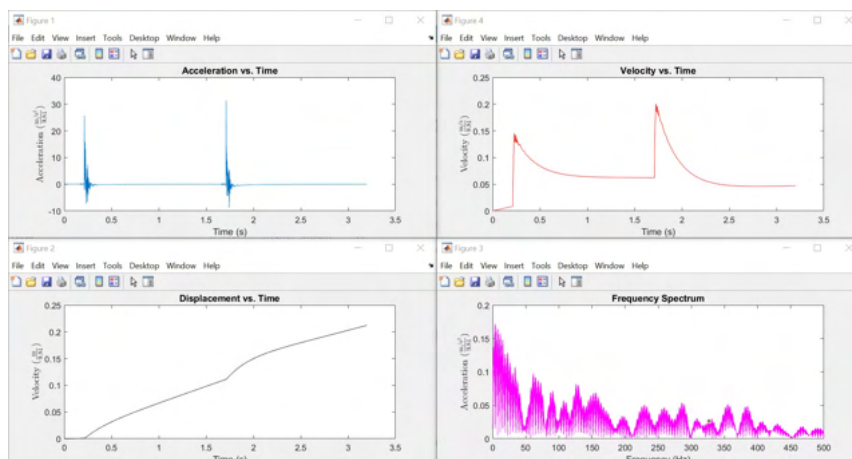


Figure 61: Results of acceleration sensor on material.

Acceleration Sensor Housing in z-direction: Figure bla below shows vibrations in the housing in the z-direction.

Sample Results: Figure 62 shows the resulting sample after it had broken.



Figure 62: The area around the impact zone.

For CN0.9, the following things are noticeable about the sample:

- There was cracking at the bottom of the block but little around the impact zone.
- The sample took approximately 20 seconds to break when hitting relatively close to the edge.

CN5

Laser in y-direction: Figure 63 below shows tool vibrations in the y-direction.

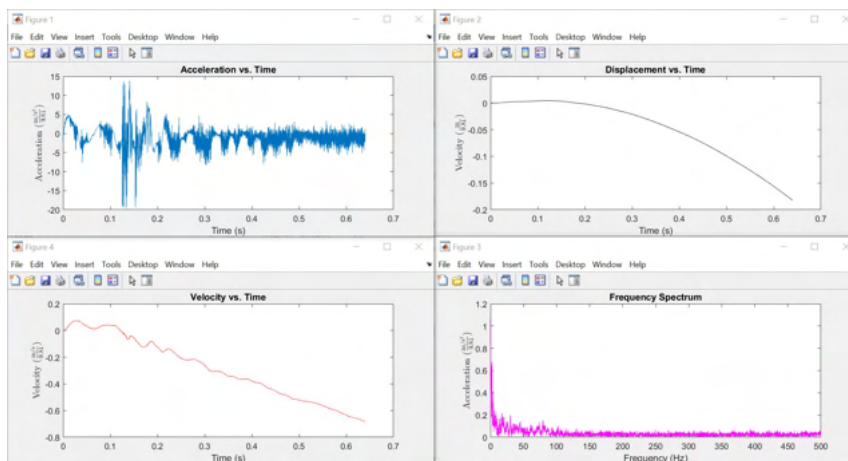


Figure 63: Results from the Laser Measurements on the Tool.

Acceleration Sensor Material in z-direction: Figure 64 below shows material vibrations in the z-direction.

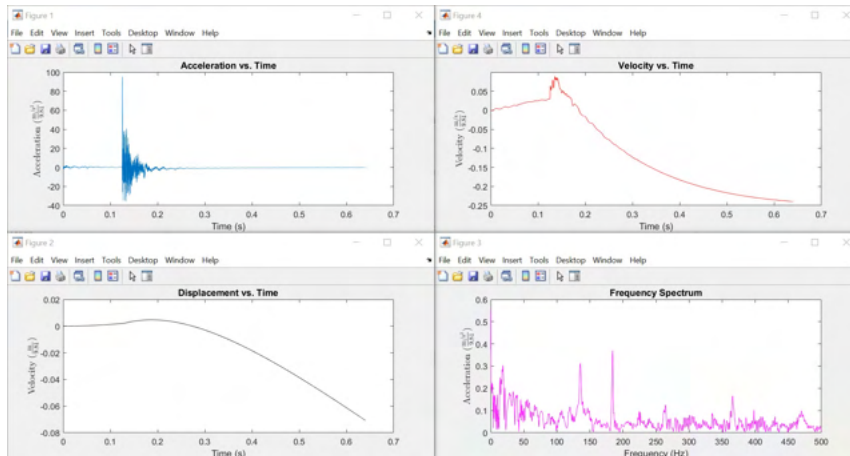


Figure 64: Results of acceleration sensor on material.

Acceleration Sensor Material in x-direction: Figure 65 below shows material vibrations in the x-direction.

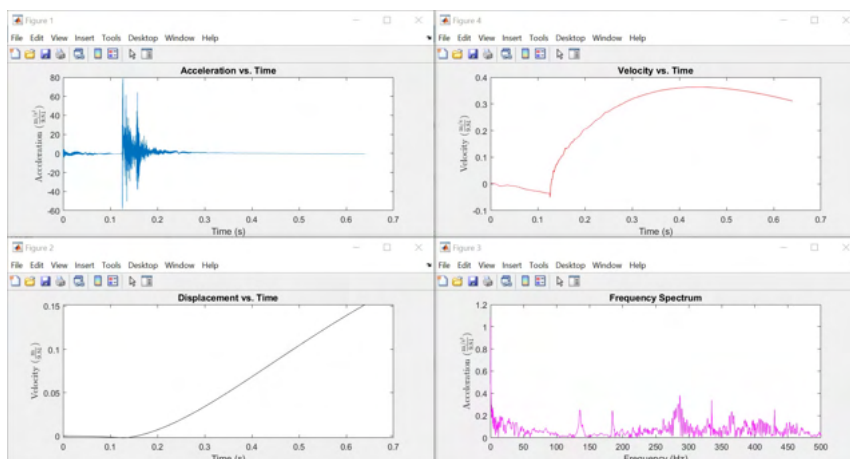


Figure 65: Results of acceleration sensor on material.

Sample Results: Figure 66 shows the resulting sample after it had broken.



Figure 66: The area around the impact zone.

For CN5, the following things are noticeable about the sample:

- There was cracking at the bottom of the block but little around the impact zone.
- The sample took approximately 8 seconds to break when hitting close to the edge

CN8

Laser in y-direction: Figure 67 below shows tool vibrations in the y-direction.

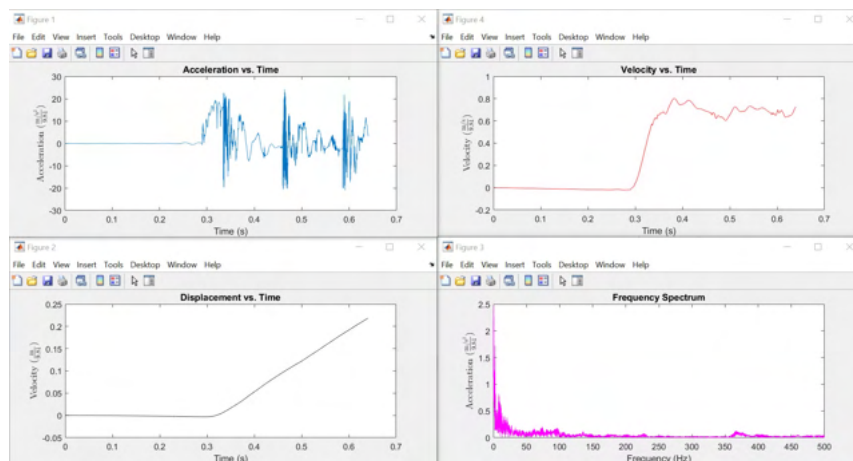


Figure 67: Results from the Laser Measurements on the Tool.

Acceleration Sensor Material in z-direction: Figure 68 below shows material vibrations in the z-direction.

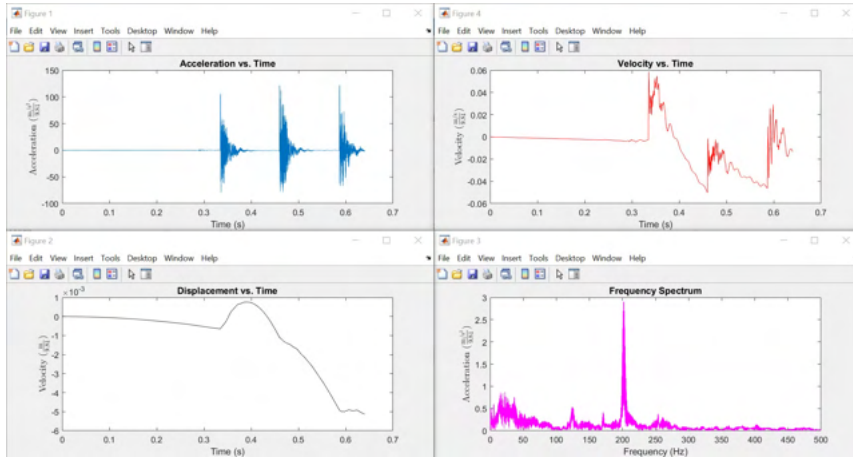


Figure 68: Results of acceleration sensor on material.

Acceleration Sensor Material in x-direction: Figure 69 below shows material vibrations in the x-direction.

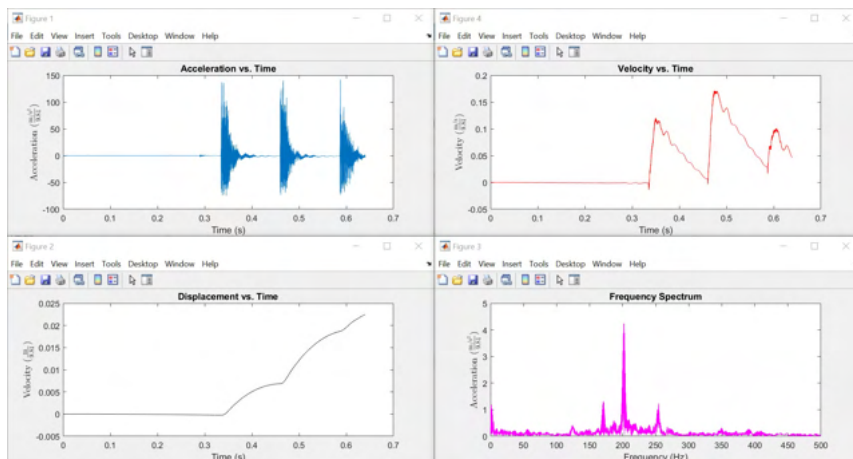


Figure 69: Results of acceleration sensor on material.

Sample Results: Figure 70 shows the resulting sample after it had broken.



Figure 70: The area around the impact zone.

For CN8, the following things are noticeable about the sample:

- There was cracking at the bottom of the block and at the side and some close to the impact zone parallel to the top surface.
- The sample took about 5 seconds to break when hitting near the side.

CN14

Laser in y-direction: Figure 71 below shows tool vibrations in the y-direction.

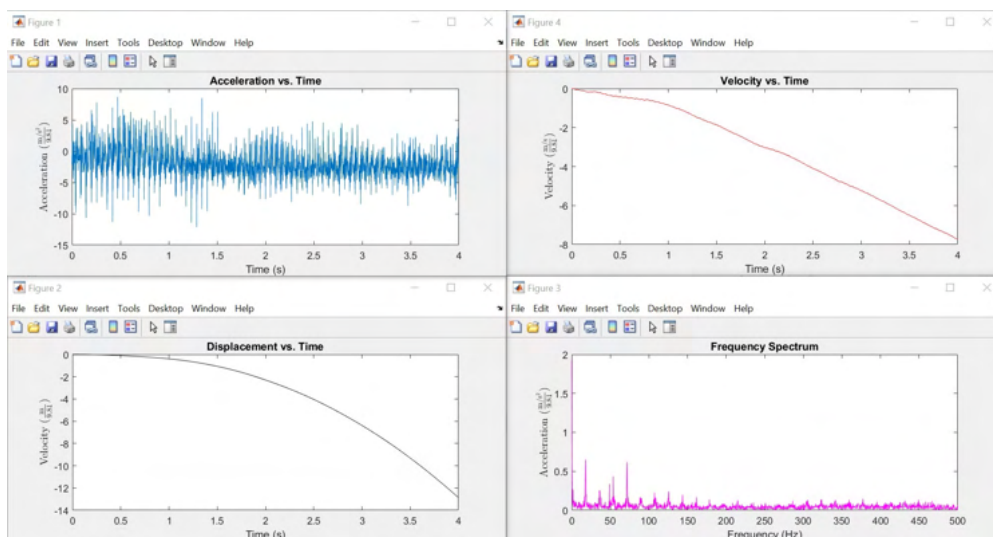


Figure 71: Results from the Laser Measurements on the Tool.

Acceleration Sensor Material in z-direction: Figure 72 below shows material vibrations in the z-direction.

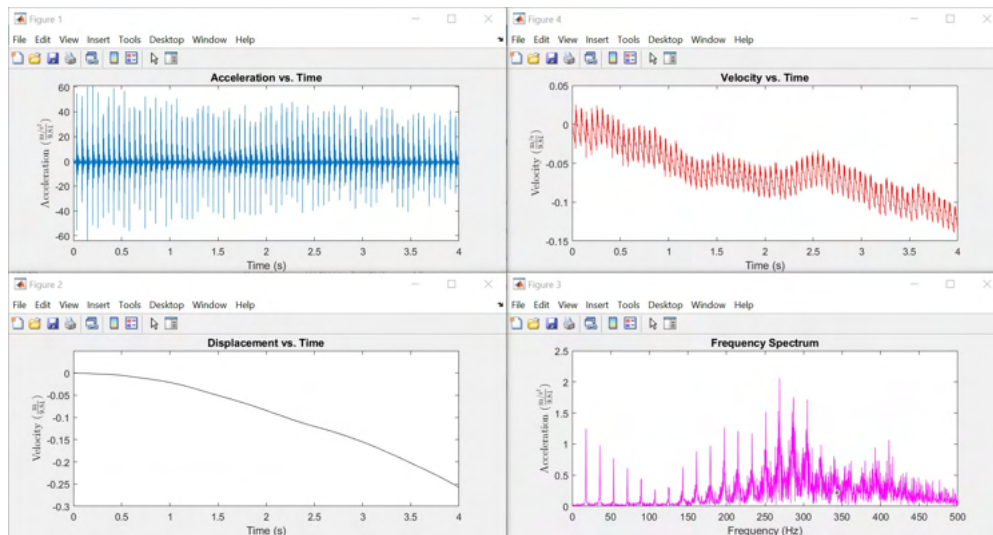


Figure 72: Results of acceleration sensor on material.

Acceleration Sensor Material in x-direction: Figure 73 below shows material vibrations in the x-direction.

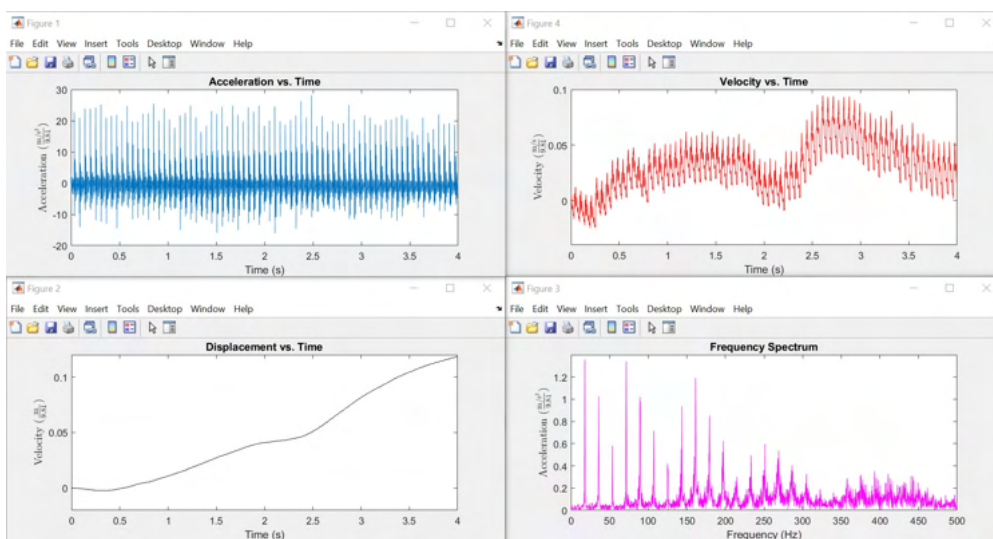


Figure 73: Results of acceleration sensor on material.

Sample Results: Figure 74 shows the resulting sample after it had broken.

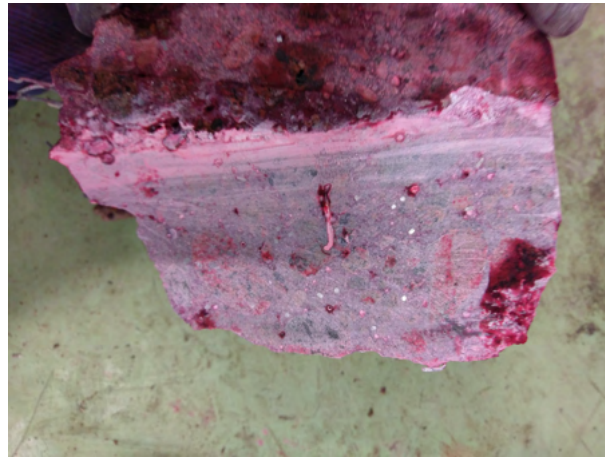


Figure 74: The area around the impact zone.

For CN14, the following things are noticeable about the sample:

- There was cracking at the bottom of the block but little around the impact zone.
- The sample took about 20 seconds to break when hitting near the edge.

CN18

Laser in y-direction: Figure 75 below shows tool vibrations in the y-direction.

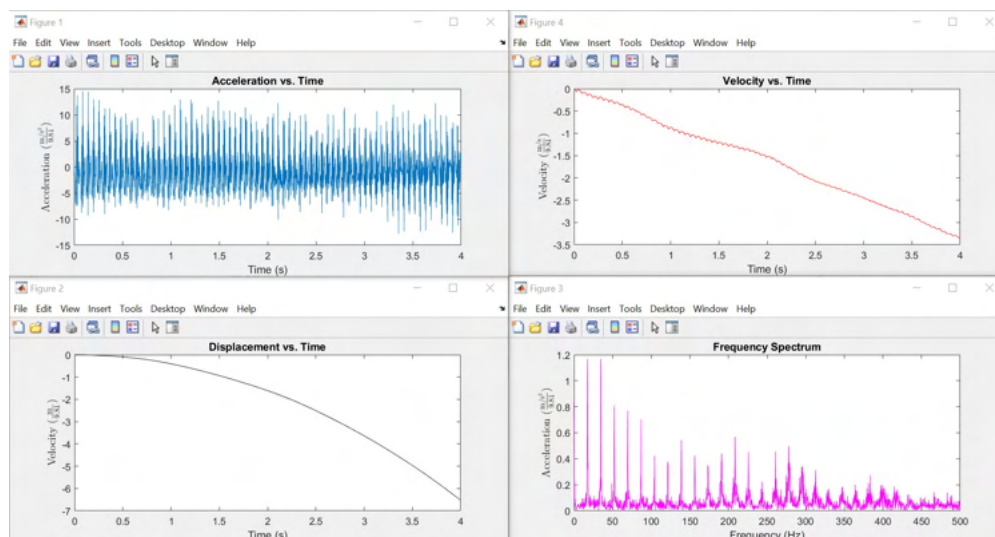


Figure 75: Results from the Laser Measurements on the Tool.

Acceleration Sensor Material in z-direction: Figure 76 below shows material vibrations in the z-direction.

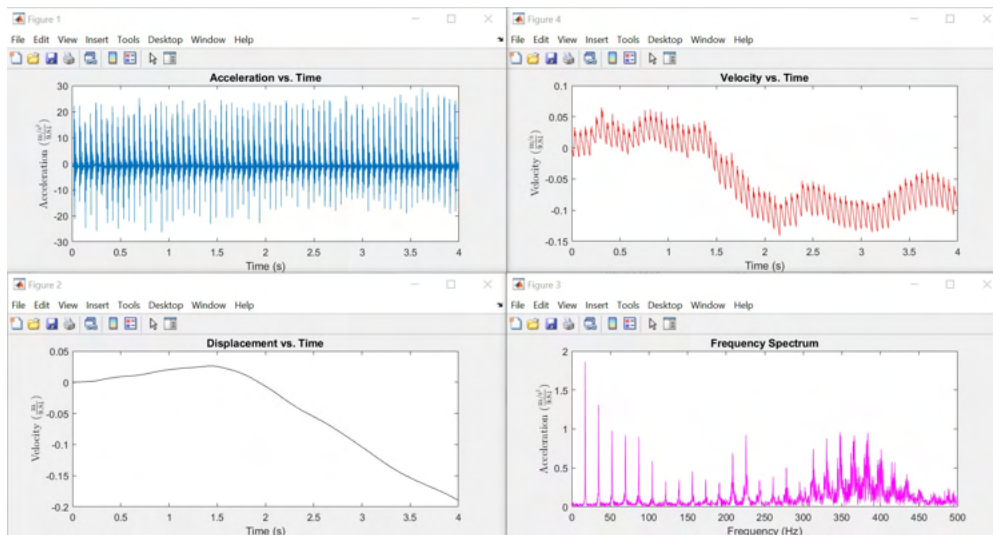


Figure 76: Results of acceleration sensor on material.

Acceleration Sensor Material in x-direction: Figure 77 below shows material vibrations in the x-direction.

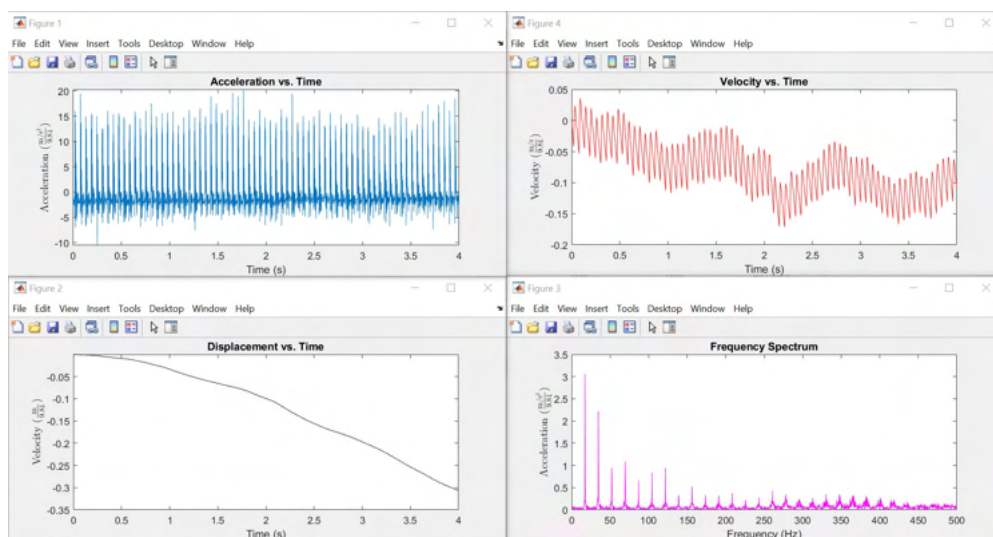


Figure 77: Results of acceleration sensor on material.

Sample Results: Figure 78 shows the resulting sample after it had broken.



Figure 78: The area around the impact zone.

For CN18, the following things are noticeable about the sample:

- There was cracking at the bottom of the block but little around the impact zone.
- The sample did not break within 45 seconds of hitting while hitting in the middle.
- The sample took about 60 seconds to break when hitting near the side at the same spot.

Therefore, it can be said that with the cone tool on the normal, steel fibre reinforced concrete, the cracking is more prominent at the bottom and sides than at the top around the impact zone.

BN0.9

Laser in y-direction: Figure 79 below shows tool vibrations in the y-direction.

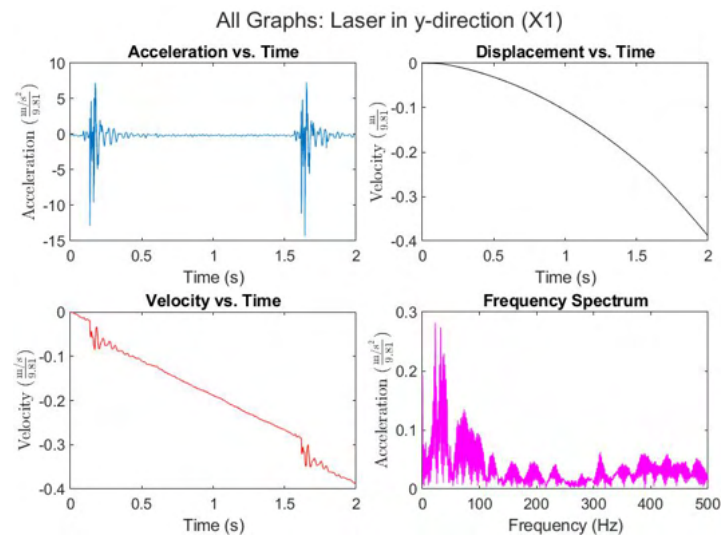


Figure 79: Results from the Laser Measurements on the Tool.

Acceleration Sensor Material in z-direction: Figure 80 below shows material vibrations in the z-direction.

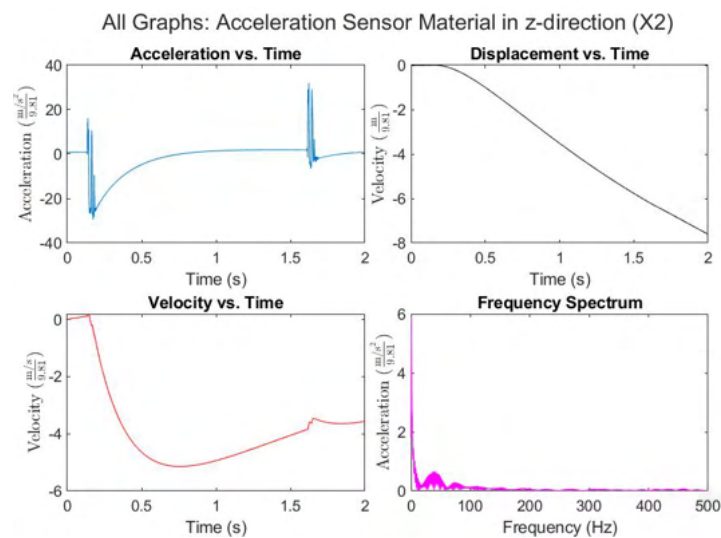


Figure 80: Results of acceleration sensor on material.

Acceleration Sensor Material in x-direction: Figure 81 below shows material vibrations in the x-direction.

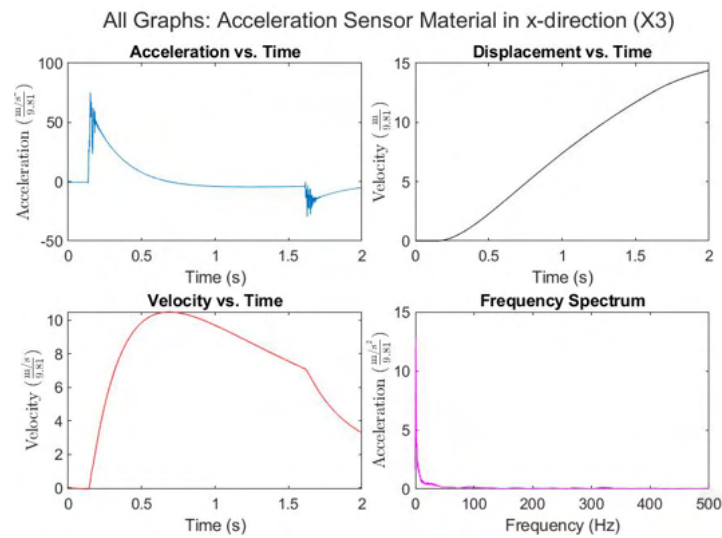


Figure 81: Results of acceleration sensor on material.

Acceleration Sensor Housing in z-direction: Figure 82 below shows housing vibrations in the z-direction.

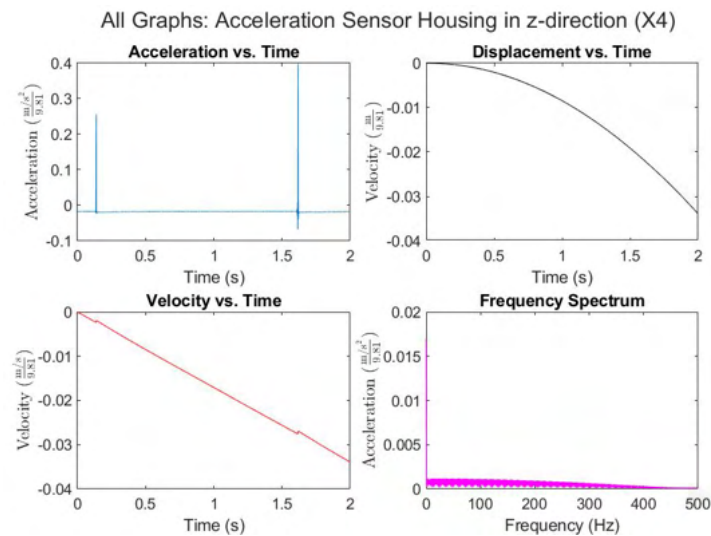


Figure 82: Results of acceleration sensor on material.

Sample Results: Figure 83 shows the resulting sample after it had broken.



Figure 83: The area around the impact zone.

For BN0.9, the following things are noticeable about the sample:

- There was cracking around the impact but only one large crack from each side to the nearest free surface. The cracks were larger at the bottom than at the top.
- The cracking took extremely long to start, with 300 seconds of hitting required to have cracking and even then fracturing not occurring when hitting close to the side of the block.

BN5

Laser in y-direction: Figure 84 below shows tool vibrations in the y-direction.

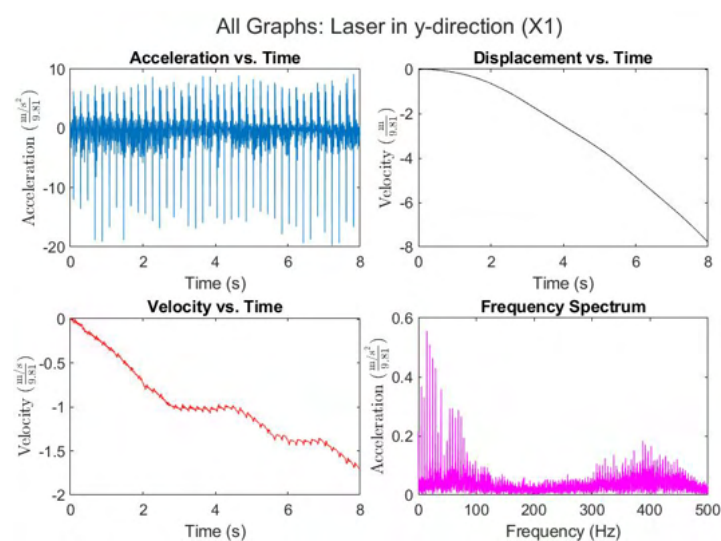


Figure 84: Results from the Laser Measurements on the Tool.

Acceleration Sensor Material in z-direction: Figure 85 below shows material vibrations in the z-direction.

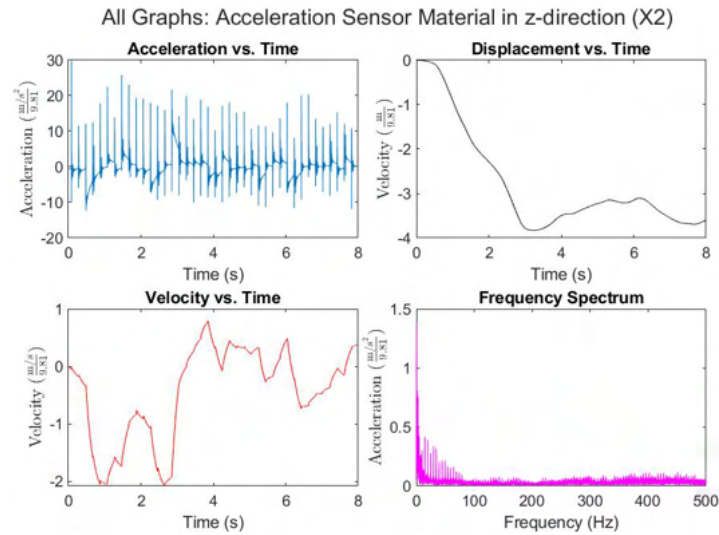


Figure 85: Results of acceleration sensor on material.

Acceleration Sensor Material in x-direction: Figure 86 below shows material vibrations in the x-direction.

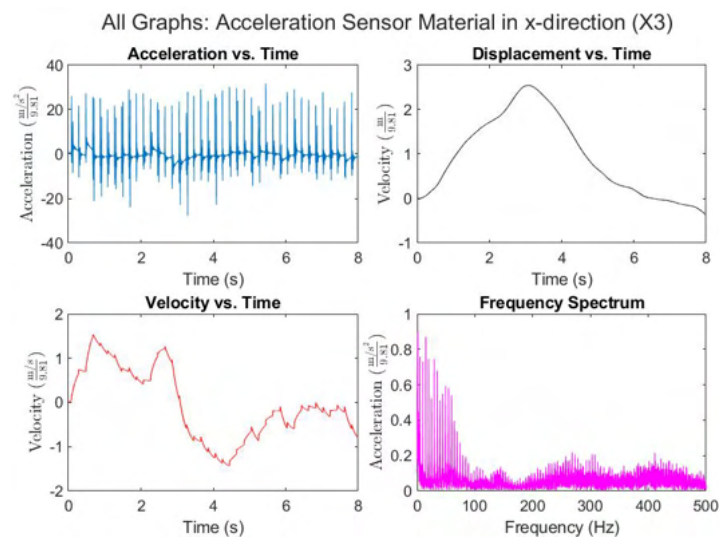


Figure 86: Results of acceleration sensor on material.

Acceleration Sensor Housing in z-direction: Figure 87 below shows housing vibrations in the z-direction.

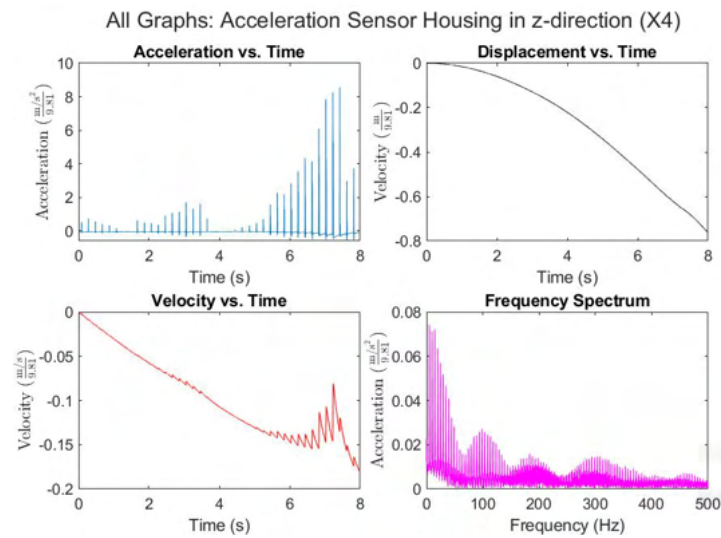


Figure 87: Results of acceleration sensor on material.

Sample Results: Figure 88 shows the resulting sample after it had broken.

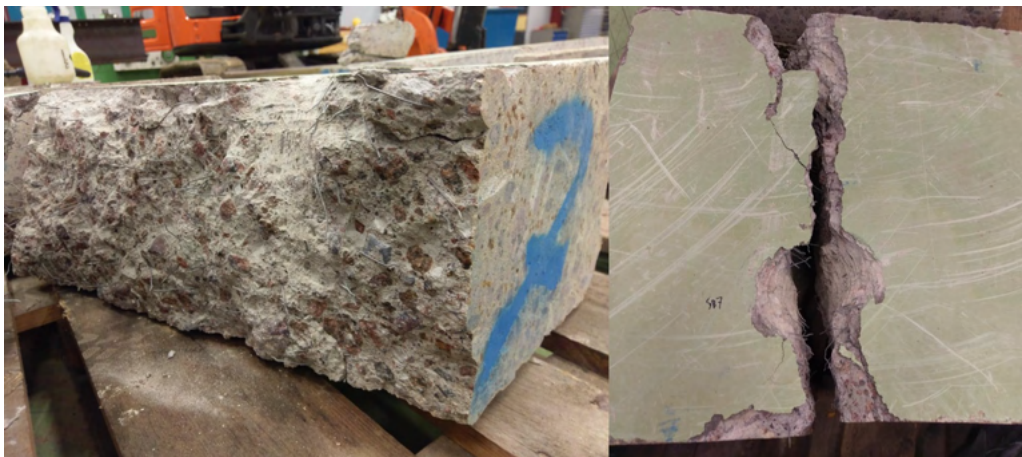


Figure 88: The area around the impact zone.

For BN5, the following things are noticeable about the sample:

- There was more small cracking and the area around the impact zone resembled rubble more, with lots of little pieces.
- The sample took around 30 seconds to break in two.

BN8

Laser in y-direction: Figure 84 below shows tool vibrations in the y-direction.

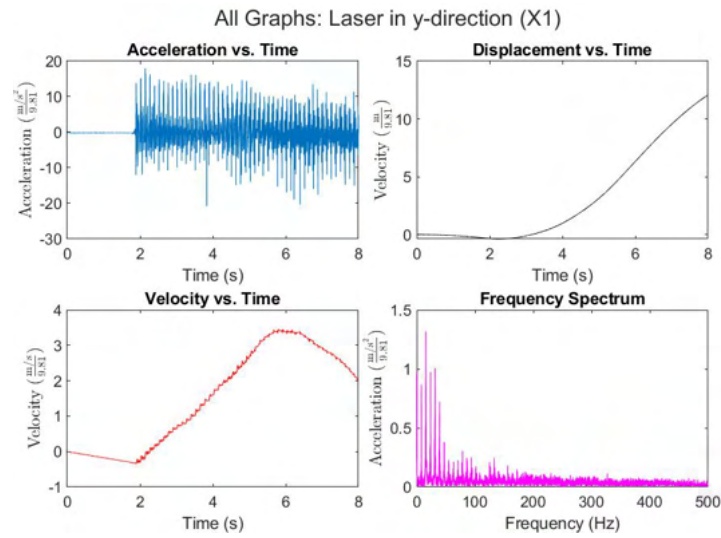


Figure 89: Results from the Laser Measurements on the Tool.

Acceleration Sensor Material in z-direction: Figure 90 below shows material vibrations in the z-direction.

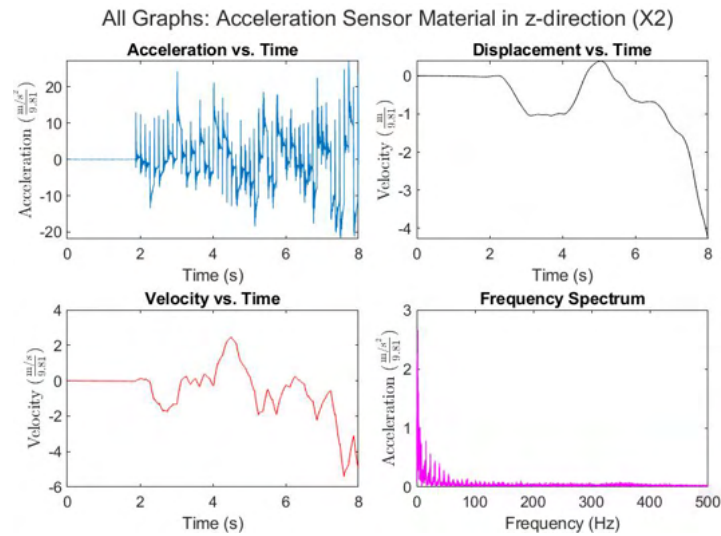


Figure 90: Results of acceleration sensor on material.

Acceleration Sensor Material in x-direction: Figure 91 below shows material vibrations in the x-direction.

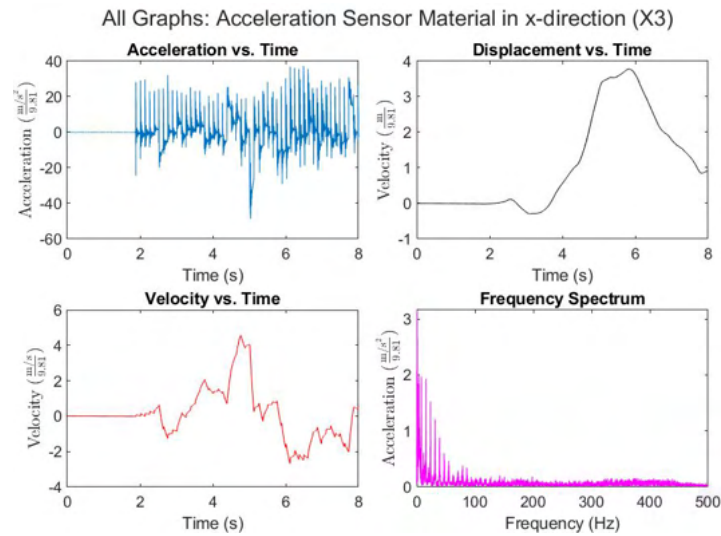


Figure 91: Results of acceleration sensor on material.

Acceleration Sensor Housing in z-direction: Figure 92 below shows housing vibrations in the z-direction.

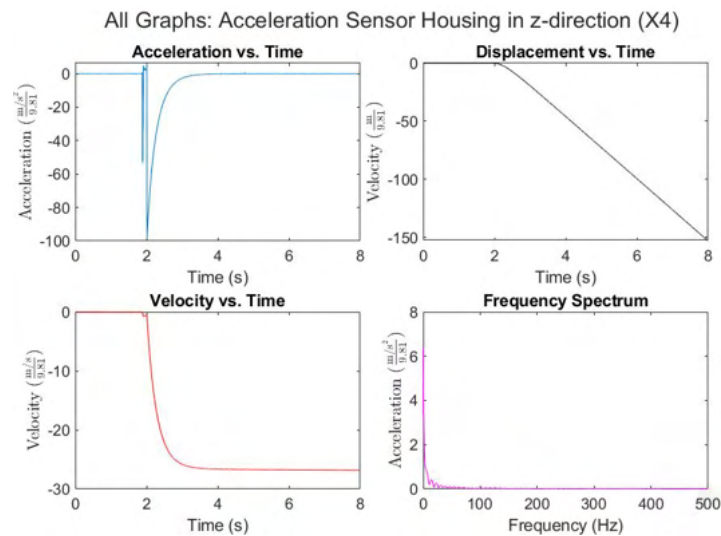


Figure 92: Results of acceleration sensor on material.

Sample Results: Figure 93 shows the resulting sample after it had broken.

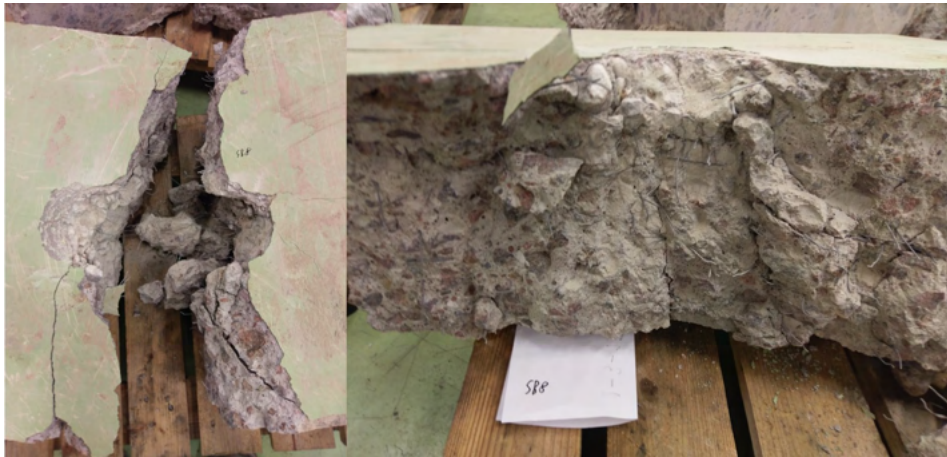


Figure 93: The area around the impact zone.

For BN8, the following things are noticeable about the sample:

- The sample broke in a messy way, with lots of cracking around the impact zone and rubble being generated. Also some loose pieces of concrete were still on the block around the impact zone.
- The sample took around 51 seconds to break when being hit near the middle of the block.

BN14

Laser in y-direction: Figure 94 below shows tool vibrations in the y-direction.

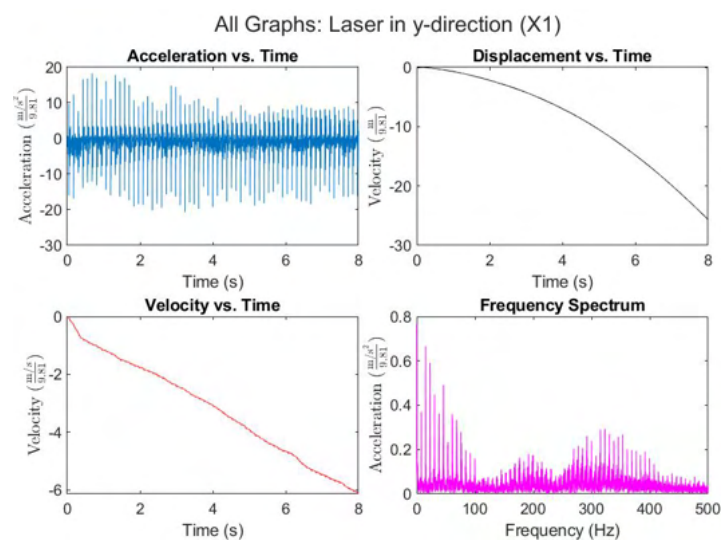


Figure 94: Results from the Laser Measurements on the Tool.

Acceleration Sensor Material in z-direction: Figure 95 below shows material vibrations in the z-direction.

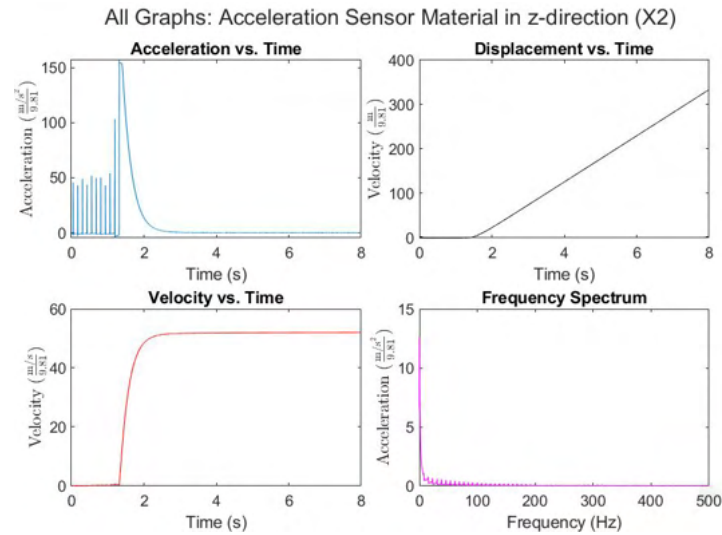


Figure 95: Results of acceleration sensor on material.

Acceleration Sensor Material in x-direction: Figure 96 below shows material vibrations in the x-direction.

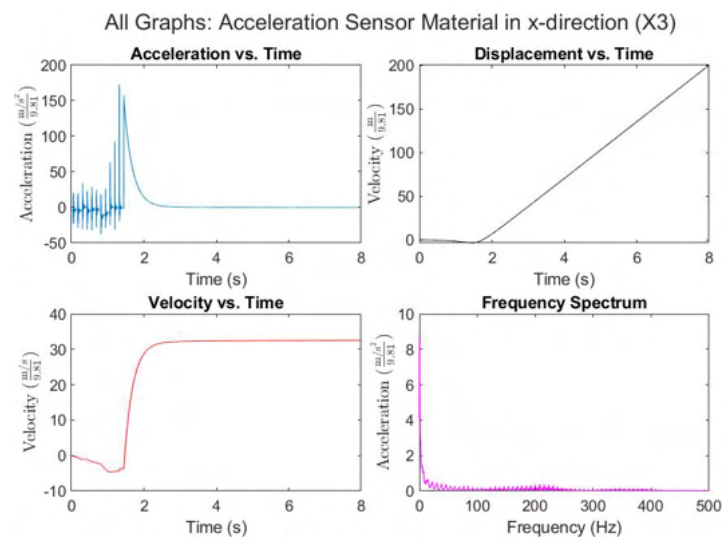


Figure 96: Results of acceleration sensor on material.

Acceleration Sensor Housing in z-direction: Figure 97 below shows housing vibrations in the z-direction.

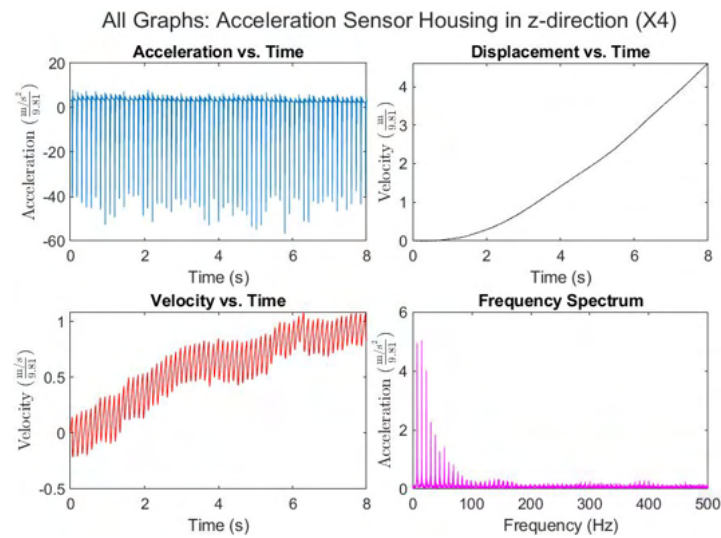


Figure 97: Results of acceleration sensor on material.

Sample Results: Figure 98 shows the resulting sample after it had broken.

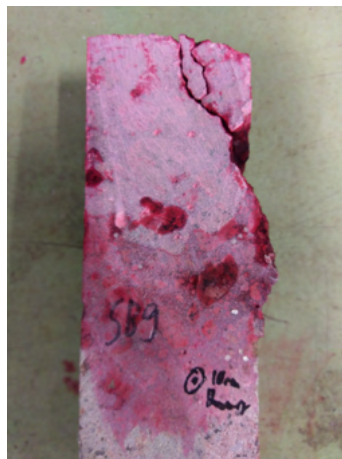


Figure 98: The area around the impact zone.

For BN14, the following things are noticeable about the sample:

- There was some cracking near the impact zone, but only a couple of cracks.
- The sample took about 120 seconds to break.

BN18

Laser in y-direction: Figure 99 below shows tool vibrations in the y-direction.

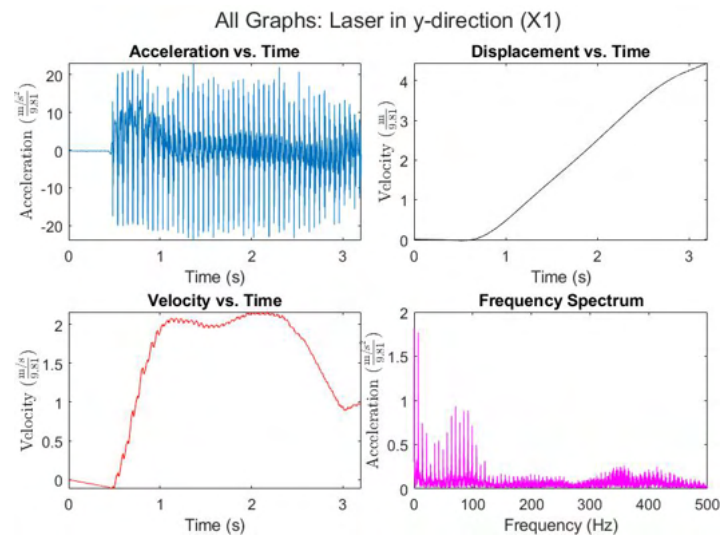


Figure 99: Results from the Laser Measurements on the Tool.

Acceleration Sensor Material in z-direction: Figure 100 below shows material vibrations in the z-direction.

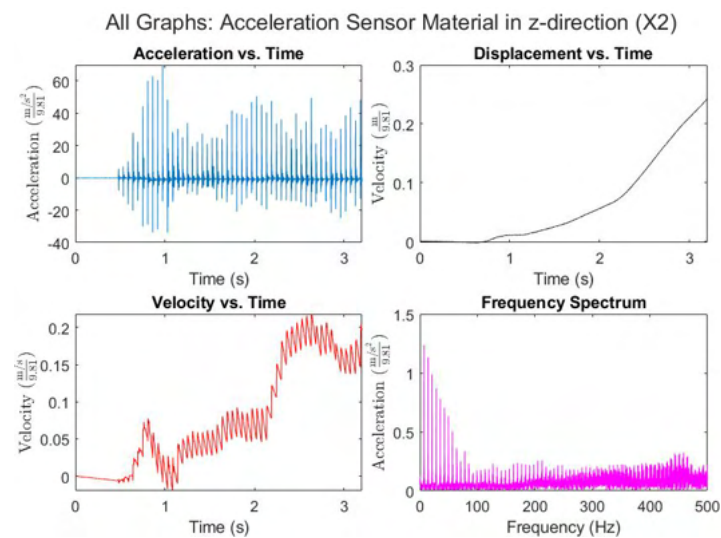


Figure 100: Results of acceleration sensor on material.

Acceleration Sensor Material in x-direction: Figure 101 below shows material vibrations in the x-direction.

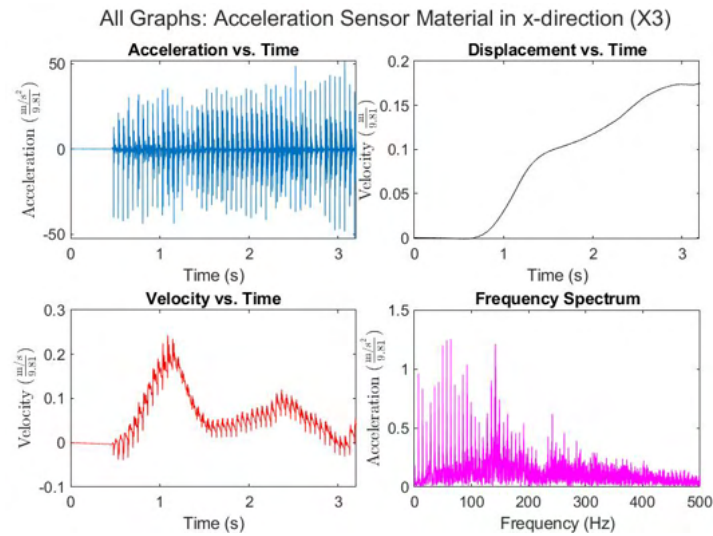


Figure 101: Results of acceleration sensor on material.

Acceleration Sensor Housing in z-direction: Figure 102 below shows housing vibrations in the z-direction.

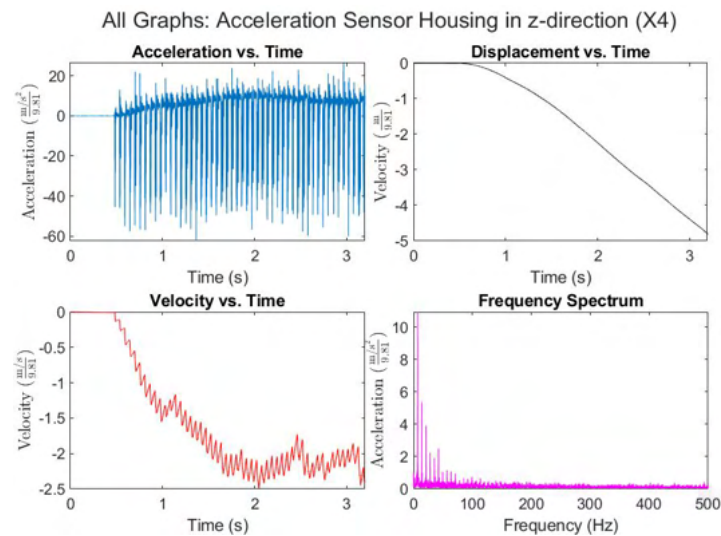


Figure 102: Results of acceleration sensor on material.

Sample Results: Figure 103 shows the resulting sample after it had broken.

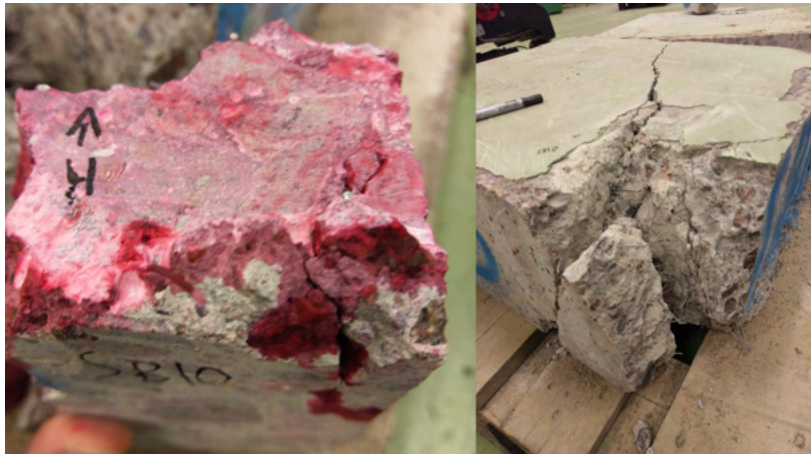


Figure 103: The area around the impact zone.

For BN18, the following things are noticeable about the sample:

- There was more cracking at the bottom of the block than at the top, immediately near the impact zone. The block disintegrated rather than cracking cleanly, with again a lot of small pieces being generated.
- The block took about 120 seconds to break when it was hit near the edge.

Therefore, it can be said that when breaking normal, steel fibre reinforced concrete with the blunt tool, the cracking is more prominent at the bottom than at the top of the block. However, cracking in general disintegrates the block rather than penetrates it, with lots of little, rubble like pieces being generated and the block overall being weakened and cracked more than with the cone tool.

WN0.9

Sample Results: Figure 104 shows the resulting sample after it had broken.



Figure 104: The area around the impact zone.

For WN5, the following things are noticeable about the sample:

- There was some slight cracking at the impact zone, apart from that there was little fragmentation and the big piece broke off cleanly from the small piece. The only fragmentation occurred at the bottom of the block.
- The sample took about 43 seconds to break when hitting near the side of the block.

WN5

Laser in y-direction: Figure 105 below shows tool vibrations in the y-direction.

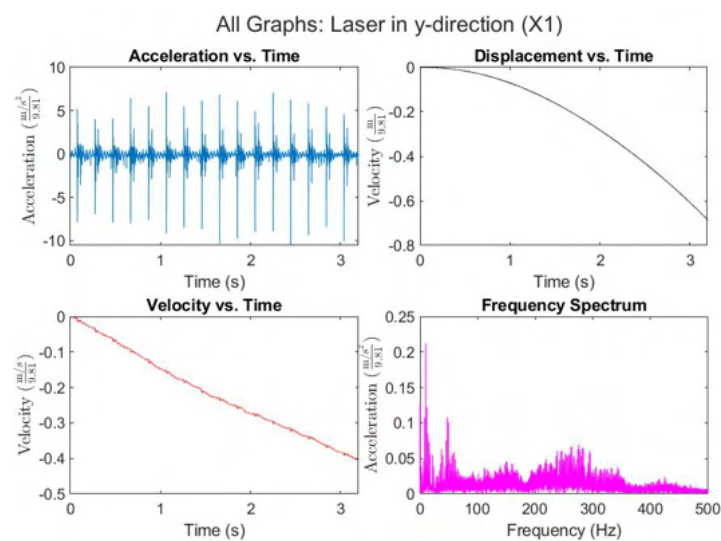


Figure 105: Results from the Laser Measurements on the Tool.

Acceleration Sensor Material in z-direction: Figure 106 below shows material vibrations in the z-direction.

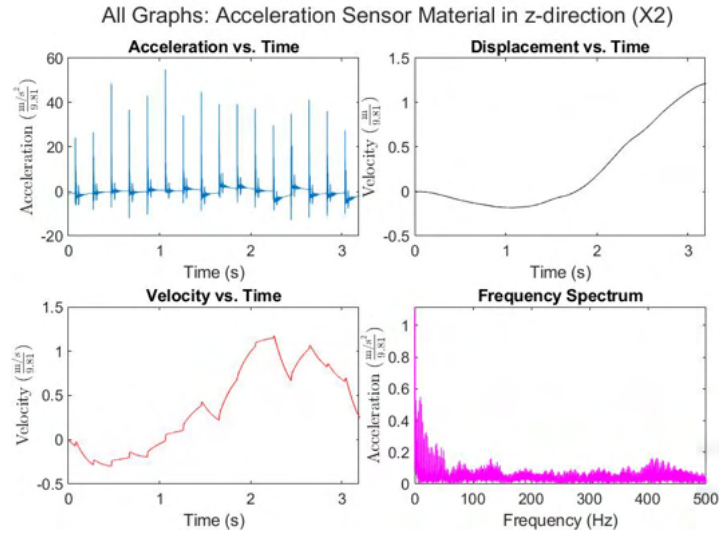


Figure 106: Results of acceleration sensor on material.

Acceleration Sensor Material in x-direction: Figure 107 below shows material vibrations in the x-direction.

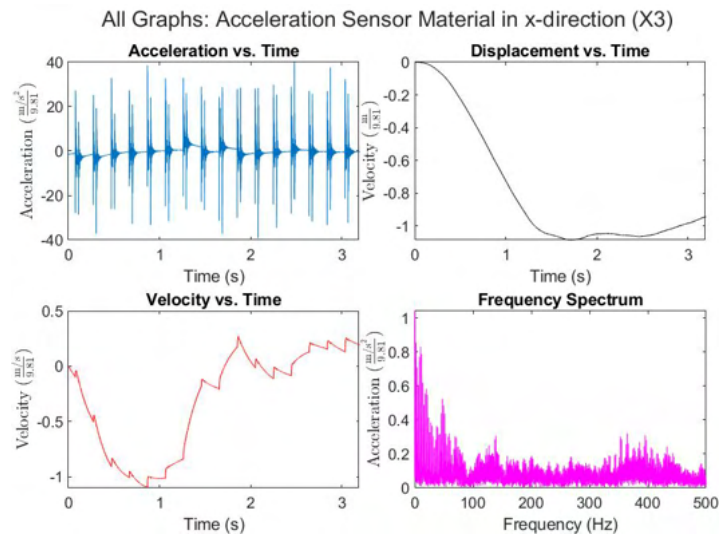


Figure 107: Results of acceleration sensor on material.

Acceleration Sensor Housing in z-direction: Figure 108 below shows housing vibrations in the z-direction.

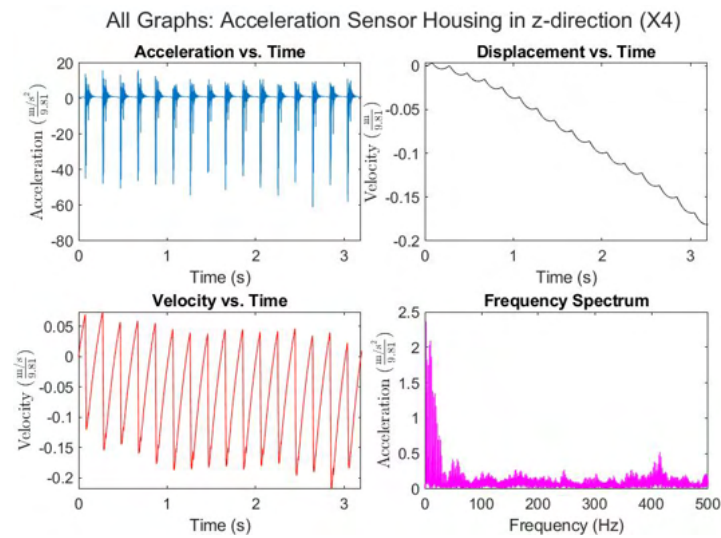


Figure 108: Results of acceleration sensor on material.

Sample Results: Figure 109 shows the resulting sample after it had broken.



Figure 109: The area around the impact zone.

For WN5, the following things are noticeable about the sample:

- There was little cracking at the impact zone and the piece broke off relatively cleanly, fragmenting into several pieces near the bottom.
- The sample took about 17 seconds to break when hitting from the side.

WN8

Laser in y-direction: Figure 110 below shows tool vibrations in the y-direction.

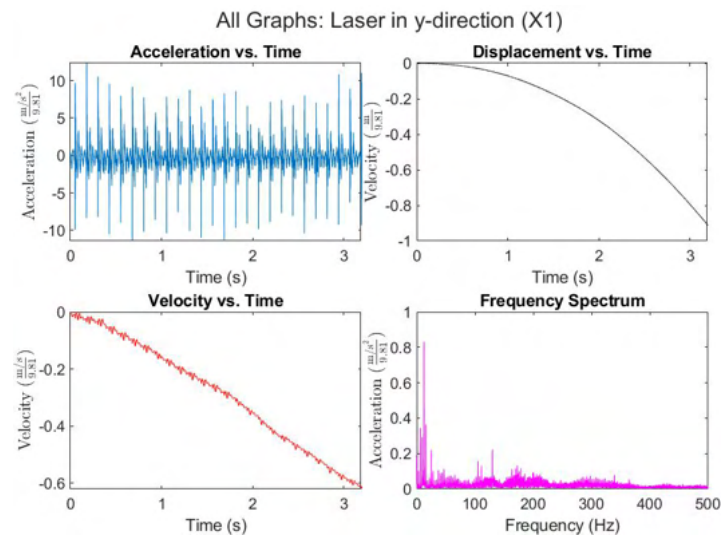


Figure 110: Results from the Laser Measurements on the Tool.

Acceleration Sensor Material in z-direction: Figure 111 below shows material vibrations in the z-direction.

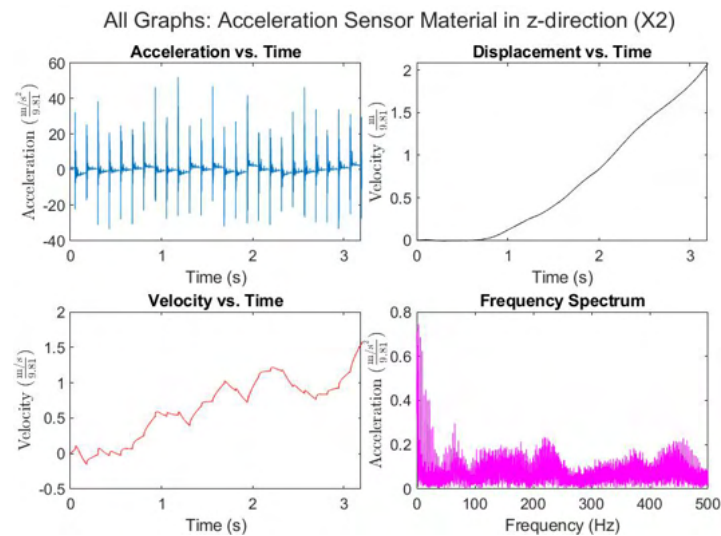


Figure 111: Results of acceleration sensor on material.

Acceleration Sensor Material in x-direction: Figure 112 below shows material vibrations in the x-direction.

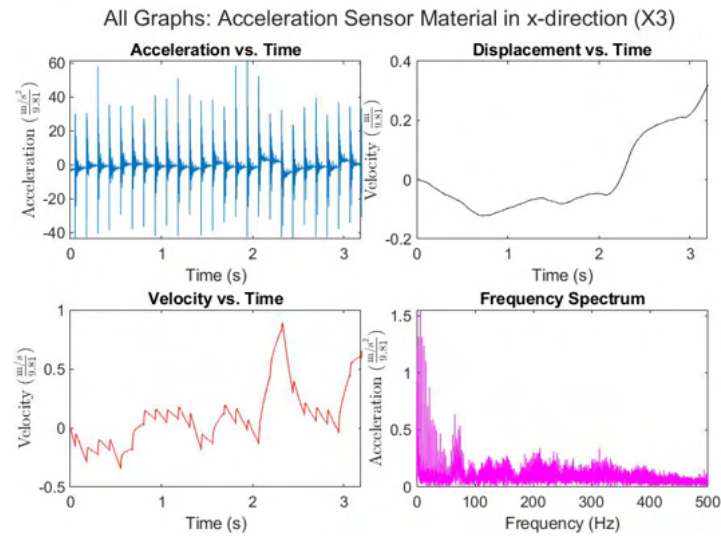


Figure 112: Results of acceleration sensor on material.

Acceleration Sensor Housing in z-direction: Figure 113 below shows housing vibrations in the z-direction.

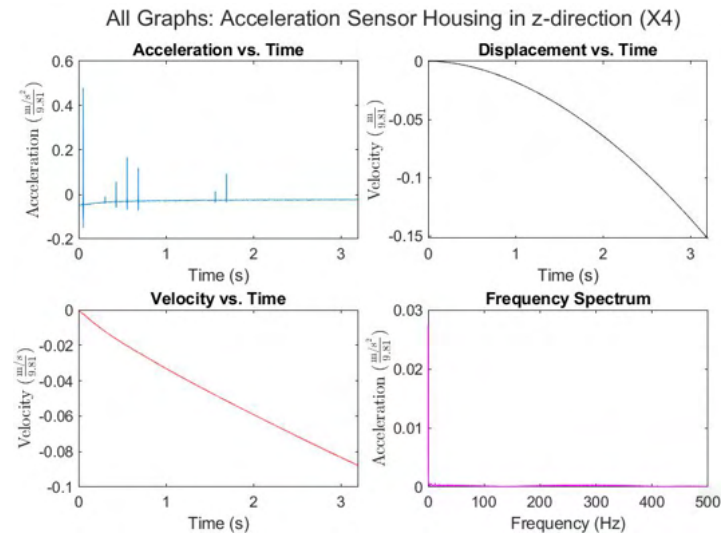


Figure 113: Results of acceleration sensor on material.

Sample Results: Figure 114 shows the resulting sample after it had broken.



Figure 114: The area around the impact zone.

For WN8, the following things are noticeable about the sample:

- There was little cracking around the impact zone but some small fragmentation at the bottom of the block. Apart from that, there was a crack that propagated perpendicular to the wedge to the free surface (left in Figure 114).
- The sample took about 38 seconds to break when hitting was done near the middle of the block.

WN14

Sample Results: Figure 115 shows the resulting sample after it had broken.



Figure 115: The area around the impact zone.

For WN14, the following things are noticeable about the sample:

- There was a little cracking around the impact zone and the block fragmented into several pieces, one main chunk that broke off and a couple of smaller pieces near the bottom.
- The sample took about 5 seconds to break when hammering was done near the side of the block.

WN18

Laser in y-direction: Figure 116 below shows tool vibrations in the y-direction.

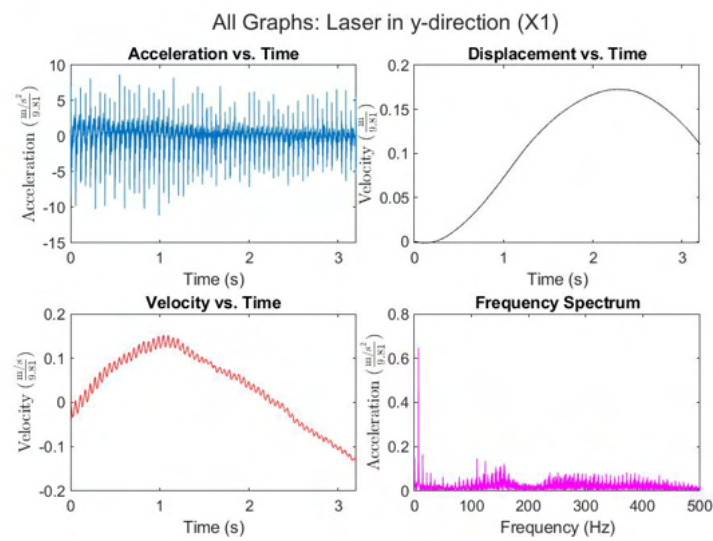


Figure 116: Results from the Laser Measurements on the Tool.

Acceleration Sensor Material in z-direction: Figure 117 below shows material vibrations in the z-direction.

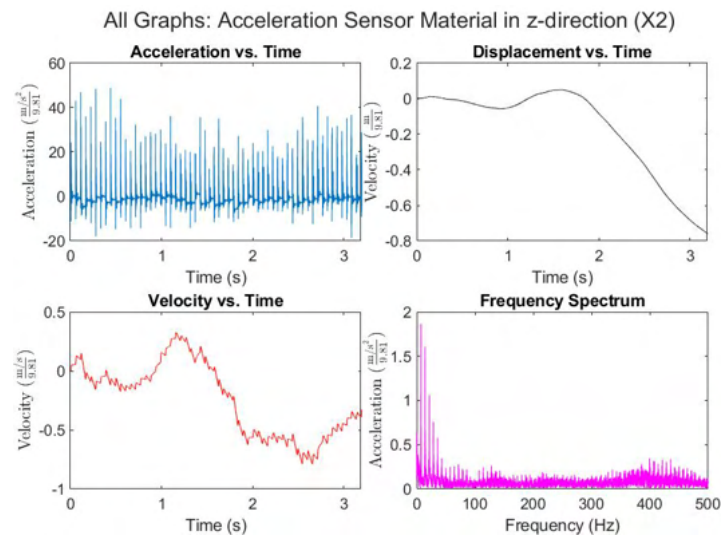


Figure 117: Results of acceleration sensor on material.

Acceleration Sensor Material in x-direction: Figure 118 below shows material vibrations in the x-direction.

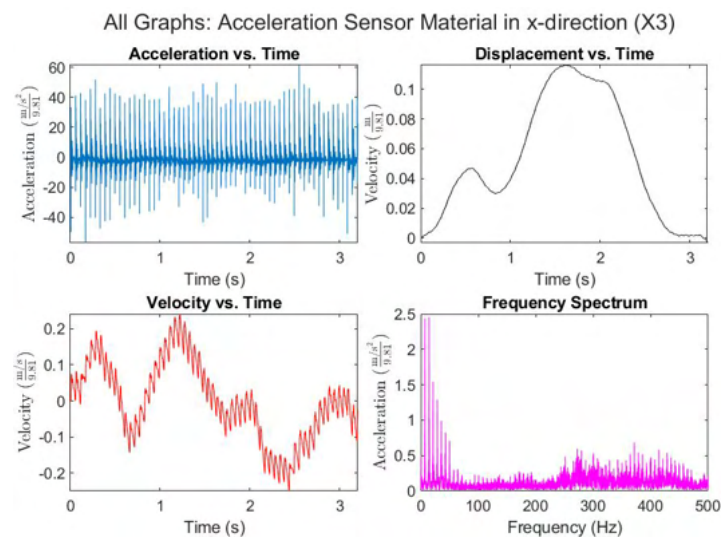


Figure 118: Results of acceleration sensor on material.

Acceleration Sensor Housing in z-direction: Figure 119 below shows housing vibrations in the z-direction.

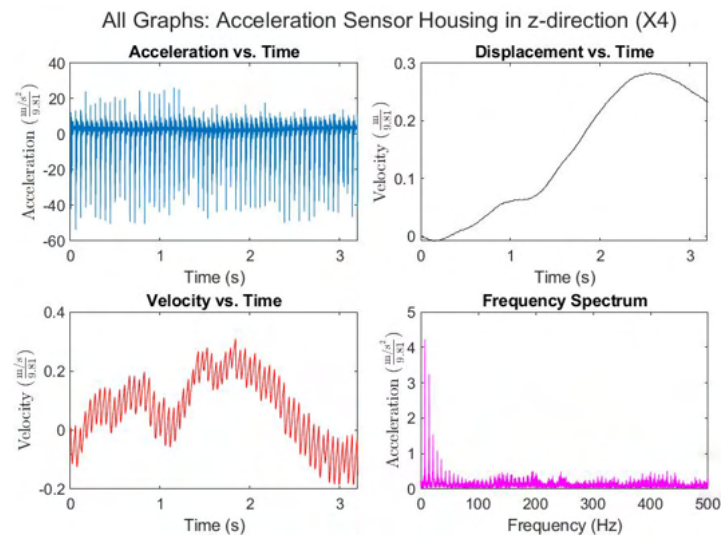


Figure 119: Results of acceleration sensor on material.

Sample Results: Figure 120 shows the resulting sample after it had broken.



Figure 120: The area around the impact zone.

For WN18, the following things are noticeable about the sample:

- There was a little cracking around the impact zone and the block fragmented into 3 pieces, one of which did not completely break off from the block.
- The sample took about 17 seconds to break when hammering was done near the side of the block

Therefore, when breaking normal concrete with the wedge tool, it can be said that the piece fragments little and tends to break off in a more “clean” way. The little fragmentation that does occur occurs at the bottom of the block.

WH0.9

Laser in y-direction: Figure 121 below shows tool vibrations in the y-direction.

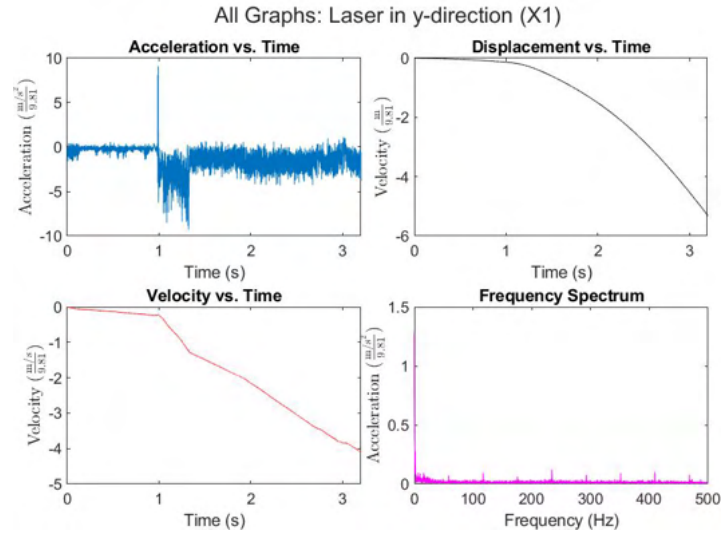


Figure 121: Results from the Laser Measurements on the Tool.

Acceleration Sensor Material in z-direction: Figure 122 below shows material vibrations in the z-direction.

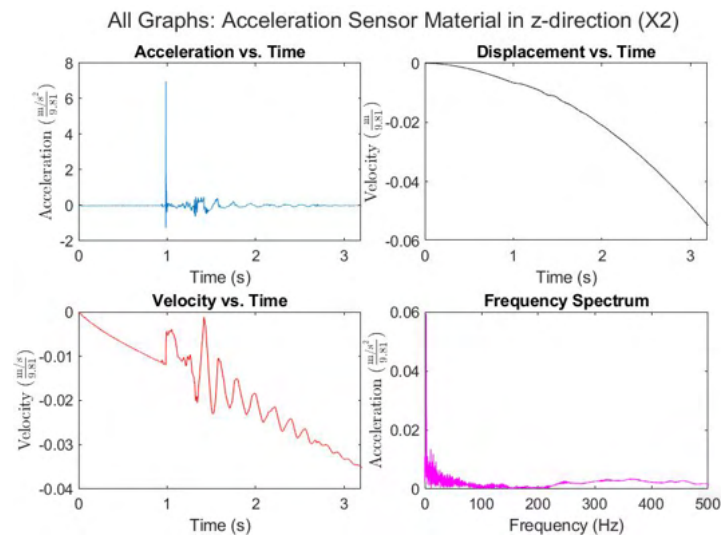


Figure 122: Results of acceleration sensor on material.

Acceleration Sensor Material in x-direction: Figure 123 below shows material vibrations in the x-direction.

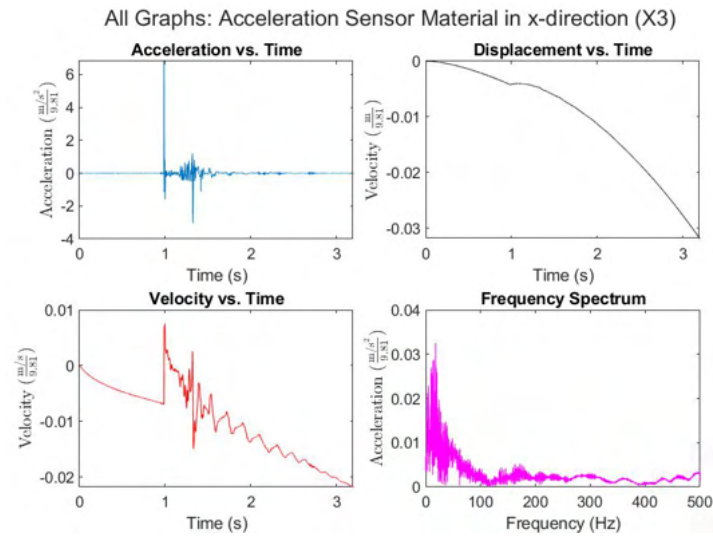


Figure 123: Results of acceleration sensor on material.

Acceleration Sensor Housing in z-direction: Figure 124 below shows housing vibrations in the z-direction.

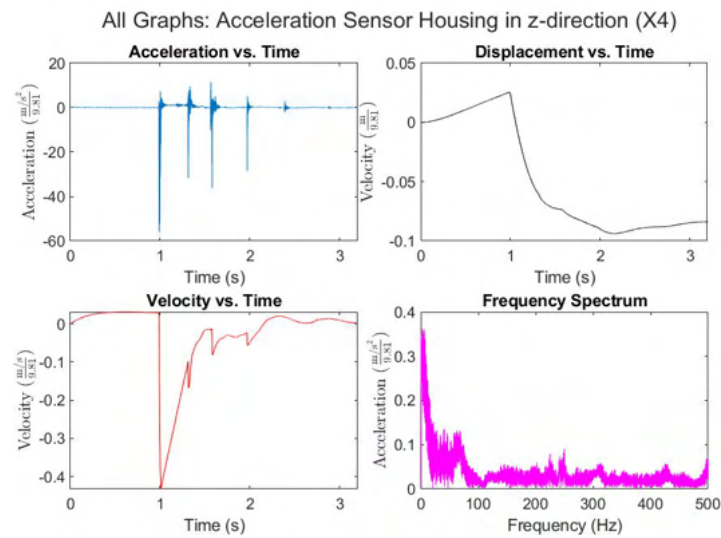


Figure 124: Results of acceleration sensor on material.

Sample Results: Figure 125 shows the resulting sample after it had broken.



Figure 125: The area around the impact zone.

- Only one piece broke off very cleanly, although this piece did have a crack perpendicular to the wedge of the tool to the free surface, where some other, fine cracks branched off from it (left image in Figure 125).
- The sample took about 5 seconds to break when hammering was done near the edge of the block.

WH5

Laser in y-direction: Figure 126 below shows tool vibrations in the y-direction.

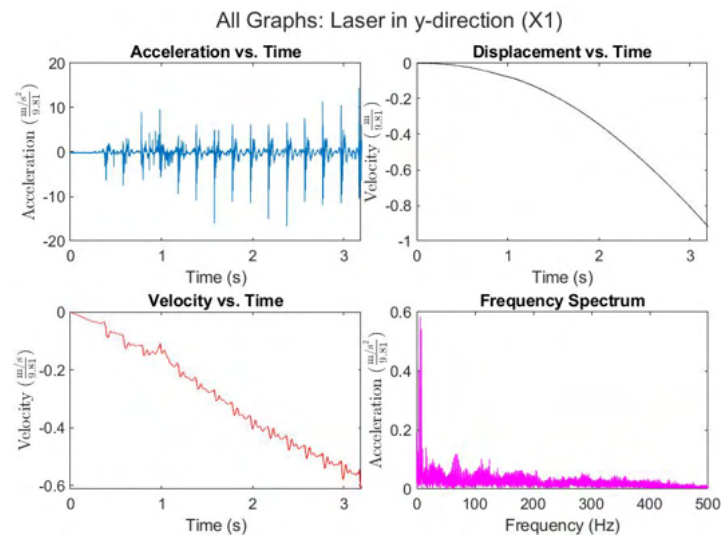


Figure 126: Results from the Laser Measurements on the Tool.

Acceleration Sensor Material in z-direction: Figure 127 below shows material vibrations in the z-direction.

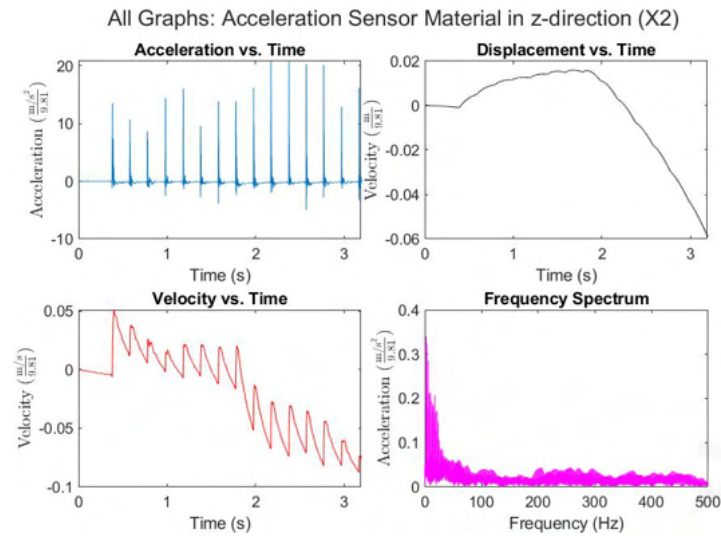


Figure 127: Results of acceleration sensor on material.

Acceleration Sensor Material in x-direction: Figure 128 below shows material vibrations in the x-direction.

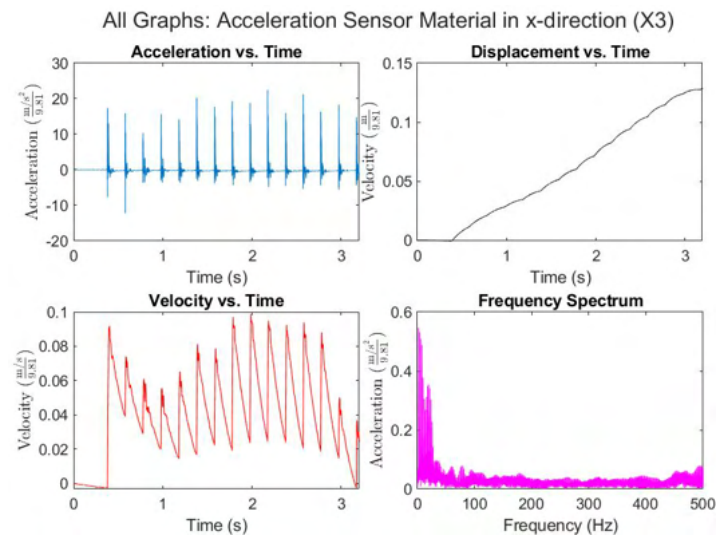


Figure 128: Results of acceleration sensor on material.

Acceleration Sensor Housing in z-direction: Figure 129 below shows housing vibrations in the z-direction.

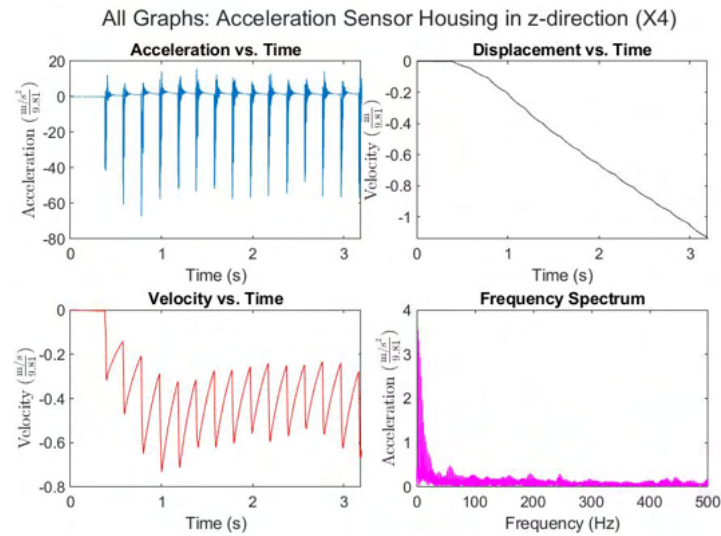


Figure 129: Results of acceleration sensor on material.

Sample Results: Figure 130 shows the resulting sample after it had broken.



Figure 130: The area around the impact zone.

For WH5, the following things are noticeable about the sample:

- A single block once again broke off very cleanly, with some slight fragmentation near one of the free surfaces.
- The block took about 9 seconds to break apart when hitting relatively close to the edge.

WH8

Laser in y-direction: Figure 131 below shows tool vibrations in the y-direction.

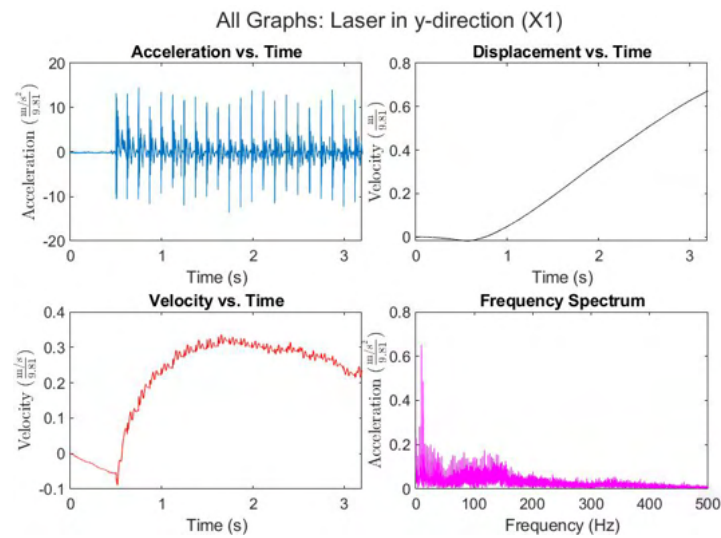


Figure 131: Results from the Laser Measurements on the Tool.

Acceleration Sensor Material in z-direction: Figure 132 below shows material vibrations in the z-direction.

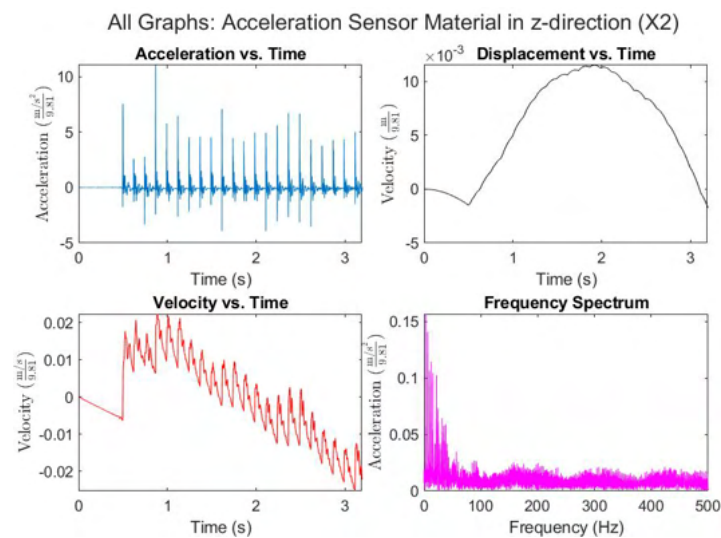


Figure 132: Results of acceleration sensor on material.

Acceleration Sensor Material in x-direction: Figure 133 below shows material vibrations in the x-direction.

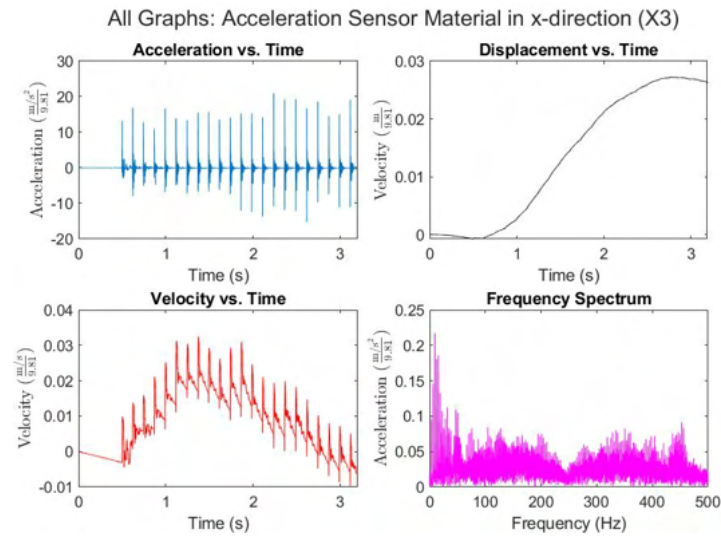


Figure 133: Results of acceleration sensor on material.

Acceleration Sensor Housing in z-direction: Figure 134 below shows housing vibrations in the z-direction.

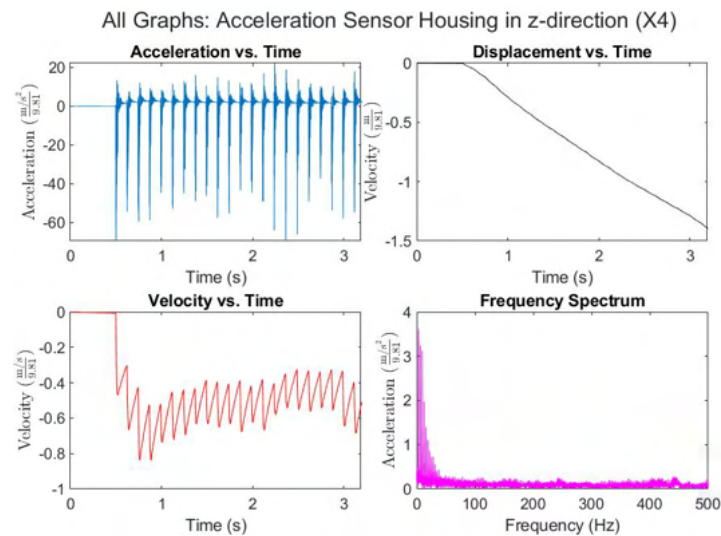


Figure 134: Results of acceleration sensor on material.

Sample Results: Figure 135 shows the resulting sample after it had broken.



Figure 135: The area around the impact zone.

For WH8, the following things are noticeable about the sample:

- There was some visible cracking around the impact zone, with some fragmentation, although the main block broke off cleanly.
- The block took around 32 seconds to break off when hitting near the edge.

WH14

Laser in y-direction: Figure 136 below shows tool vibrations in the y-direction.

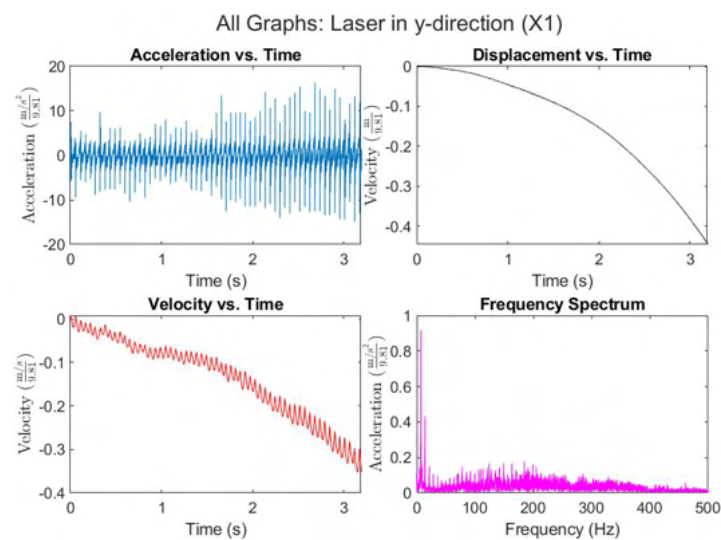


Figure 136: Results from the Laser Measurements on the Tool.

Acceleration Sensor Material in z-direction: Figure 137 below shows material vibrations in the z-direction.

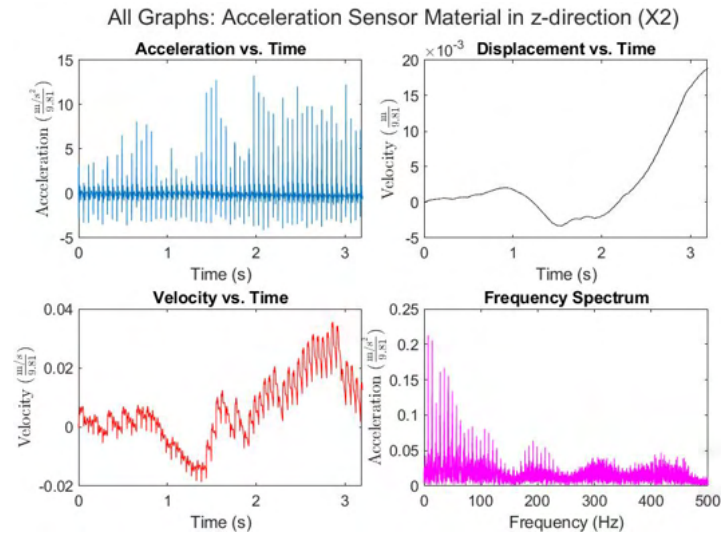


Figure 137: Results of acceleration sensor on material.

Acceleration Sensor Material in x-direction: Figure 138 below shows material vibrations in the x-direction.

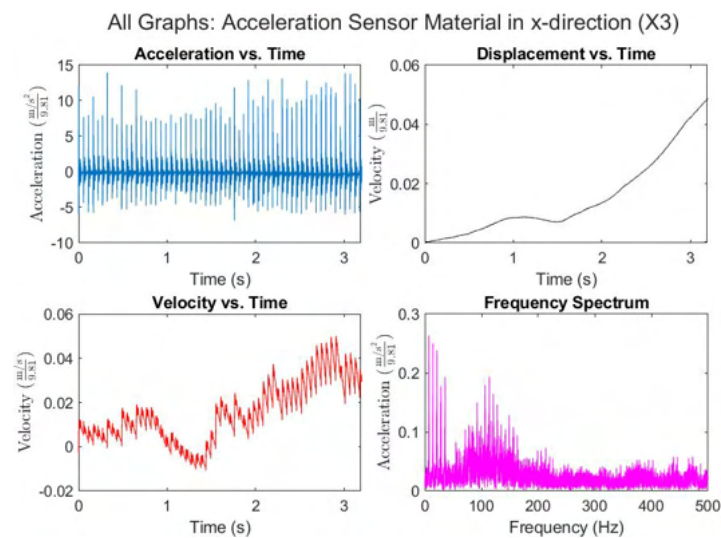


Figure 138: Results of acceleration sensor on material.

Acceleration Sensor Housing in z-direction: Figure 139 below shows housing vibrations in the z-direction.

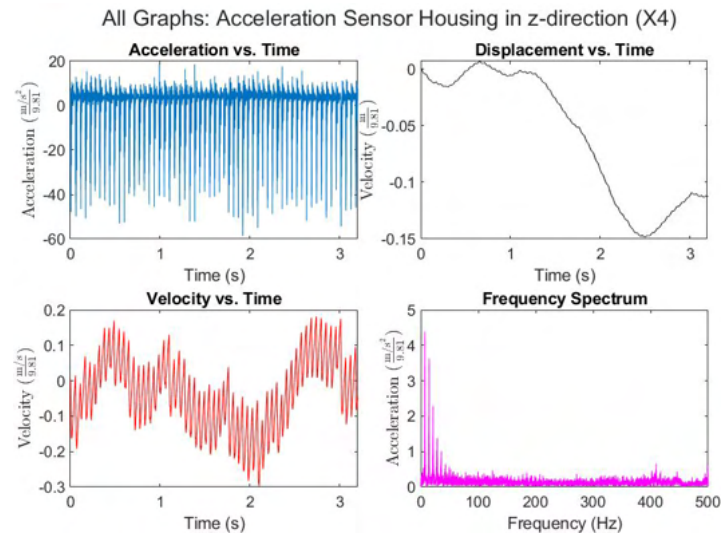


Figure 139: Results of acceleration sensor on material.

Sample Results: Figure 140 shows the resulting sample after it had broken.



Figure 140: The area around the impact zone.

For WH8, the following things are noticeable about the sample:

- There was some slight fragmentation around the impact zone, otherwise the block broke off cleanly in two pieces, with one crack again perpendicular to the wedge of the tool.
- The block took around 10 seconds to break off when hitting near the edge.

WH18

Laser in y-direction: Figure 141 below shows tool vibrations in the y-direction.

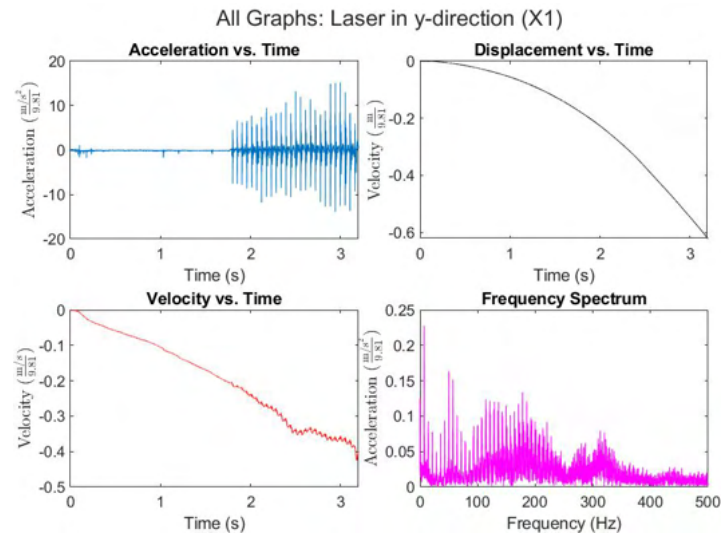


Figure 141: Results from the Laser Measurements on the Tool.

Acceleration Sensor Material in z-direction: Figure 142 below shows material vibrations in the z-direction.

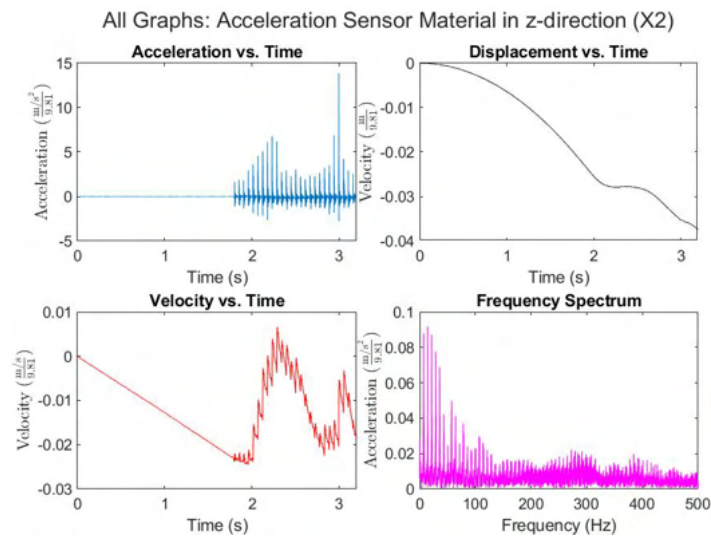


Figure 142: Results of acceleration sensor on material.

Acceleration Sensor Material in x-direction: Figure 143 below shows material vibrations in the x-direction.

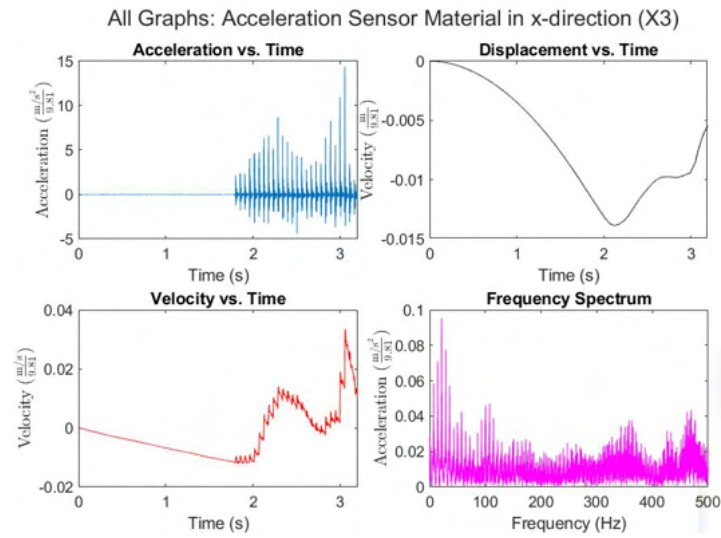


Figure 143: Results of acceleration sensor on material.

Acceleration Sensor Housing in z-direction: Figure 144 below shows housing vibrations in the z-direction.

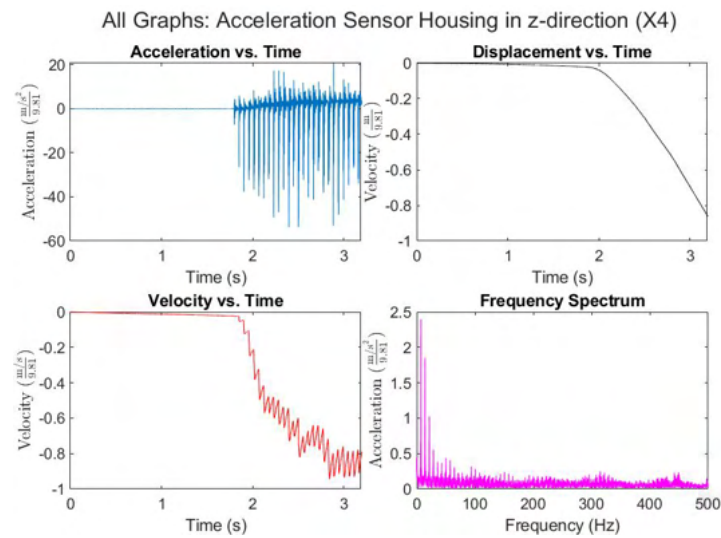


Figure 144: Results of acceleration sensor on material.

Sample Results: Figure 145 shows the resulting sample after it had broken.



Figure 145: The area around the impact zone.

For WH18, the following things are noticeable about the sample:

- There was some slight fragmentation and minor cracking around the impact zone, otherwise the block broke off cleanly in one piece.
- The block took around 5 seconds to break off when hitting near the edge.

Therefore, it can be said that with the wedge tool on the high strength concrete, the cracking is very clean, with sometimes a little fragmentation visible around the impact zone. It is also noticeable that sometimes, a crack develops perpendicular to the wedge of the tool.

BH0.9

Laser in y-direction: Figure 146 below shows tool vibrations in the y-direction.

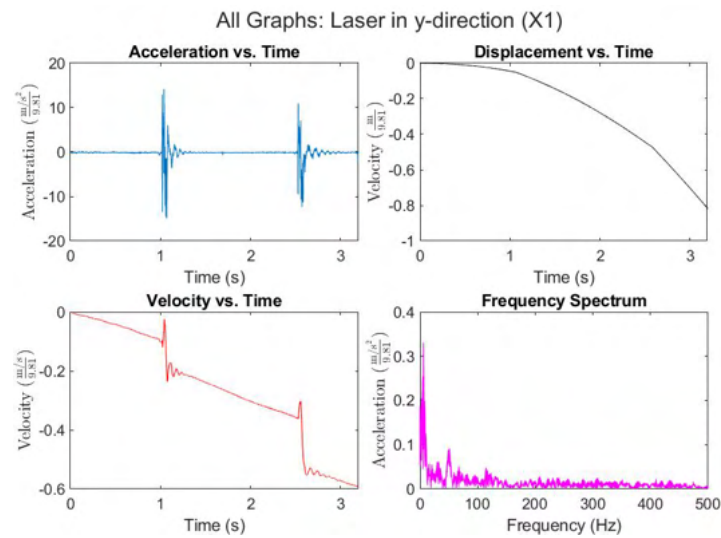


Figure 146: Results from the Laser Measurements on the Tool.

Acceleration Sensor Material in z-direction: Figure 147 below shows material vibrations in the z-direction.

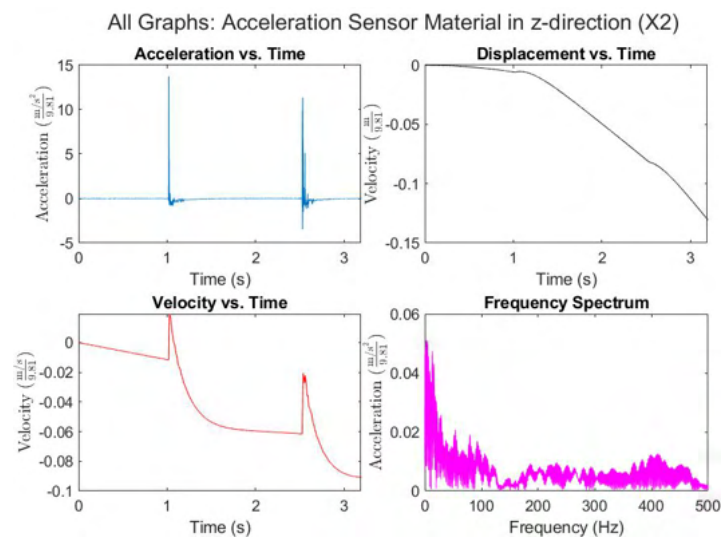


Figure 147: Results of acceleration sensor on material.

Acceleration Sensor Material in x-direction: Figure 148 below shows material vibrations in the x-direction.

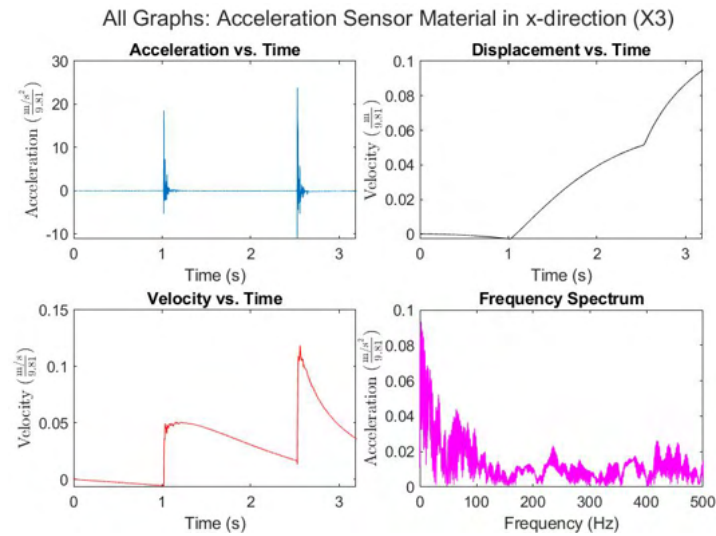


Figure 148: Results of acceleration sensor on material.

Acceleration Sensor Housing in z-direction: Figure 149 below shows housing vibrations in the z-direction.

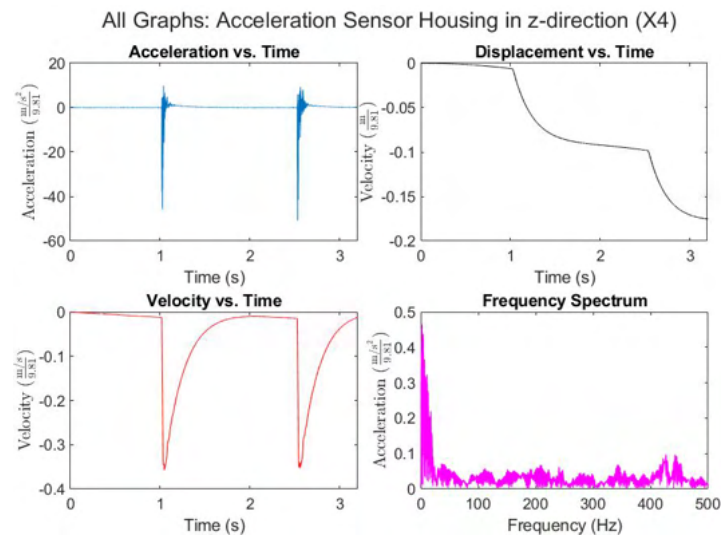


Figure 149: Results of acceleration sensor on material.

Sample Results: Figure 150 shows the resulting sample after it had broken.



Figure 150: The area around the impact zone.

- There was some fragmentation and minor cracking around the impact zone, otherwise the block broke off relatively cleanly in one piece. The crack propagation started from the side of the tool.
- The block took around 77 seconds to break when hitting near the edge.

BH5

Laser in y-direction: Figure 151 below shows tool vibrations in the y-direction.

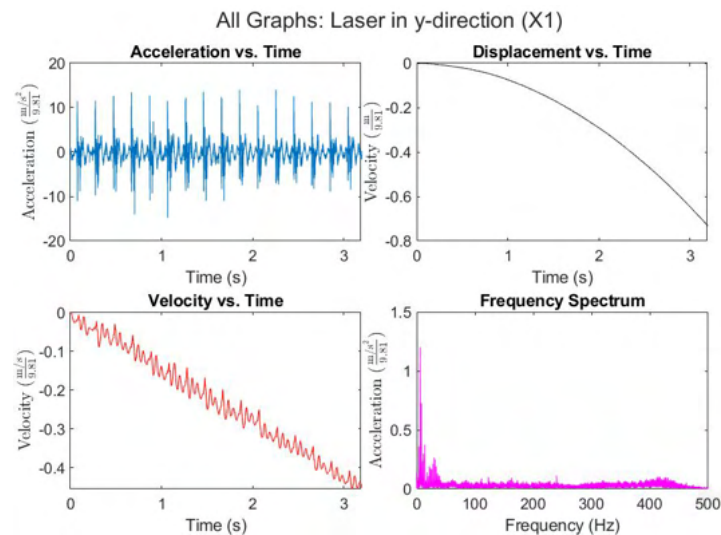


Figure 151: Results from the Laser Measurements on the Tool.

Acceleration Sensor Material in z-direction: Figure 152 below shows material vibrations in the z-direction.

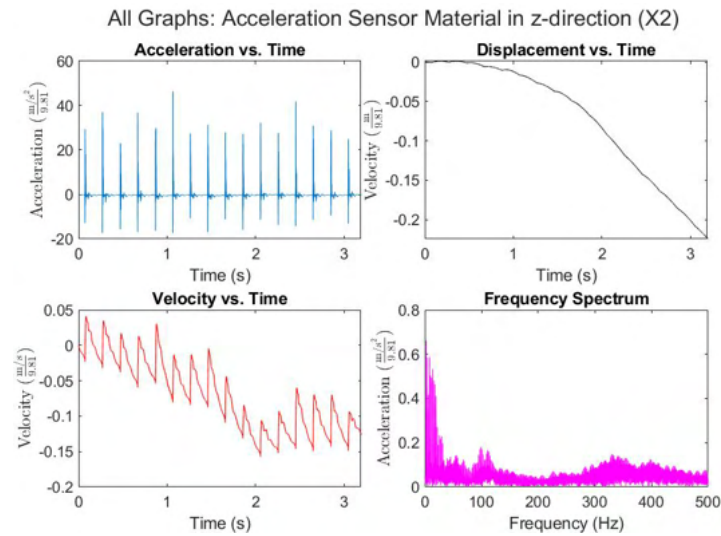


Figure 152: Results of acceleration sensor on material.

Acceleration Sensor Material in x-direction: Figure 153 below shows material vibrations in the x-direction.

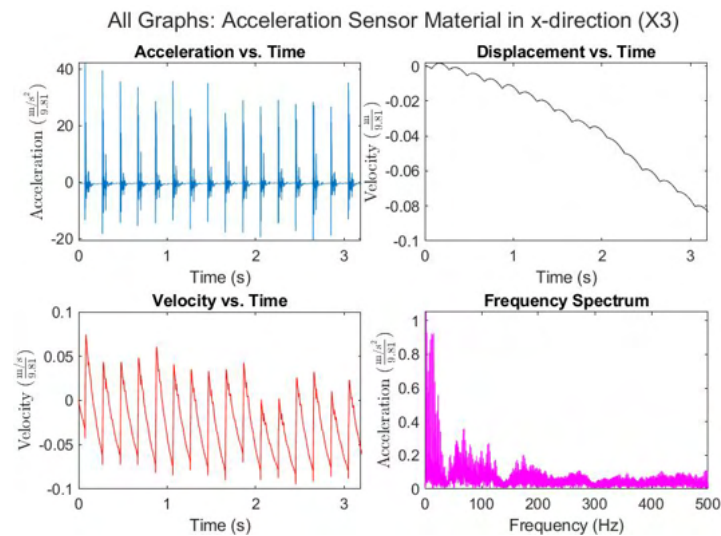


Figure 153: Results of acceleration sensor on material.

Acceleration Sensor Housing in z-direction: Figure 154 below shows housing vibrations in the z-direction.

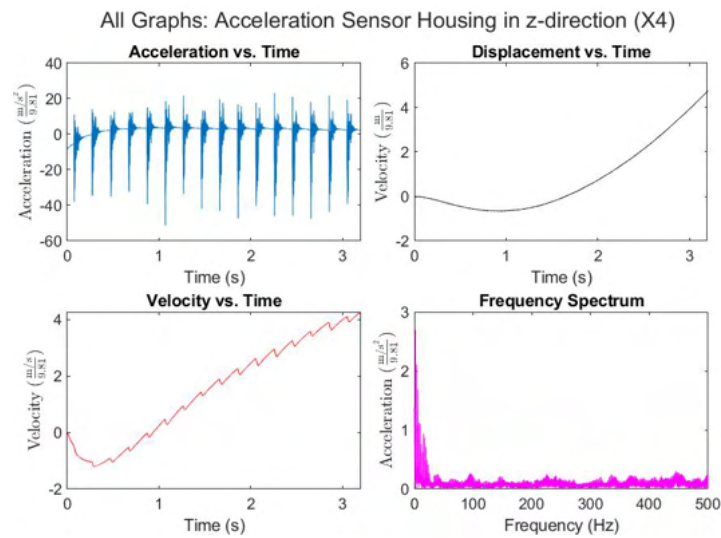


Figure 154: Results of acceleration sensor on material.

Sample Results: Figure 155 shows the resulting sample after it had broken.



Figure 155: The area around the impact zone.

- There was significant fragmentation and cracking around the impact zone, and the main crack went deep from the tool to the free surface at the bottom of the block. A second, smaller piece also broke off.
- The block took around 50 seconds to break when hitting near the edge.

BH8

Laser in y-direction: Figure 156 below shows tool vibrations in the y-direction.

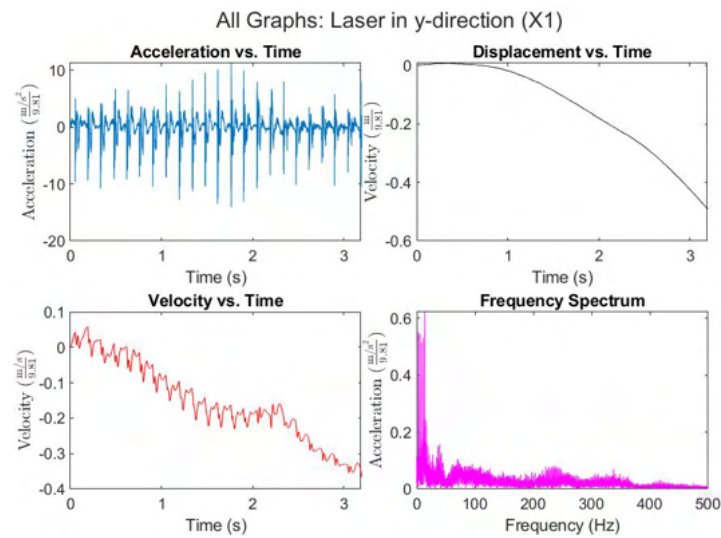


Figure 156: Results from the Laser Measurements on the Tool.

Acceleration Sensor Material in z-direction: Figure 157 below shows material vibrations in the z-direction.

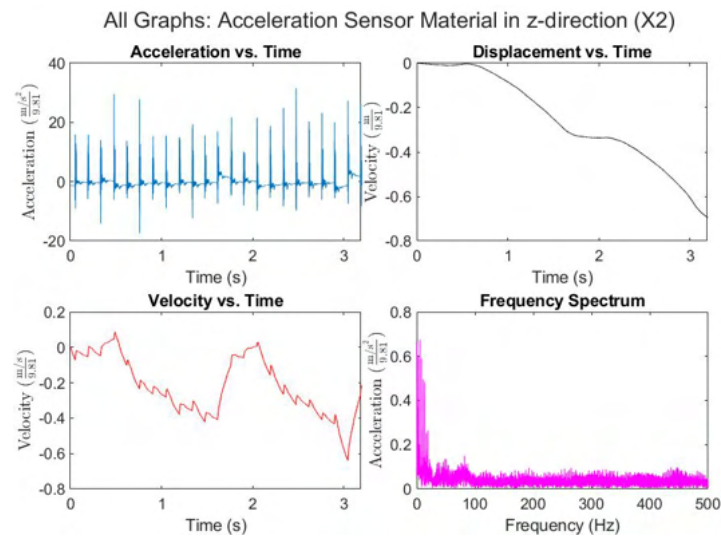


Figure 157: Results of acceleration sensor on material.

Acceleration Sensor Material in x-direction: Figure 158 below shows material vibrations in the x-direction.

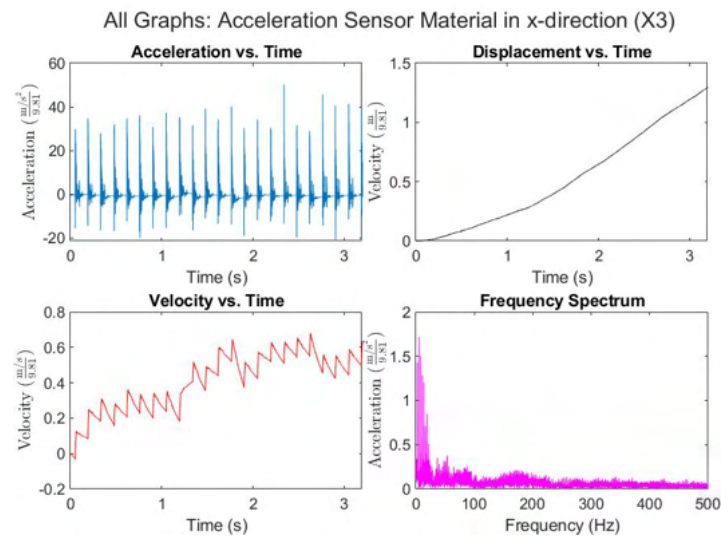


Figure 158: Results of acceleration sensor on material.

Acceleration Sensor Housing in z-direction: Figure 159 below shows housing vibrations in the z-direction.

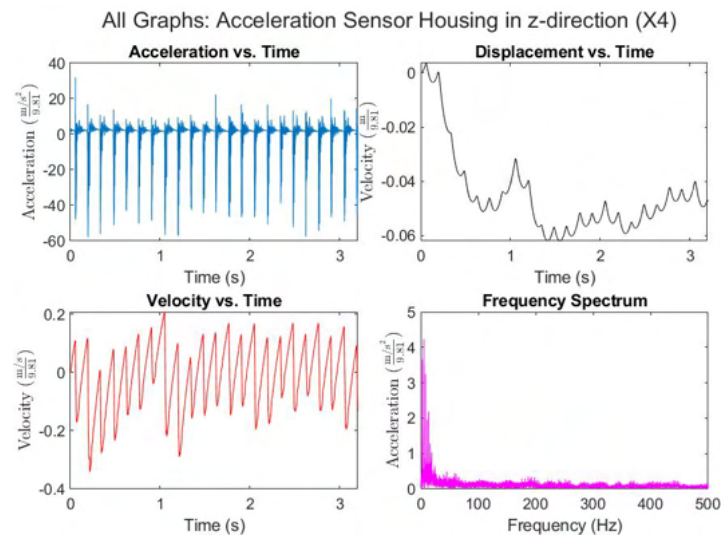


Figure 159: Results of acceleration sensor on material.

Sample Results: Figure 160 shows the resulting sample after it had broken.



Figure 160: The area around the impact zone.

- There was again some significant fragmentation and cracking around the impact zone of the tool but the main piece broke off cleanly apart from this, with a small crack forming to the free surface perpendicular to the main crack.
- The block took around 97 seconds to break when hitting near the edge.

BH14

Laser in y-direction: Figure 161 below shows tool vibrations in the y-direction.

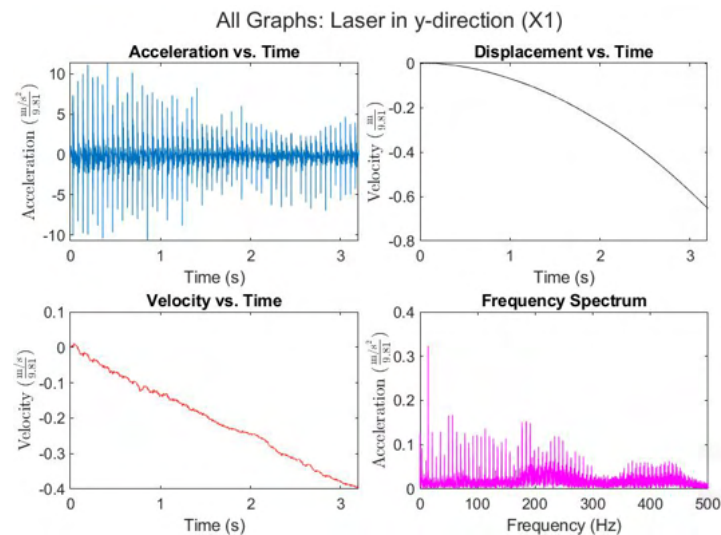


Figure 161: Results from the Laser Measurements on the Tool.

Acceleration Sensor Material in z-direction: Figure 162 below shows material vibrations in the z-direction.

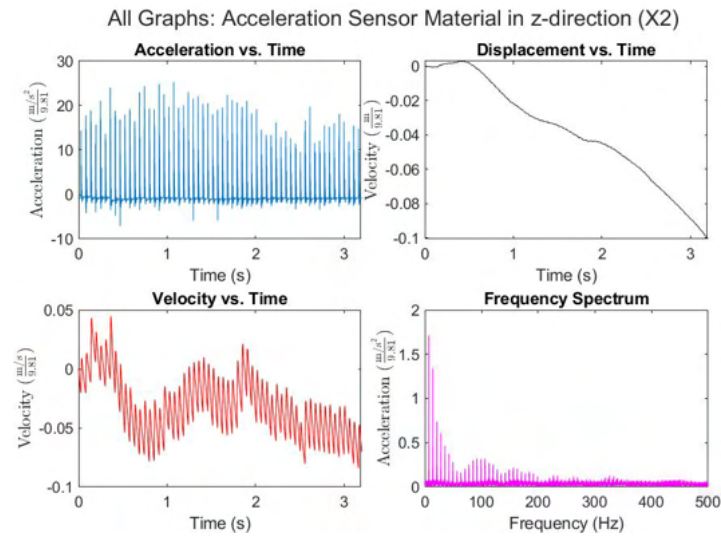


Figure 162: Results of acceleration sensor on material.

Acceleration Sensor Material in x-direction: Figure 163 below shows material vibrations in the x-direction.

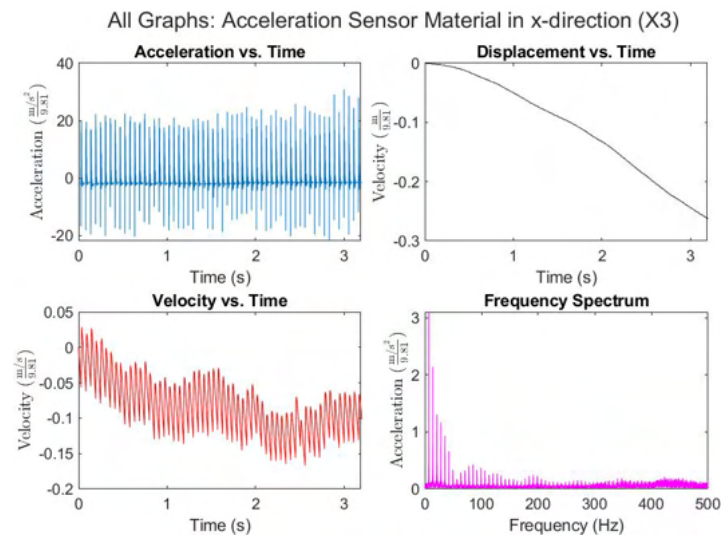


Figure 163: Results of acceleration sensor on material.

Acceleration Sensor Housing in z-direction: Figure 164 below shows housing vibrations in the z-direction.

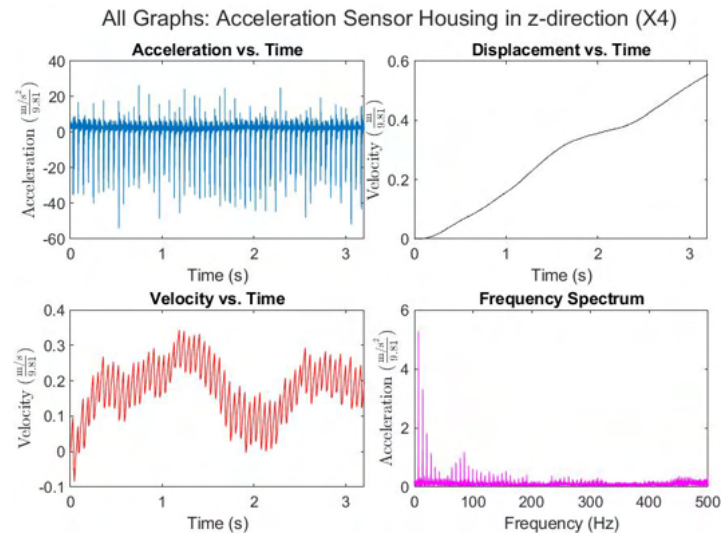


Figure 164: Results of acceleration sensor on material.

Sample Results: Figure 165 shows the resulting sample after it had broken.



Figure 165: The area around the impact zone.

- There was significant fragmentation and cracking around the impact zone of the tool and a couple of main pieces broke off the main block, but their cracks were parallel to each other.
- The block took around 99 seconds to break when hitting near the edge.

BH18

Laser in y-direction: Figure 166 below shows tool vibrations in the y-direction.

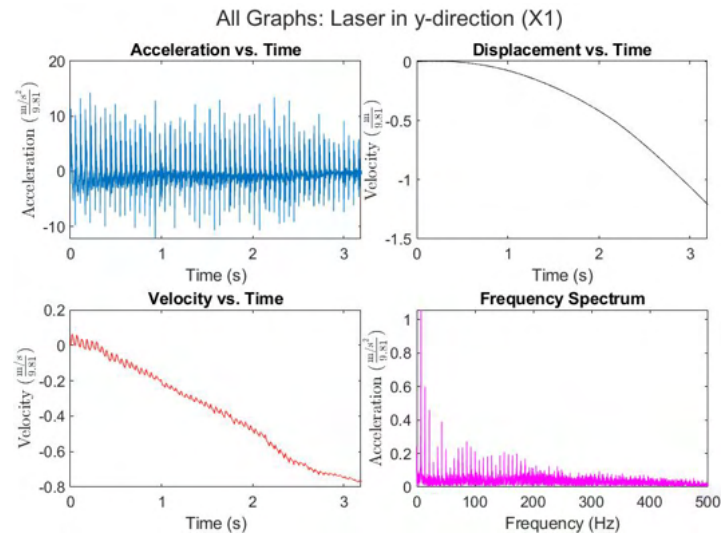


Figure 166: Results from the Laser Measurements on the Tool.

Acceleration Sensor Material in z-direction: Figure 167 below shows material vibrations in the z-direction.

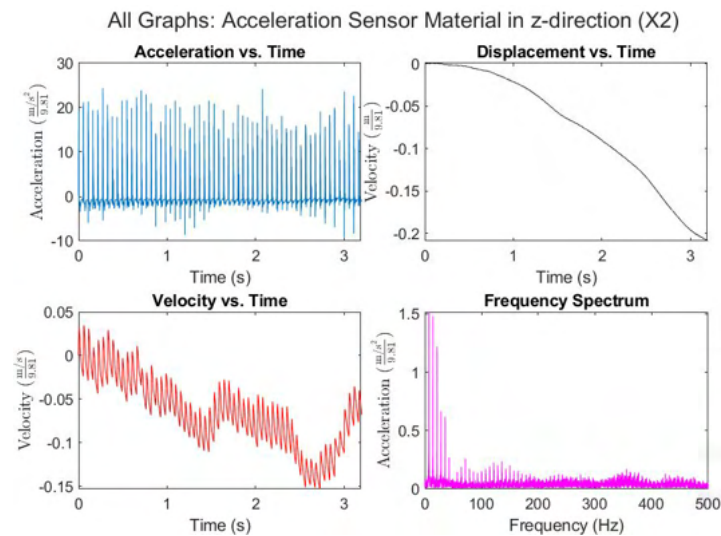


Figure 167: Results of acceleration sensor on material.

Acceleration Sensor Material in x-direction: Figure 168 below shows material vibrations in the x-direction.

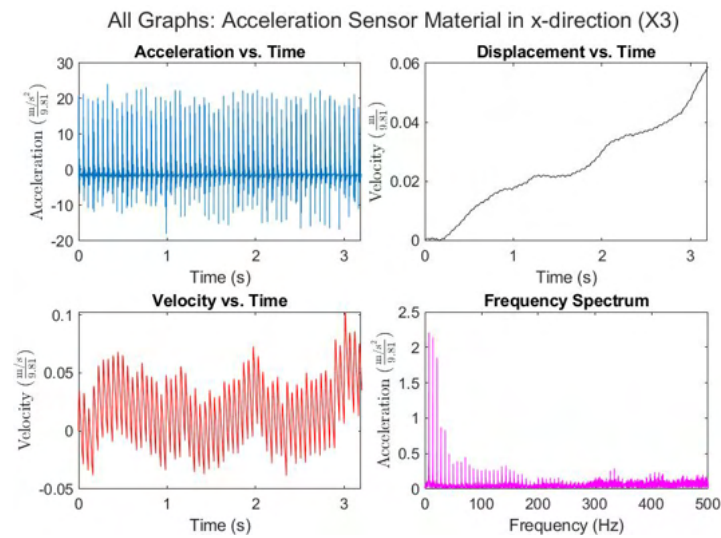


Figure 168: Results of acceleration sensor on material.

Acceleration Sensor Housing in z-direction: Figure 169 below shows housing vibrations in the z-direction.

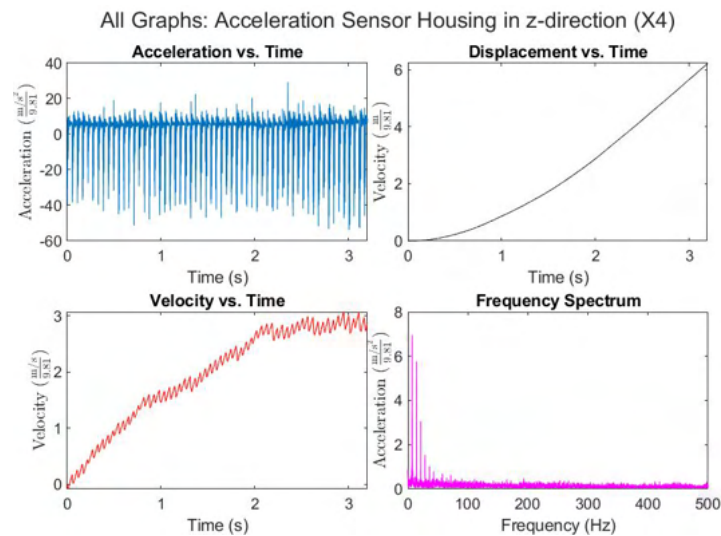


Figure 169: Results of acceleration sensor on material.

Sample Results: Figure 170 shows the resulting sample after it had broken.



Figure 170: The area around the impact zone.

- A relatively small piece broke off from the edge. It did not fragment into multiple larger pieces, but there was fragmentation around the impact zone and around the main crack near the free surface.
- The block took around 61 seconds to break when hitting near the edge.

Therefore, the blunt tool clearly causes more fragmentation than the wedge tool on the high strength concrete, but the high strength concrete also breaks off much more cleanly than the normal concrete. Fragmentation usually occurred around the impact zone. If another large crack developed from the main crack, it was not necessarily perpendicular to the main crack.

CH0.9

Laser in y-direction: Figure 171 below shows tool vibrations in the y-direction.

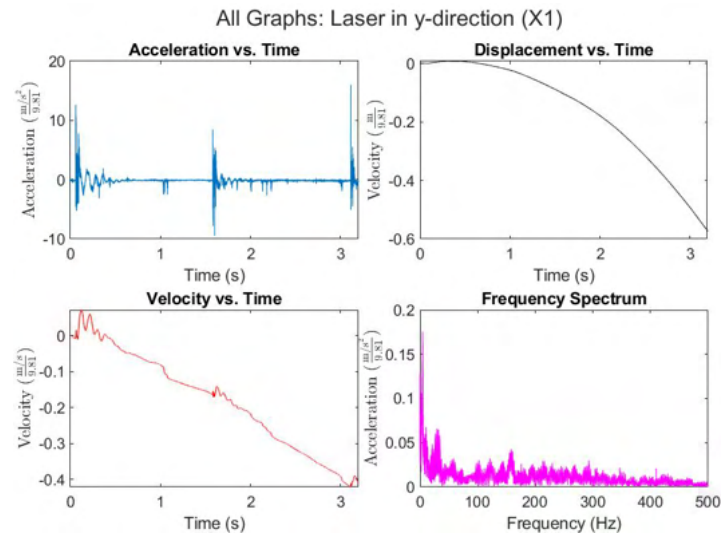


Figure 171: Results from the Laser Measurements on the Tool.

Acceleration Sensor Material in z-direction: Figure 172 below shows material vibrations in the z-direction.

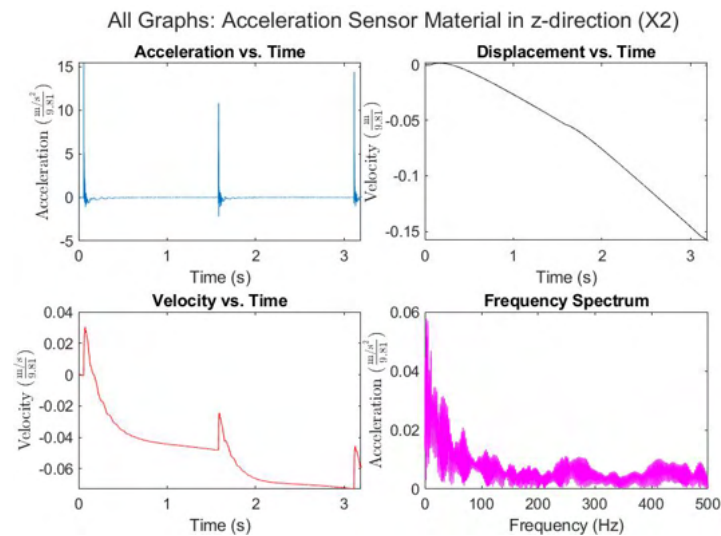


Figure 172: Results of acceleration sensor on material.

Acceleration Sensor Material in x-direction: Figure 173 below shows material vibrations in the x-direction.

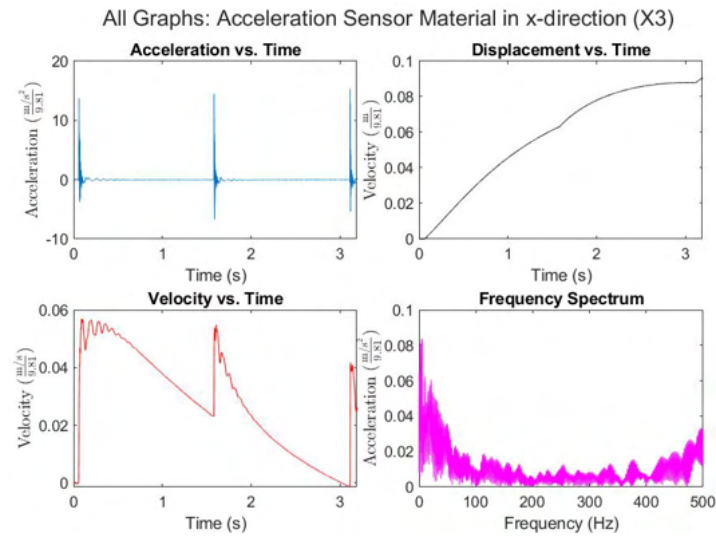


Figure 173: Results of acceleration sensor on material.

Acceleration Sensor Housing in z-direction: Figure 174 below shows housing vibrations in the z-direction.

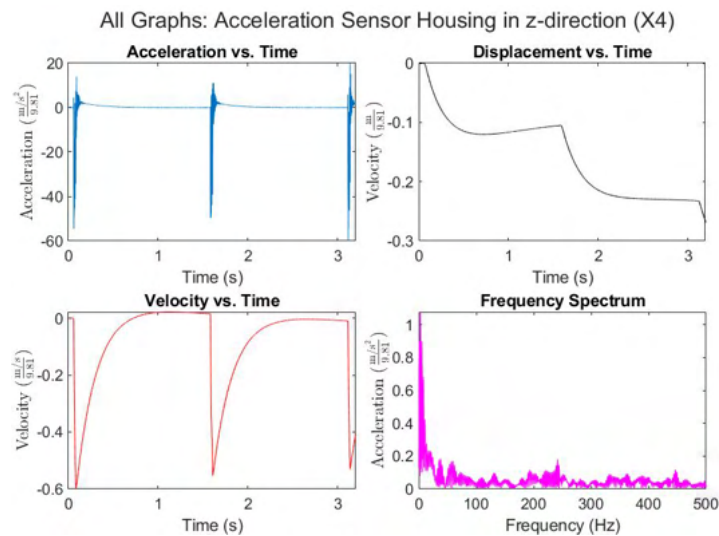


Figure 174: Results of acceleration sensor on material.

Sample Results: Figure 175 shows the resulting sample after it had broken.



Figure 175: The area around the impact zone.

For CH0.9, the following things are noticeable about the sample:

- There was no fragmentation or cracking around the impact zone. The piece broke off cleanly in one piece.
- The block took about 30 seconds to break when it was hit near the edge.

CH5

Laser in y-direction: Figure 176 below shows tool vibrations in the y-direction.

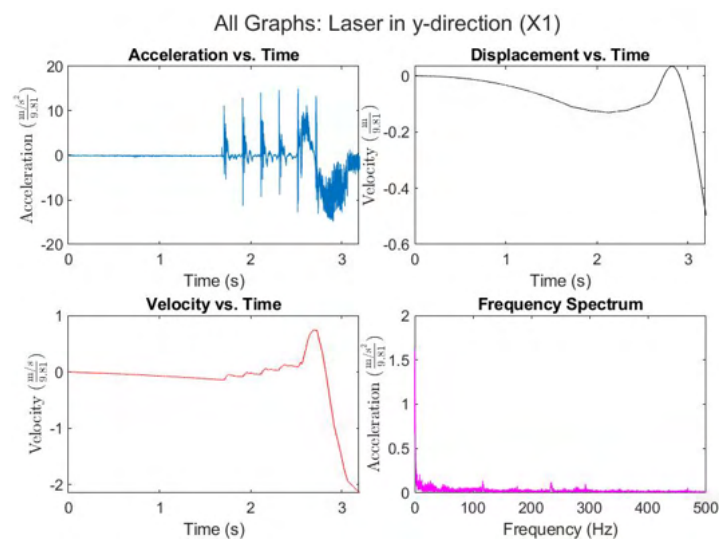


Figure 176: Results from the Laser Measurements on the Tool.

Acceleration Sensor Material in z-direction: Figure 177 below shows material vibrations in the z-direction.

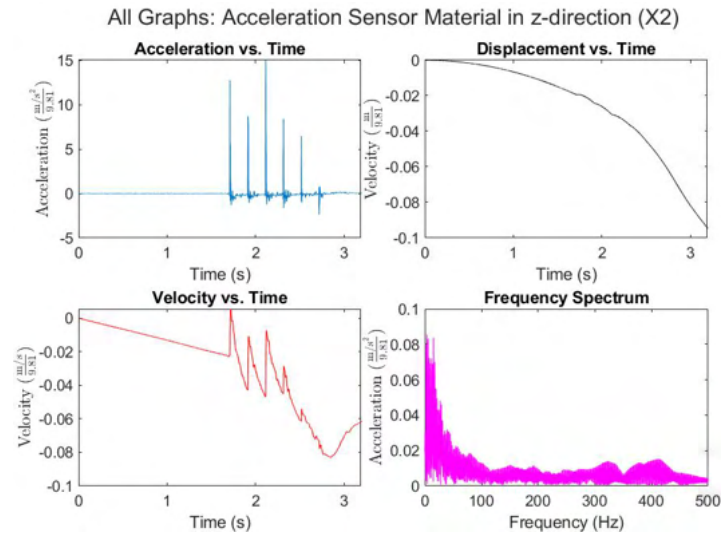


Figure 177: Results of acceleration sensor on material.

Acceleration Sensor Material in x-direction: Figure 178 below shows material vibrations in the x-direction.

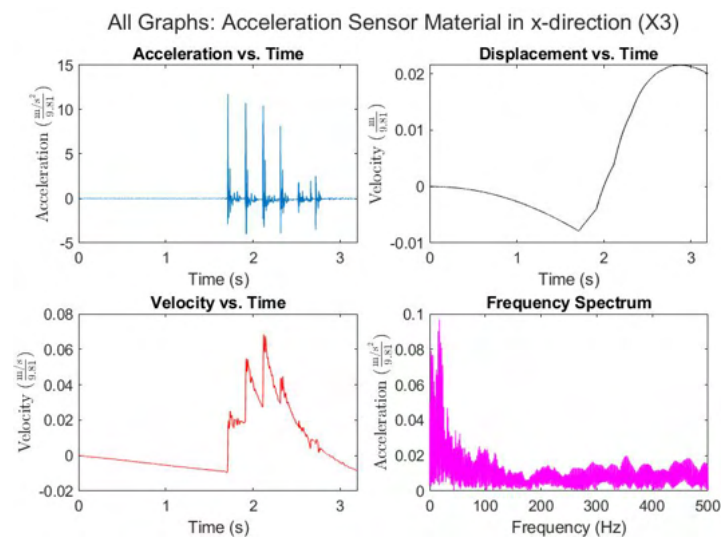


Figure 178: Results of acceleration sensor on material.

Acceleration Sensor Housing in z-direction: Figure 179 below shows housing vibrations in the z-direction.

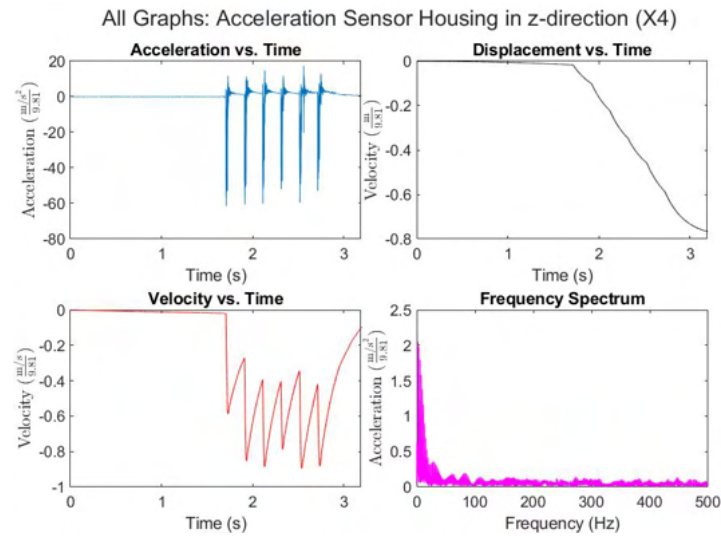


Figure 179: Results of acceleration sensor on material.

Sample Results: Figure 180 shows the resulting sample after it had broken.

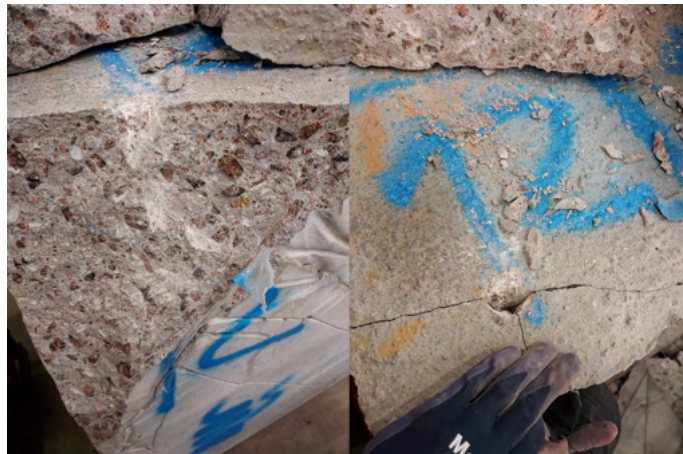


Figure 180: The area around the impact zone.

For CH5, the following things are noticeable about the sample:

- Fragmentation was again minimal to nonexistent and there were two clear pieces that broke off, with their cracks perpendicular to each other, as can be seen in figure 180 on the right.
- The block took only 2 seconds to break when it was hit near the edge.

CH8

Laser in y-direction: Figure 181 below shows tool vibrations in the y-direction.

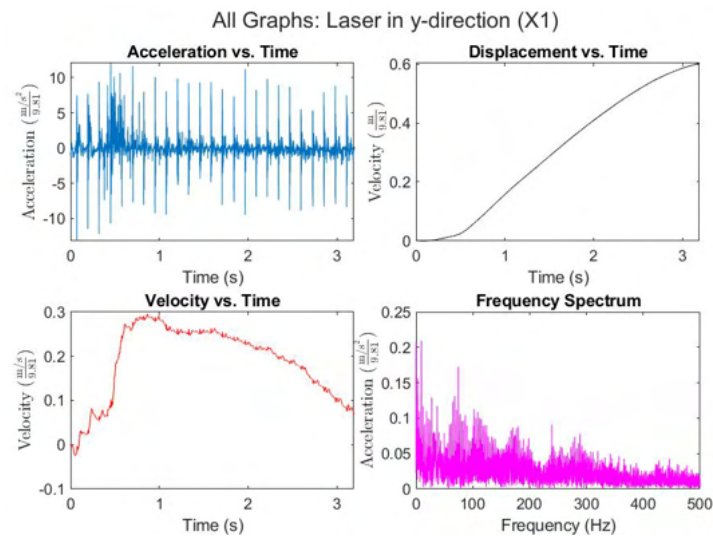


Figure 181: Results from the Laser Measurements on the Tool.

Acceleration Sensor Material in z-direction: Figure 182 below shows material vibrations in the z-direction.

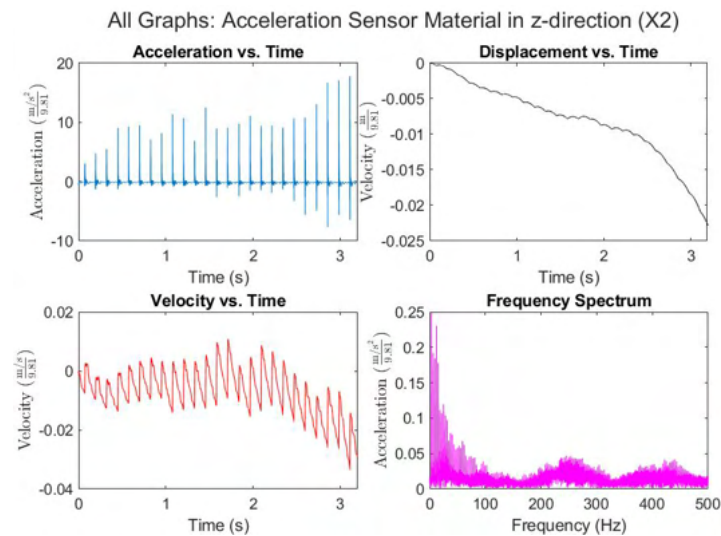


Figure 182: Results of acceleration sensor on material.

Acceleration Sensor Material in x-direction: Figure 183 below shows material vibrations in the x-direction.

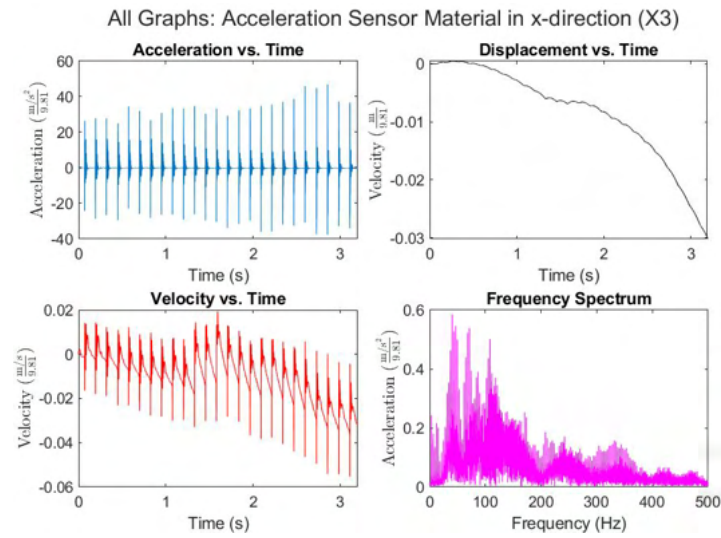


Figure 183: Results of acceleration sensor on material.

Acceleration Sensor Housing in z-direction: Figure 184 below shows housing vibrations in the z-direction.

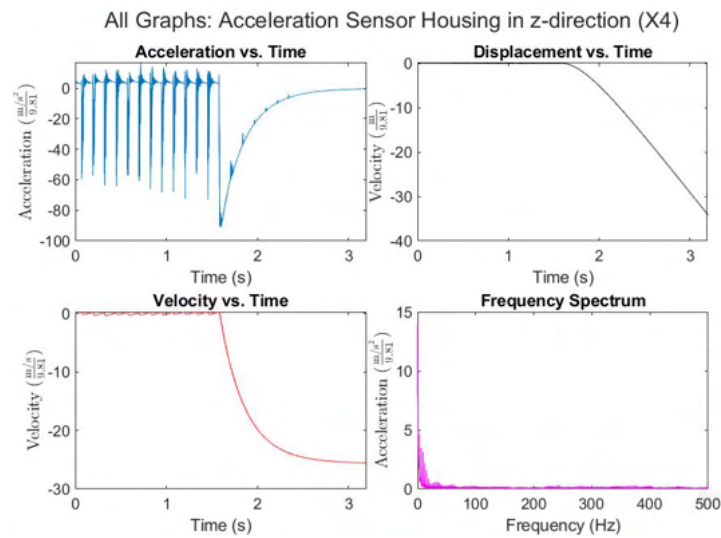


Figure 184: Results of acceleration sensor on material.

Sample Results: Figure 185 shows the resulting sample after it had broken.



Figure 185: The area around the impact zone.

For CH8, the following things are noticeable about the sample:

- Fragmentation was basically nonexistent and only one piece broke off from the main block in a clean manner.
- The block took only 5 seconds to break when it was hit near the edge.

CH14

Laser in y-direction: Figure 186 below shows tool vibrations in the y-direction.

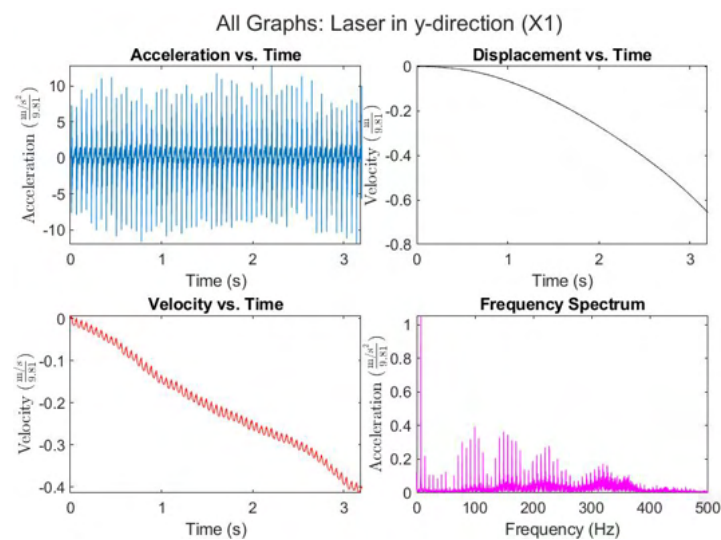


Figure 186: Results from the Laser Measurements on the Tool.

Acceleration Sensor Material in z-direction: Figure 187 below shows material vibrations in the z-direction.

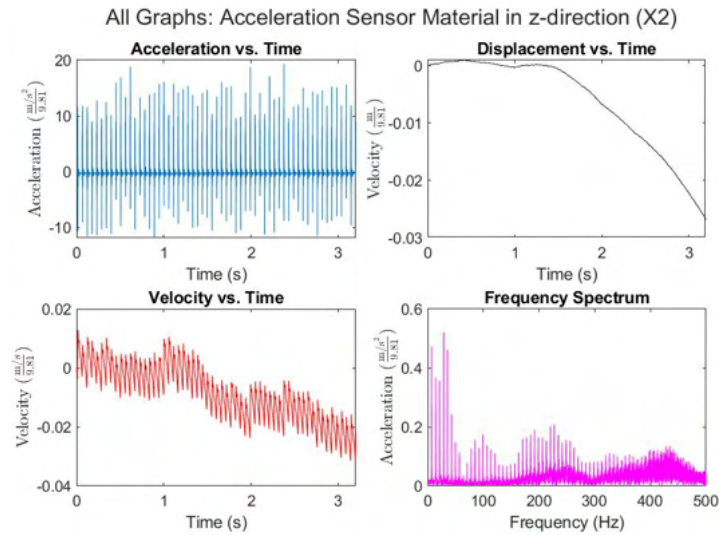


Figure 187: Results of acceleration sensor on material.

Acceleration Sensor Material in x-direction: Figure 188 below shows material vibrations in the x-direction.

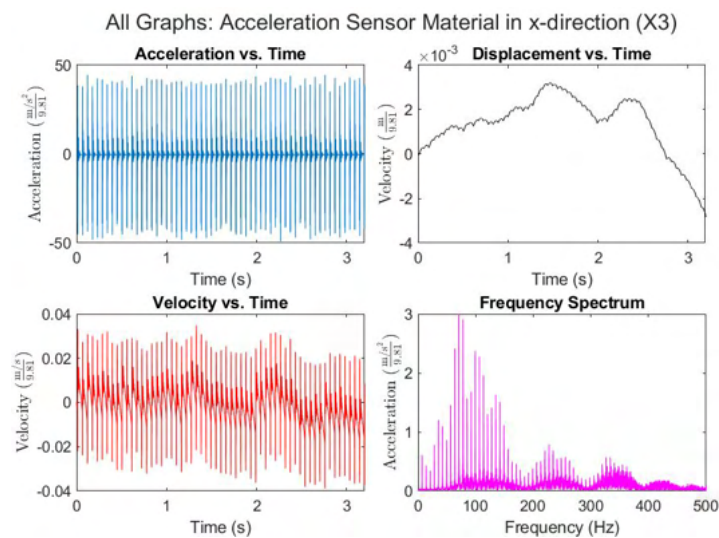


Figure 188: Results of acceleration sensor on material.

Acceleration Sensor Housing in z-direction: Figure 189 below shows housing vibrations in the z-direction.

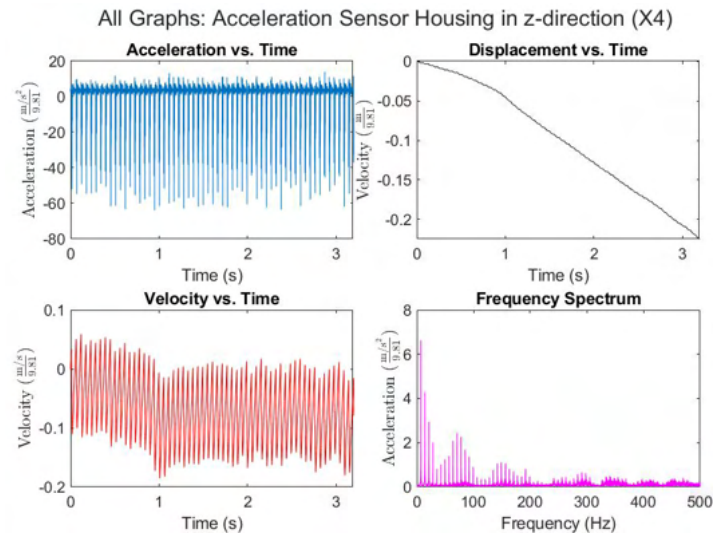


Figure 189: Results of acceleration sensor on material.

Sample Results: Figure 190 shows the resulting sample after it had broken.



Figure 190: The area around the impact zone.

For CH14, the following things are noticeable about the sample:

- The block broke off in one piece but it was not as clean as the previous ones, with some fragmentation near the impact zone.
- The block took about 52 seconds to break when it was hit near the edge.

CH18

Laser in y-direction: Figure 191 below shows tool vibrations in the y-direction.

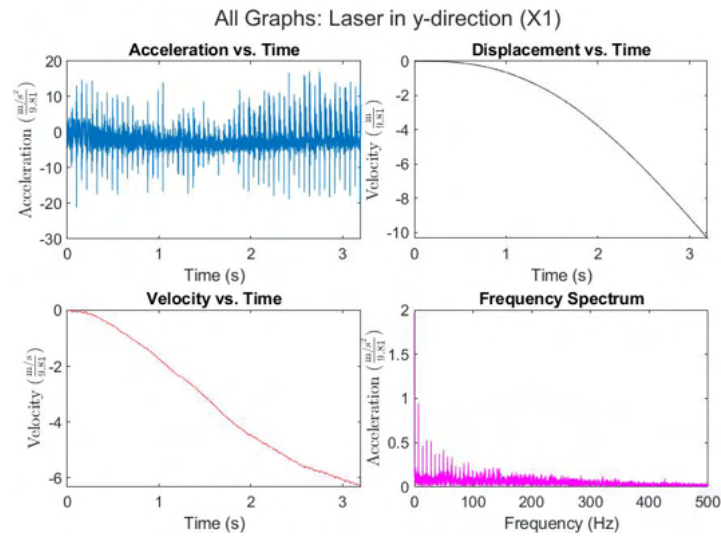


Figure 191: Results from the Laser Measurements on the Tool.

Acceleration Sensor Material in z-direction: Figure 192 below shows material vibrations in the z-direction.

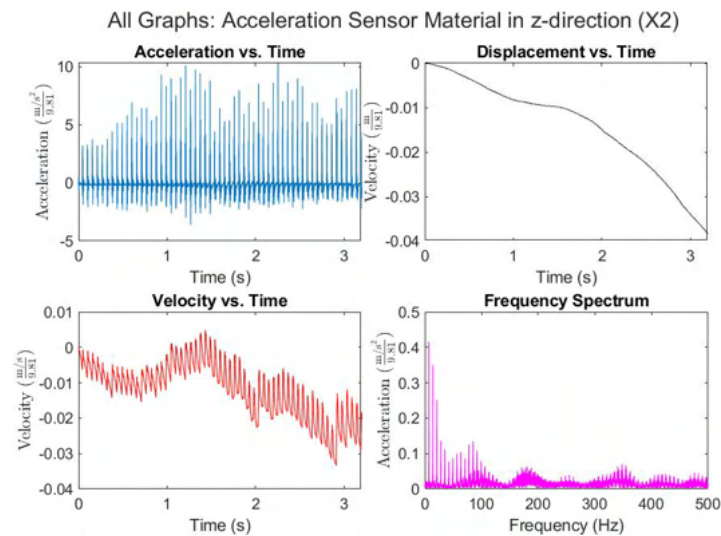


Figure 192: Results of acceleration sensor on material.

Acceleration Sensor Material in x-direction: Figure 193 below shows material vibrations in the x-direction.

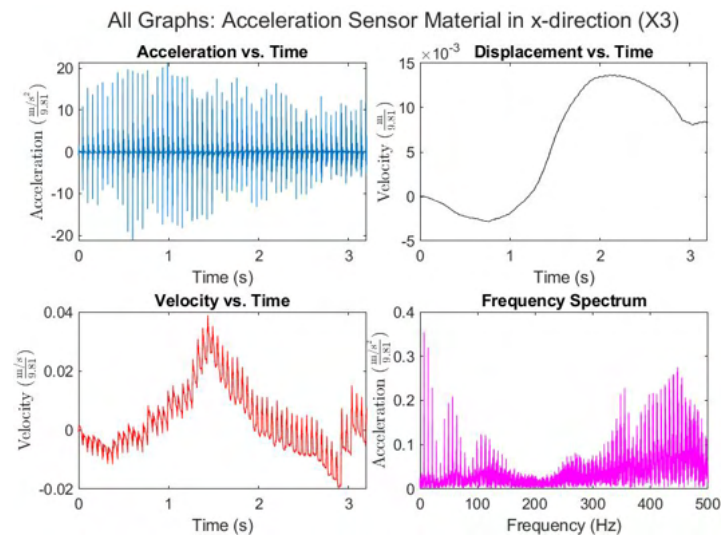


Figure 193: Results of acceleration sensor on material.

Acceleration Sensor Housing in z-direction: Figure 194 below shows housing vibrations in the z-direction.

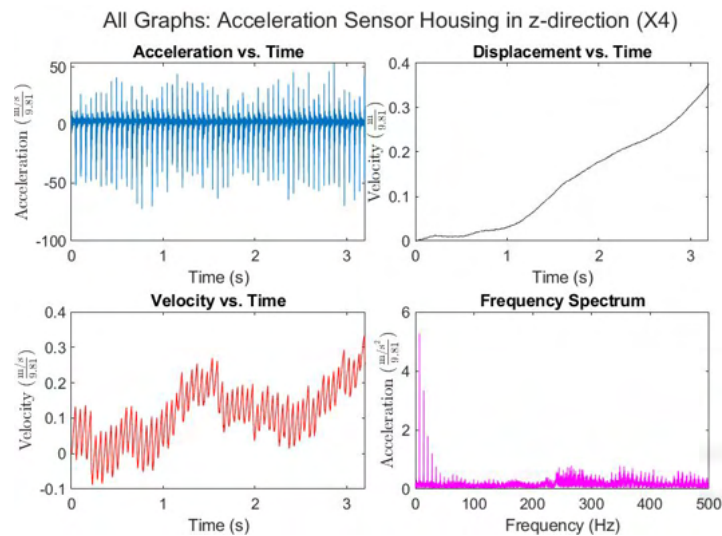


Figure 194: Results of acceleration sensor on material.

Sample Results: Figure bla shows the resulting sample after it had broken.
insert picture here

For CH18, the following things are noticeable about the sample:

- There

Therefore...